

関西学院大学審査 博士学位論文

Endothelin Induced Contractile Mechanism in

Airway Smooth Muscle

Signal Transduction Mechanism Mediated by Endothelin_A and

Endothelin_B Receptors

乾 隆

関西学院大学博士論文

**Endothelin Induced Contractile Mechanism in
Airway Smooth Muscle**
Signal Transduction Mechanism Mediated by Endothelin_A and
Endothelin_B Receptors

(エンドセリンによる気管平滑筋収縮の機構に関する研究：
エンドセリン ET_A、ET_B受容体を介した細胞内情報伝達機構の解析)

by
Takashi Inui
1997

To Kyoshi

This thesis is approved as to style and content by

Professor Susumu Takayama

Professor Asako Kawasumi

Professor Tatsuo Yagura

&

Professor Tomohi Matsuki

To Kiyoshi

CONTENTS

GENERAL INTRODUCTION

SUMMARY

References

This thesis is approved as to style and content by

CHAPTER 1

ET_A and ET_B receptors on single smooth muscle cells regulate in vivo airway smooth

muscle contraction

Professor Susumu Takayama

14

1-1. Abstract

Professor Asako Kawamori

15

1-2. Introduction

Professor Tatsuo Yagura

17

1-3. Materials and Methods

&

17

1-4. Results

Professor Tomoh Masaki

22

1-4-1. Binding Sites of ET_A and ET_B in Tracheal Smooth Muscle Membranes

1-4-2. ET_A and ET_B in Primary Cultures of Tracheal Smooth Muscle Cells

1-4-3. Increase in [Ca²⁺]_i Mediated by ET_A and ET_B in Pura Dissociated Primary Cultured Cells

1-4-4. Distributions of ET_A and ET_B in Single Tracheal Smooth Muscle Cells by Monitoring [Ca²⁺]_i Changes after Stimulation with ETx

1-4-5. Spatial Distribution of Ca²⁺ Levels of Single Smooth Muscle Cells after Stimulation with ETx

1-4-6. Tracheal Contraction Induced by ET-1 and ET-2

1-5. Discussion

29

1-6. References

31

CONTENTS

GENERAL INTRODUCTION	1
SUMMARY	8
References	9
CHAPTER 1	
<i>ET_A and ET_B receptors on single smooth muscle cells cooperate in mediating guinea pig tracheal contraction*</i>	14
1-1. Abstract	15
1-2. Introduction	15
1-3. Materials and Methods	17
1-4. Results	22
1-4-1. Binding Sites of ET _A and ET _B in Tracheal Smooth Muscle Membranes.	
1-4-2. ET _A and ET _B in Primary Cultures of Tracheal Smooth Muscle Cells.	
1-4-3. Increases in [Ca ²⁺] _i Mediated by ET _A and ET _B in Fura-2-loaded Primary Cultured Cells.	
1-4-4. Distribution of ET _A and ET _B in Single Tracheal Smooth Muscle Cells by Monitoring [Ca ²⁺] _i Changes after Stimulation with ETs.	
1-4-5. Spatial Distribution of Ca ²⁺ Levels of Single Smooth Muscle Cells after Stimulation with ETs.	
1-4-6. Tracheal Contraction Induced by ET-1 and ET-3.	
1-5. Discussion	29
1-6. References	33

1-7. Tables and Figures	37
-------------------------	----

CHAPTER 2

<i>Selective activation of pharmacomechanical and electromechanical excitation-contraction coupling pathways by ET_A and ET_B in guinea pig tracheal smooth muscle</i>	47
2-1. Abstract	48
2-2. Introduction	48
2-3. Materials and Methods	52
2-4. Results	58
2-4-1. Tracheal Contraction Induced by ET-1, ET-3 and IRL 1620.	
2-4-2. Simultaneous Measurements of [Ca ²⁺] _i and Muscle Tension.	
2-4-3. Contribution of Transient and Sustained Increases in [Ca ²⁺] _i to Contraction.	
2-4-4. ET _A -selective Activation of Phospholipase C and ET _B -mediated Ca ²⁺ Influx via L-type Voltage-dependent Ca ²⁺ Channel.	
2-4-5. Membrane Depolarization in ET _B -mediated Response.	
2-4-6. Phosphatidylinositol Turnover.	
2-4-7. Translocation of Protein Kinase C from Cytosol to Membrane Fractions.	
2-4-8. Cumulative Substitution of Extracellular Ca ²⁺ .	
2-5. Discussion	66
2-6. References	71
2-7. Tables and Figures	75
CONCLUSION	88
LIST OF PUBLICATIONS	91
ACKNOWLEDGMENTS	94

General introduction

Identification and Characterization of Endothelins and Receptors

Endothelin is a 21-amino acid vasoconstrictor belonging to a new class of peptides. It was originally discovered in the supernatant of cultured bovine aortic endothelial cells, and subsequently isolated from cultured porcine aortic endothelial cells (11, 36). The primary sequence of human endothelin has been deduced from a human placental cDNA library and found to be identical to that of porcine endothelin, now referred to as endothelin-1 (ET-1) (13). Since the initial identification of ET-1, two other related peptides have been reported and designated endothelin-2 (ET-2) and endothelin-3 (ET-3), differing by 2 and 6 amino acid residues, respectively (Fig. G-1) (12, 28). All three forms appear to be distinct gene products (35). Two endothelin-related genes were identified by cloning and sequence analysis of the mouse genome (24). One encoded the peptide ET-1, while the other encoded a new peptide differing by three amino acid residues. The gene for this novel peptide is only expressed in the intestine and has been referred to as "vasoactive intestinal constrictor" (VIC) (24).

ET-1 is derived from a 203 amino acid peptide precursor known as preproendothelin, which is cleaved after translation by endopeptidases specific for the paired dibasic residues to form a 38 (human) or 39 (porcine) amino acid peptide, proendothelin or big ET (Fig. G-2) (33). The biological significance of differences in the amino acid sequence between the prepropeptides and the presence of an ET-like peptide within preproET are presently unclear. The identity of the dibasic endopeptidase is not currently known. Big ET is then converted to active ET by a putative endothelin converting enzyme (ECE, Fig. G-2) (36, 37). The physiological importance of cleavage of ET (1-39) is indicated by the reported 140-fold increase in vasoconstrictor activity upon cleavage to ET-1 (14).

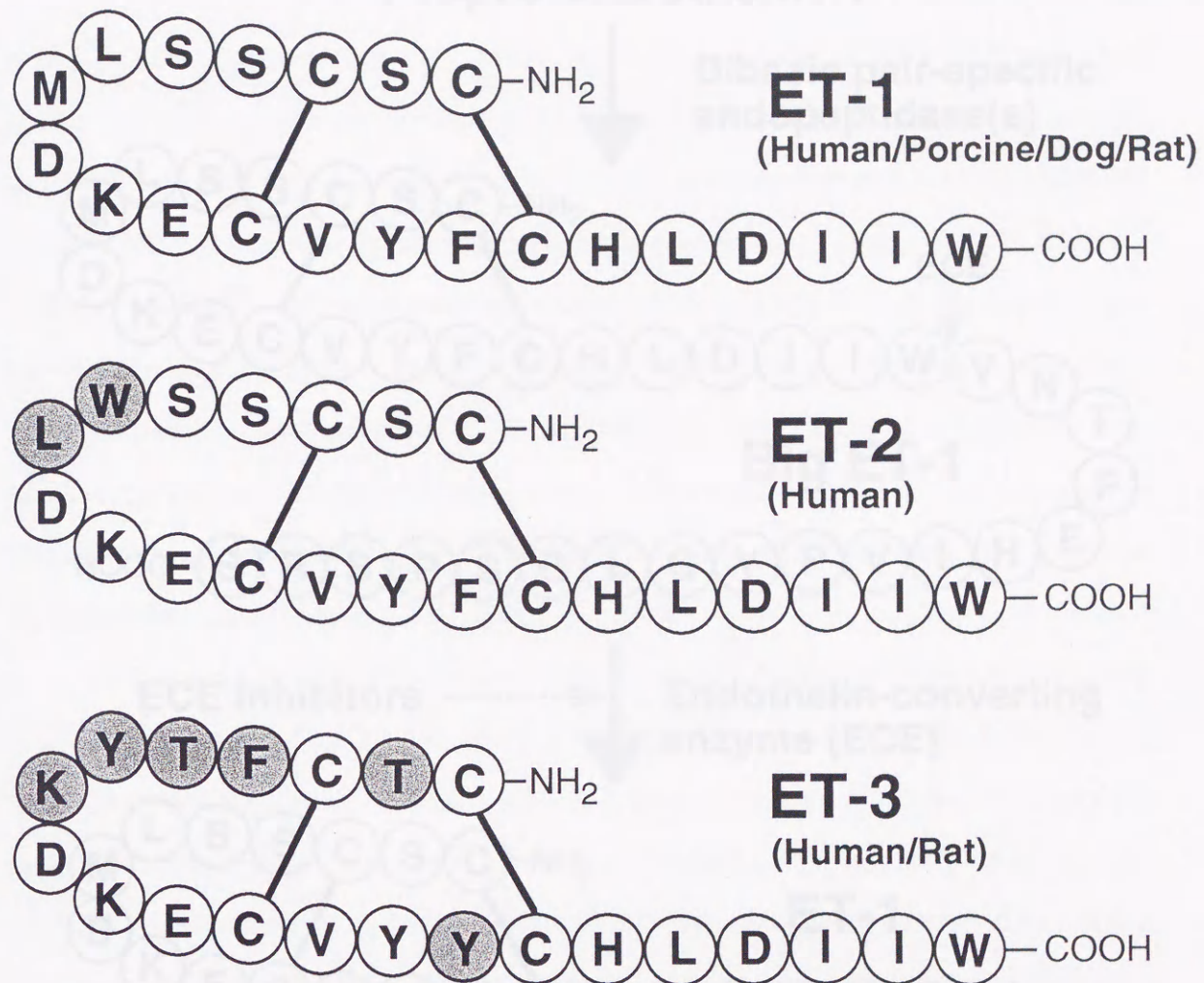


Fig. G-1. Amino acid sequences for endothelins. C-C lines indicate disulfide bonds.

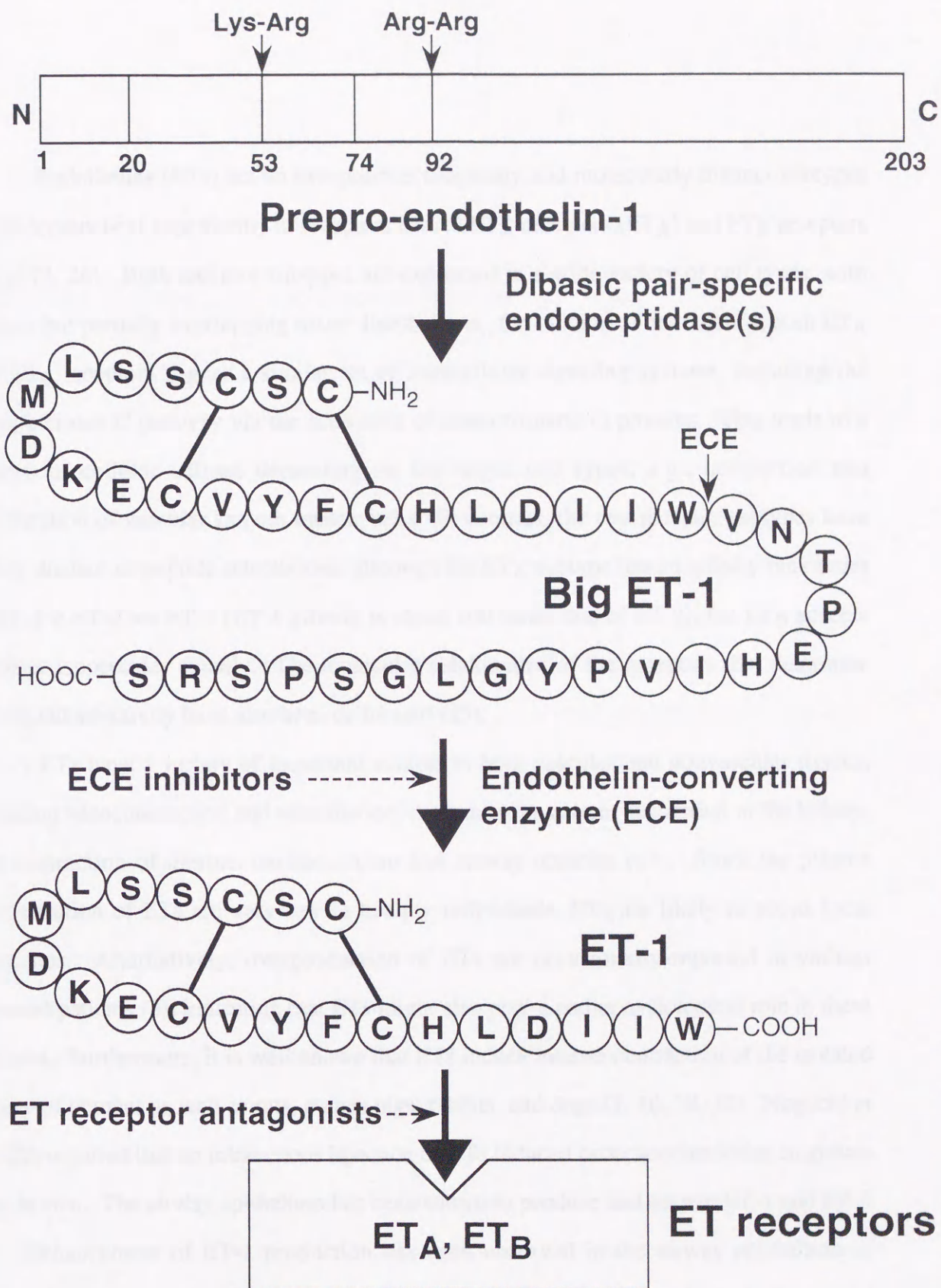


Fig. G-2. Endothelin-1 (ET-1) biosynthetic pathway and potential molecular targets for novel therapeutic agents.

Endothelins (ETs) act on two pharmacologically and molecularly distinct subtypes of the heptahelical superfamily of receptors named ET_A receptors (ET_A) and ET_B receptors (ET_B) (2, 26). Both receptor subtypes are expressed in a wide variety of cell types, with distinct but partially overlapping tissue distributions. On binding of endothelins, both ET_A and ET_B receptors trigger a similar set of intracellular signaling systems, including the phospholipase C pathway via the activation of heterotrimeric G proteins. This leads to a variety of cellular actions depending on the target cell types, e.g., contraction and proliferation of vascular smooth muscle cells. In contrast, the two receptor subtypes have highly distinct isopeptide selectivities: although the ET_A subtype has an affinity rank order of ET-1 ≥ ET-2 >> ET-3 (ET-1 affinity is about 100 times that of ET-3), the ET_B accepts all three isopeptides equally. The molecular subdomains of the receptors that determine this ligand selectivity have also been delineated (25).

ETs have a variety of important actions in both vascular and nonvascular tissues, including vasoconstriction and vasodilation, decrement in sodium absorption in the kidney, and contraction of uterine, cardiac, ileum and airway muscles (17). Since the plasma concentration of ETs are very low in healthy individuals, ETs are likely to act as local hormones. Alternatively, overproduction of ETs are occasionally reported in various diseased patients (8), indicating that ETs might also play a pathophysiological role in these diseases. Furthermore, it is well known that ETs induce intense contraction of the isolated airway of humans as well as rats, guinea pigs, rabbits, and dogs (1, 10, 18, 32). Noguchi *et al.* (20) reported that an intravenous injection of ETs induced bronchoconstriction in guinea pigs *in vivo*. The airway epithelium has been shown to produce and secrete ET-1 and ET-3 (3). Enhancement of ET-1 production has been observed in the airway epithelium of patients with asthma (30). ETs are, therefore, predicted to play an important pathophysiological role in the regulation of airway contraction. In guinea pigs, ET_B are thought to be responsible for the tracheal and bronchial contractions induced by ETs (5,

20). However, the identity of the subtypes of ET receptor, and the responses mediated by these receptors, require clarification in spite of their prime importance.

Activation of Contraction in Smooth Muscles

The rise in intracellular free Ca^{2+} is the principal mechanisms that initiated contraction in smooth muscles (6, 29). Ca^{2+} binds to calmodulin, and the association of the regulatory, calcium-calmodulin complex with the catalytic subunit of myosin light-chain kinase (MLCK) activates this enzyme to phosphorylate serine at position 19 on the regulatory light chain (MLC_{20}) of myosin (9). Phosphorylation of Ser 19 of MLC_{20} allows the myosin ATPase to be activated by actin and the muscle to contract (9, 31). On the other hand, it is now universally that two forms of excitation-contraction (E/C) coupling exist: electromechanical and pharmacomechanical. Electromechanical coupling, as the term suggests, depend on either electrical depolarization of the plasma membrane which opens Ca^{2+} channels leading to Ca^{2+} influx from the extracellular space, and hence an increase in intracellular concentration of free Ca^{2+} , or a voltage-dependent release of Ca^{2+} from intracellular stores such as the sarcoplasmic reticulum. In contrast, the pharmacomechanical coupling mechanism is voltage-independent. It may involve either extracellular Ca^{2+} influx via ligand-gated Ca^{2+} channels or release of activator Ca^{2+} from intracellular stores. The release mechanism is mediated either via ligand-generated intracellular second messenger or via a direct action of a ligand on the intracellular sarcoplasmic reticular stores. When the contractile agonist interacts with its cell surface receptor, the intracellular concentration of Ca^{2+} in airway smooth muscle cells rises abruptly from its resting level (< 200 nM) to between 500 - 1000 nM. These activator Ca^{2+} , so called because they initiate the contractile sequence, can only be derived from two sources: the extracellular compartment where they reside in abundance or from intracellular stores such as the sarcoplasmic reticulum. The relative contribution of activator Ca^{2+} from

these two sources is dependent on both the nature and concentration of the contractile agonist and component (phasic or tonic) of the contractile response being considered.

The resting membrane potential of airway smooth muscle cells lies somewhere between -45 and -60 mV. Under normal circumstances, most species (guinea pig and man being notable exceptions) do not exhibit spontaneous oscillations of the membrane potential (slow waves), i.e. the cells are electrically quiescent. A further characteristic feature is the cell membrane's remarkable propensity for outward electrical rectification consequent upon a depolarizing stimulus. This rectification behavior is thought to be due to largely to a voltage-dependent Ca^{2+} -insensitive delayed rectifier K^+ current (15). Additionally, G-protein-regulated (both G_s and G_i), Ca^{2+} -activated K^+ channels of either low (about 90 pS) or high (250-290 pS) conductance are abundant in the airway smooth muscle plasma membrane (16, 27). This rectification ability, in addition to limiting the magnitude of any depolarization, effectively prevents the membrane potential from attaining the threshold necessary for eliciting opening of voltage-dependent Ca^{2+} channels. Given that the cell membrane effectively and efficiently partitions the intracellular and extracellular environments, it is self-evident that activator Ca^{2+} originating in the extracellular compartment can only gain admission to the cell once the membrane has been rendered permeable to them. This is achieved via the opening of Ca^{2+} channels in the plasma membrane through which the Ca^{2+} flow down their electrochemical and concentration gradients. Two types of Ca^{2+} channels have been proposed: voltage-dependent (VDC) and receptor-operated (ROC) (4).

VDCs, as the term implies, possess a Ca^{2+} conductance that is directly proportional to the potential difference that exists across the plasma membrane. Thus membrane depolarization increases both the probability of VDC opening and the duration of the open channel time. Furthermore, VDCs display a susceptibility to blockade by Ca^{2+} -entry-blocking drugs, for example, verapamil and the dihydropyridines. As far as airway smooth muscle is concerned, there is ample convincing evidence that VDCs are present (22, 34).

Indeed, opening of such VDCs in response to the depolarizing action of substances such as KCl and tetraethylammonium is the principal mechanism that underlies entry of extracellular Ca^{2+} into the cells, so initiating contraction. In stark contrast, there is no evidence that supports the involvement of VDCs in the mechanisms underlying contraction of airway smooth muscle elicited by a range of physiologically relevant agonists, for example, cholinomimetics, histamine, eicosanoids, endothelin and the tachykinins substance P and neurokinin A (7, 23).

On the other hand, ROCs are ion channels opened, or operated, by a receptor for a stimulant substance. It is accepted that ROCs are not wholly selective for Ca^{2+} , have an ionic permeability determined by the controlling receptor, can be gated by either voltage-dependent or voltage-independent events and are not readily inhibited by organic Ca^{2+} antagonists such as the dihydropyridines. In airway smooth muscle, most pharmacological agonists elicit contraction that is associated with graded membrane depolarization (the magnitudes differ substantially between different agonists) but without action potential discharge. Furthermore, the same agonists can elicit contractions in fully depolarized airway preparations. Contractions produced by such agonists are resistant to the effects of Ca^{2+} -channel-blocking drugs, but, using the "lanthanum technique", it has not proved possible to detect extracellular Ca^{2+} influx in response to agonists (21). Notwithstanding, the results of a recent study (19), using Fura-2 fluorescence to measure intracellular Ca^{2+} concentrations in cultured human airway smooth muscle cells, provide new evidence concerning Ca^{2+} movements. The implications from this study are that intracellular activator Ca^{2+} ions are responsible for the initiation of contraction but that tonic or sustained phase of the contraction is associated with a low level of extracellular Ca^{2+} influx, via a mechanism that bears all the hallmarks of an ROC-mediated event. Although these findings clearly require substantiation, they may well signal for the first time not only the presence but also the active participation of ROCs in the E/C coupling process in airway smooth muscle. Unambiguous definition of such a role, through development of more

selective inhibitors of Ca^{2+} influx via these ROCs, may very well lead to the development of novel therapeutic agents for use in diseases such as asthma.

Summary

In the present study, to evaluate the contribution of ET_A and ET_B to the ET-induced contraction of guinea pig trachea, I firstly studied the existence of these receptors by binding assays with ^{125}I -ET-1 and ^{125}I -ET-3, and examined their distribution in guinea pig tracheal smooth muscle cells by monitoring intracellular calcium levels after stimulation with ETs. Furthermore, it was found that the two subtypes of ET receptor coexist in a major population of single tracheal smooth muscle cells in primary culture. These results indicate that ET_A and ET_B on individual smooth muscle cells cooperate in mediating ET-1-induced contractions of the guinea pig trachea (Chapter 1).

Secondarily, the intracellular signal transduction mechanism via ET receptors on tracheal smooth muscle contraction was investigated. I suggest that the ability of ET-1 to activate diverse sets of Ca^{2+} channels, by activating both ET_A and ET_B , may underlie the high potency of the peptide as a smooth muscle constrictor. The ET_A -selective activation of phosphatidylinositol (PI) cascade, which in turn leads to the activation of protein kinase C (PKC), potentiates the effect of ET-1. The combination of the non-selective ligand ET-1 and the two receptor subtypes coupled with distinct signaling pathways enables the full mobilization of the contractile apparatus. Thus, ET-1 is the first example of a single ligand which activates both pharmacomechanical and electromechanical pathways, via two receptor subtypes specialized to each E/C coupling pathway (Chapter 2).

References

1. **Advenier, C., B. Sarria, E. Naline, L. Puybasset, and V. Lagente.** Contractile activity of three endothelins (ET-1, ET-2 and ET-3) on the human isolated bronchus. *Br. J. Pharmacol.* 100: 168-172, 1990.
2. **Arai, H., S. Hori, I. Aramori, H. Ohkubo, and S. Nakanishi.** Cloning and expression of a cDNA encoding an endothelin receptor. *Nature.* 348: 730-732, 1990.
3. **Black, P. N., M. A. Ghatei, K. Takahashi, D. Bretherton-Watt, T. Krausz, C. T. Dollery, and S. R. Bloom.** Formation of endothelin by cultured airway epithelial cells. *FEBS Lett.* 255: 129-132, 1989.
4. **Bolton, T. B.** Mechanisms of action of transmitters and other substances on smooth muscle. *Physiol. Rev.* 59: 606-718, 1979.
5. **Cardell, L. O., R. Uddman, and L. Edvinsson.** A novel ET_A-receptor antagonist, FR139317, inhibits endothelin-induced contractions of guinea-pig pulmonary arteries, but not trachea. *Br. J. Pharmacol.* 108: 448-452, 1993.
6. **Filo, R. S., D. F. Bohr, and J. C. Ruegg.** Glycerinated skeletal and smooth muscle: calcium and magnesium dependence. *Science.* 147: 1581-1583, 1965.
7. **Giembycz, M. A., and I. W. Rodger.** Electrophysiological and other aspects of excitation-contraction coupling and uncoupling in mammalian airway smooth muscle. *Life Sci.* 41: 111-132, 1987.
8. **Gulati, A., and R. C. Strimal.** Endothelin mechanisms in the central nervous system: a target for drug development. *Drug Dev. Res.* 26: 361-387, 1992.
9. Hartshorne, D. J., *Biochemistry of the contractile process in smooth muscle.* 2nd edn ed. Physiology of the gastrointestinal tract., ed. L.R. Johnson. 1987, New York: Raven press. 423-482.

10. **Henry, P. J., P. J. Rigby, G. J. Self, J. M. Preuss, and R. G. Goldie.** Relationship between endothelin-1 binding site densities and constrictor activities in human and animal airway smooth muscle. *Br. J. Pharmacol.* 100: 786-792, 1990.
11. **Hickey, K. A., G. Rubanyi, R. J. Paul, and R. F. Highsmith.** Characterization of a coronary vasoconstrictor produced by endothelial cells in culture. *Am. J. Physiol.* 248: C550-C556, 1985.
12. **Inoue, A., M. Yanagisawa, S. Kimura, Y. Kasuya, T. Miyauchi, K. Goto, and T. Masaki.** The human endothelin family: three structurally and pharmacologically distinct isopeptides predicted by three separate genes. *Proc. Natl. Acad. Sci. USA.* 86: 2863-2867, 1989.
13. **Ito, Y., M. Yanagisawa, S. Ohkubo, C. Kimura, T. Kosaka, A. Inoue, N. Ishida, Y. Mitsui, H. Onda, M. Fujino, and T. Masaki.** Cloning and sequence of cDNA encoding the precursor of a human endothelium-derived vasoconstrictor peptide, endothelin: Identify of human and porcine endothelin. *FEBS Lett.* 231: 440-444, 1988.
14. **Kimura, S., Y. Kasuya, T. Sawamura, O. Shinimi, Y. Sugita, M. Yanagisawa, K. Goto, and T. Masaki.** Conversion of big endothelin-1 to 21-residue endothelin-1 is essential for expression of full vasoconstrictor activity: structure-activity relationships of big endothelin-1. *J. Cardiovasc. Pharmacol.* 13: S5-S7, 1989.
15. **Kotlikoff, M. I.** Potassium currents in canine airway smooth muscle cells. *Am. J. Physiol.* 259: L384-L395, 1990.
16. **Kume, H., and M. I. Kotlikoff.** Muscarinic inhibition of single KCa-channels in smooth muscle cells by a pertussis-sensitive G-protein. *Am. J. Physiol.* 261: C1204-C1209, 1991.
17. **Masaki, T., M. Yanagisawa, and K. Goto.** Physiology and pharmacology of endothelins. *Medical Research Reviews.* 12: 391-421, 1992.

18. **McKay, K. O., J. L. Black, and C. L. Armour.** Phosphoramidon potentiates the contractile response to endothelin-3, but not endothelin-1 in isolated airway tissue. *Br. J. Pharmacol.* 105: 929-932, 1992.
19. **Murray, R. K., and M. I. Kotlikoff.** Receptor-activated calcium influx in human airway smooth muscle cells. *J. Physiol.* 435: 123-144, 1991.
20. **Noguchi, K., Y. Noguchi, H. Hirose, M. Nishikibe, M. Ihara, K. Ishikawa, and M. Yano.** Role of endothelin ET_B receptors in bronchoconstrictor and vasoconstrictor responses in guinea-pig. *Eur. J. Pharmacol.* 233: 47-51, 1993.
21. **Raeburn, D., and I. W. Rodger.** Lack of effect of leukotriene D₄ on Ca-uptake in airway smooth muscle. *Br. J. Pharmacol.* 83: 499-504, 1984.
22. **Rodger, I. W.** Calcium channels. *Am. Rev. Resp. Dis.* 136: S15-S17, 1987.
23. Rodger, I. W., and N. J. Pyne, *Airway smooth muscle*. 2nd edn ed. Asthma: Basic Mechanisms and Clinical Management, ed. P.J. Barnes, I.W. Rodger, and N.C. Thomson. 1992, London: Academic Press. 59-84.
24. **Saida, K., Y. Mitsui, and N. Ishida.** A novel peptide, vasoactive intestinal contractor, of a new (endothelin) peptide family. Molecular cloning, expression, and biological activity. *J. Biol. Chem.* 264: 14623-14616, 1989.
25. **Sakamoto, A., M. Yanagisawa, T. Sawamura, T. Enoki, T. Ohtani, T. Sakurai, K. Nakao, T. Toyo-oka, and T. Masaki.** Distinct subdomains of human endothelin receptors determine their selectivity to ET_A-selective antagonist and ET_B-selective agonists. *J. Biol. Chem.* 268: 8547-8553, 1993.
26. **Sakurai, T., M. Yanagisawa, Y. Takuwa, H. Miyazaki, S. Kimura, K. Goto, and T. Masaki.** Cloning of cDNA encoding a non-isopeptide-selective subtype of the endothelin receptor. *Nature.* 348: 732-735, 1990.
27. **Saunders, H.-M. H., and J. M. Farley.** Spontaneous transient outward currents and Ca²⁺-activated K⁺ channels in swine tracheal smooth muscle cells. *J. Pharmacol. Exp. Ther.* 257: 1114-1120, 1991.

28. **Shinmi, O., S. Kimura, T. Sawamura, Y. Sugita, T. Yoshizawa, Y. Uchiyama, M. Yanagisawa, K. Goto, T. Masaki, and I. Kanazawa.** Endothelin-3 is a novel neuropeptide: isolation and sequence determination of endothelin-1 and endothelin-3 in porcine brain. *Biochem. Biophys. Res. Commun.* 164: 587-593, 1989.
29. **Somlyo, A. P., and B. Himpens.** Cell calcium and its regulation in smooth muscle. *FASEB J.* 3: 2266-2276, 1989.
30. **Springall, D. R., P. H. Howarth, H. Counihan, R. Djukanovic, S. T. Holgate, and J. M. Polak.** Endothelin immunoreactivity of airway epithelium in asthmatic patients. *The Lancet.* 337: 697-701, 1991.
31. **Sweeney, H. L., Z. Yang, G. Zhi, J. T. Stull, and K. M. Trybus.** Charge replacement near the phosphorylatable serine of the myosin regulatory light chain mimics aspects of phosphorylation. *Proc. Natl. Acad. Sci. USA.* 91: 1490-1494, 1994.
32. **Tschirhart, E. J., J. W. Drijfhout, J. T. Pelton, R. C. Miller, and C. R. Jones.** Endothelin: functional and autoradiographic studies in guinea pig trachea. *J. Pharmacol. Exp. Ther.* 258: , 1991.
33. **Watanabe, T., Y. Itoh, K. Ogi, C. Kimura, N. Suzuki, and H. Onda.** Synthesis of human endothelin-1 precursors in *Escherichia coli*. *FEBS Lett.* 251: 257-260, 1989.
34. **Worley, J. F., and M. I. Kotlikoff.** Dihydropyridine-sensitive single calcium channels in airway smooth muscle cells. *Am. J. Physiol.* 259: L468-L480, 1990.
35. **Yanagisawa, M., A. Inoue, T. Ishikawa, Y. Kasuya, S. Kimura, S. Kumegaye, K. Nakajima, T. Watanabe, S. Sakakibara, K. Goto, and T. Masaki.** Primary structure, synthesis, and biological activity of rat endothelin, an endothelium-derived vasoconstrictor peptide. *Proc. Natl. Acad. Sci. USA.* 85: 6964-6967, 1988.
36. **Yanagisawa, M., H. Kurihara, S. Kimura, Y. Tomobe, M. Kobayashi, Y. Mitsui, Y. Yazaki, K. Goto, and T. Masaki.** A novel potent vasoconstrictor peptide produced by vascular endothelial cells. *Nature.* 332: 411-415, 1988.

37. **Yanagisawa, M., and T. Masaki.** Molecular biology and biochemistry of the endothelins. *Trends Pharmacol. Sci.* 10: 374-378, 1989.

CHAPTER 1

*ET_A and ET_B receptors on single smooth muscle cells cooperate in mediating guinea pig tracheal constriction**

CHAPTER 1

*ET_A and ET_B receptors on single smooth muscle cells cooperate in mediating guinea pig tracheal contraction**

In Chapter 1, an identification of ET_A and ET_B receptors in single smooth muscle cells and their contribution to endothelin-induced contraction of guinea pig trachea were investigated. ET_A and ET_B receptors were detected in smooth muscle membranes autoradiographically in primary cultured cells. ET_A and ET_B showed concentration-dependent increases in intracellular Ca²⁺ concentration and contractile force. The half-maximally effective concentrations of ET-1 and ET-3 at various concentrations were 1.9 and 2.7 nM, respectively. The Ca²⁺ responses showed biphasic nature in both cells stimulated with ET-1, but only in ET-3 after stimulation with ET-3. Competitive applications of ET-3 and ET-1 (10 nM each) abolished only the ET_A-dominant (~95%) response to only ET-3, ET_B showed (~25%) depending to only ET-3 and ET_A and ET_B-possessing (~55%) cells depending on cells. The ET_A antagonist, 10 μM BQ123, abolished ET-1-induced contractions but did not affect the ET-3-induced contractions. The results indicate that both receptors occur in a single population of smooth muscle cells and cooperate in mediating ET-1-induced contractility.

Introduction

Endothelin (ET) now denoted as ET-1, was initially identified as a potent vasoconstrictor peptide in culture medium conditioned by vascular endothelial cells (1). It is one of a family of three heptapeptides (ET-1, ET-2 and ET-3) collectively termed ETs (2). ETs have a variety of biological actions in both vascular and non-vascular tissues including vasoconstriction and proliferation, decrement in sodium absorption in the kidney, and contraction of smooth muscle, heart, bronchial and airway muscles (3). Since the plasma

Abstract

In Chapter 1, the distribution of ET_A and ET_B receptors in single smooth muscle cells and their contribution to endothelin (ET)-induced contractions of guinea pig trachea were investigated. ET_A and ET_B receptors were detected in smooth muscle membranes (maximum binding capacities of 810 and 360 fmol/mg protein and dissociation constants of 38 and 5.1 pM for ^{125}I -ET-1 and ^{125}I -ET-3, respectively) and visualized autoradiographically in primary cultured cells. ET-1 and ET-3 evoked concentration-dependent increases in intracellular Ca^{2+} concentration and smooth muscle tension. The half-maximally effective concentrations of ET-1 and ET-3 at inducing contractions were 1.9 and 2.7 nM, respectively. The Ca^{2+} responses showed tachyphylaxis to both ETs after stimulation with ET-1, but only to ET-3 after stimulation with ET-3. Consecutive applications of ET-3 and ET-1 (10 nM each) classified the cells into ET_A -dominant (~30%) responding to only ET-1, ET_B -dominant (~20%) responding to only ET-3, and ET_A - and ET_B -possessing (~50%) cells responding to both. The ET_A antagonist, 10 μ M BQ-123, attenuated ET-1-induced contractions but did not affect the ET-3-induced contractions. The results indicate that both receptors coexist in a major population of smooth muscle cells and cooperate in mediating ET-1-induced contractions.

Introduction

Endothelin (ET), now denoted as ET-1, was initially identified as a potent vasoconstrictor peptide in culture medium conditioned by vascular endothelial cells (33). It is one of a family of three isopeptides (ET-1, ET-2 and ET-3) collectively termed ETs (17). ETs have a variety of important actions in both vascular and non-vascular tissues, including vasoconstriction and vasodilation, decrement in sodium absorption in the kidney, and contraction of uterine, cardiac, ileum and airway muscles (19). Since the plasma

concentration of ETs are very low in healthy individuals, ETs are likely to act as local hormones. On the other hand, overproduction of ETs are occasionally reported in various diseased patients (9), indicating that ETs might also play a pathophysiological role in these diseases. The functions of ETs are mediated by at least two distinct subtypes of receptors, ET_A receptors (ET_A) and ET_B receptors (ET_B). Cloning and expression studies of cDNAs for each subtype of ET receptors revealed that ET_A have much greater selectivity for ET-1 and ET-2 than ET-3 (2) while ET_B show almost equal affinities for the three isopeptides (29). The distinct distribution of ET_A and ET_B has been demonstrated in various tissues and cells (22).

It is well known that ETs induce intense contraction of the isolated airway of humans as well as rats, guinea pigs, rabbits, and dogs (1, 14, 20, 32). Noguchi *et al.* (25) reported that an intravenous injection of ETs induced bronchoconstriction in guinea pigs *in vivo*. The airway epithelium has been shown to produce and secrete ET-1 and ET-3 (5). Enhancement of ET-1 production has been observed in the airway epithelium of patients with asthma (31). ETs are, therefore, predicted to play an important pathophysiological role in the regulation of airway contraction. In guinea pigs, ET_B are thought to be responsible for the tracheal and bronchial contractions induced by ETs (7, 25). However, the identity of the subtypes of ET receptor, and the responses mediated by these receptors, require clarification in spite of their prime importance.

In this chapter, to evaluate the contribution of ET_A and ET_B to the ET-induced contraction of guinea pig trachea, I studied the existence of these receptors by binding assays with ¹²⁵I-ET-1 and ¹²⁵I-ET-3, and examined their distribution in guinea pig tracheal smooth muscle cells by monitoring intracellular calcium levels after stimulation with ETs. Then, it was found that the two subtypes of ET receptor coexist in a major population of single tracheal smooth muscle cells in primary culture. The results indicate that ET_A and ET_B on individual smooth muscle cells cooperate in mediating ET-1-induced contractions of the guinea pig trachea.

Materials and Methods

Materials. ET-1 and ET-3 were obtained from the Peptide Institute Inc. (Osaka, Japan), fura-2-acetoxymethyl ester was from Dojin (Kumamoto, Japan) and BQ-123 (16) was from Peninsula Laboratories Inc. (Belmont, CA). ^{125}I -ET-1 (74 TBq/mmol) and ^{125}I -ET-3 (74 TBq/mmol) were purchased from Amersham International (Bucks, U.K.). All other chemicals were of analytical grade.

Animals. Male Hartley guinea pigs weighing 350-500 g were used in this study. The animals were housed in a temperature- ($25 \pm 2^\circ\text{C}$) and moisture- (50%) controlled room with a 12-hr light/dark cycle (light on at 6:00 A.M. and off at 6:00 P.M.). They were given standard guinea pig chow (CLEA Japan, Inc., Osaka, Japan) and tap water *ad libitum*.

Membrane Preparation. The tracheal smooth muscles (220 mg wet weight) from 10 animals were homogenized using a Polytron homogenizer (Kinematica, Lucern, Switzerland) three times at top speed for 30 s each in 9 volumes of ice-cold 0.25 M sucrose solution containing 20 mM tris(hydroxymethyl)aminomethane-HCl (pH 7.4), 0.2 mM phenylmethylsulfonyl fluoride, 1 μM leupeptin, 1 μM pepstatin, 0.1 mM EDTA and 0.5 mM EGTA. After centrifugation of the homogenates at 1,000 x g for 10 min at 4°C , the supernatants were centrifuged again at 20,000 x g for 20 min. The resulting pellets were washed three times as described above and used as membrane sources. The membranes were stocked in aliquots at -80°C until use.

Cell Preparation. The trachea was removed and immediately placed in oxygenated (95% O_2 , 5% CO_2) Hank's balanced saline solution (mM): NaCl 138, KCl 5.4, CaCl_2 0.2, MgCl_2 0.8, KH_2PO_4 0.4, Na_2HPO_4 0.3, NaHCO_3 4.2, N-2-hydroxyethylpiperazine-N'-2-ethanesulfonic acid (HEPES, pH 7.4) 10, D-glucose 20, Na-pyruvate 0.1, containing penicillin-G 5000 units/ml and streptomycin 5 mg/ml. Following careful removal of the adherent fat and connective tissue, the cartilaginous portion of the trachea was cut open

along its longitudinal axis, and the epithelium was removed by gently rubbing the luminal surface. The membranous portion of the trachea was cut into two pieces (2 cm x 1 mm), each of which was incubated in 5 ml of the Hank's solution containing 200 units/ml collagenase (Worthington type I), 0.5 units/ml elastase (Biozyme type E2) and 100 units/ml DNase (Sigma) with mild shaking (120 strokes/min) for 60 min at 37°C. After removal of the loosened connective tissues, the pieces were minced to a size of approximately 2 x 1 mm and incubated for a further 120 min. The partially digested tissues were centrifuged at 1,000 x g for 5 min after adding an equal volume of Dulbecco's modified Eagle's medium (DMEM) containing 10% fetal bovine serum, penicillin-G 50 units/ml, streptomycin 50 µg/ml and L-glutamine 0.5 mM. The pellet was unraveled by gently sucking in and out 5-10 times in DMEM using a syringe, changing the needle from 18 to 19 and then 20 gauge in sequence. The suspension was then centrifuged for 5 min at 1,000 x g. The final pellet was suspended at a density of 7×10^4 cells/ml in DMEM. The suspended cells were cultured for up to 8 days in a humidified atmosphere of 5% CO₂ and 95% O₂ at 37°C. The smooth muscle cells were identified by immunofluorescent staining with rabbit anti-(actin) antibody (Biomedical Technologies, Inc., Stoughton, MA, U.S.A.), anti-(myosin) antibody (Transformation Research, Inc., Framingham, MA, U.S.A.) and fluorescein isothiocyanate-labeled anti-(rabbit IgG) antibody (Biosys S.A., Compiègne, France).

Binding Assays. The membranes (~4 µg protein) were incubated at 37°C for 1 h with 10 pM ¹²⁵I-ET-1 and ¹²⁵I-ET-3, for competitive binding studies, in the presence or absence of various amounts of unlabeled ligands in a total volume of 0.5 ml of 20 mM HEPES-buffered salt solution (pH 7.4) (HBSS) containing 140 mM NaCl, 4 mM KCl, 1 mM K₂HPO₄, 1 mM MgCl₂, 1 mM CaCl₂, 10 mM D-glucose, and 0.1% bovine serum albumin. The specific saturable binding was investigated by adding increasing concentrations of ¹²⁵I-ETs to the membranes. After incubation, unbound ¹²⁵I-ETs were separated by centrifugation at 20,000 x g for 20 min at 4°C followed by aspiration of the supernatant. The radioactivity in the membrane pellet was measured in an autogamma

counter. Nonspecific binding was defined as the membrane-associated radioactivity in the presence of a saturating concentration (100 nM) of unlabeled ET-1 or ET-3. Nonspecific binding was subtracted from the total binding and the difference was defined as specific binding. Total binding was always <10% of the total radioactivity added. Protein was determined with a BCA protein assay reagent (Pierce).

Binding assays were also performed on the cultured cells. The cells were cultured for 7 to 8 days on 12-well plates to semi-confluency (1.2×10^5 cells/well). After washing with HBSS, the cells were incubated with various concentrations of ^{125}I -ET-1 or ^{125}I -ET-3 in HBSS at 37°C for 1 h. The reaction was stopped by aspiration of the reaction buffer, then the cells were washed twice with ice-cold HBSS and solubilized in 1N NaOH. The cell-associated radioactivity was measured in a gamma counter.

Light Microscopic Autoradiography. The cells, cultured in slide-glass wells for 5 to 6 days, were fixed with 2% paraformaldehyde in 0.1 M sodium phosphate (pH 7.5) for 10 min at 4°C. After incubation at room temperature for 10 min in HBSS, the cells were incubated at 37°C for 1 h with 30 pM ^{125}I -ET-1 or ^{125}I -ET-3. This was defined as the total binding. Nonspecific binding was determined in parallel assays by incubation in the presence of 100 nM unlabeled ET-1 or ET-3. After incubation, the cells were rinsed twice in HBSS. After dehydration in 50% ethanol for 15 min, the slides were air-dried, dipped into Konica NR-M2 emulsion and stored in the dark. After exposure for 14 to 21 days, the slides were developed with Konidol X for 6 min at 20°C and then observed under a light microscope.

Monitoring of Intracellular Ca^{2+} Levels. The cells, cultured on quartz slide-glass for 5 to 6 days, were washed three times in a serum-free DMEM and incubated with 5 μM fura-2-acetoxymethyl ester at 37°C for 1.5 h in a CO_2 incubator. After washing three times in HBSS, the fura-2-loaded cells were transferred to a temperature-controlled (37°C) chamber on the microscope stage of a Ca^{2+} analyzer (FES-300, SCHOLAR-TEC CORP.,

Osaka, Japan) developed in the laboratories of Ciba-Geigy. The fura-2-loaded cells were excited alternately with light wavelengths of 340 and 380 nm provided by a grating monochromator. The emitted fluorescence was passed through the objective lens (Nikon Fluor x40) to a dichroic mirror (> 400 nm), separated into two pathways by a half mirror and each signal was passed through band-pass filters (510 nm). The two fluorescence signals at 510 nm were simultaneously passed to a photomultiplier tube (Hamamatsu Photonics) and an intensified CCD camera (Model XC-77, SONY). The signal was recorded at a normal video rate (33.3 msec). The ratio of the video signals at 340 nm and 380 nm was obtained from 5 successive video frames. The first frame of each sequence of 5 comprised the signal at 340 nm, the second frame was blank, the third frame comprised the signal at 380 nm and the remaining two frames were also left blank. Frames were left blank for recognition of each signal during computer analysis. The fluorescence signal from the photomultiplier tube was synchronized to the video rate. Therefore, successive ratio values were obtained at 167 msec intervals.

The intracellular calcium levels were monitored by the ratio of the fluorescence emitted after excitation at 340 nm and 380 nm. The intracellular calcium concentrations were tentatively estimated ($[Ca^{2+}]_i$) from a standard curve obtained using HEPES-buffered solutions (pH 7.4) containing 147 mM KCl, 1 mM $MgCl_2$, 2 mM EGTA, 1 μ M fura-2 (free acid form) with various concentrations of added $CaCl_2$. The free calcium concentrations of these solutions were calculated with a BASIC program using the stability constants of Ca^{2+} , Mg^{2+} and H^+ for EGTA (18) and taking into consideration the purity of EGTA and the activity of H^+ (27).

Contraction Assays. The trachea was removed quickly and placed in oxygenated (95% O_2 , 5% CO_2) Krebs-Henseleit solution of the following composition (mM): NaCl 113.0, KCl 4.8, $CaCl_2$ 2.5, KH_2PO_4 1.2, $MgSO_4$ 1.2, $NaHCO_3$ 25.0 and glucose 5.5, pH 7.4 at 37°C. After adherent fat and connective tissue had been carefully removed, the

trachea was cut into rings of approximately 2 mm width. The epithelium was removed by gently turning the rings on the shaft of a pair of watchmaker's forceps. The two rings were tied together carefully and placed into a 30 ml water-jacketed organ bath (Ugobasile, Comerio-Varese, Italy) containing the oxygenated Krebs-Henseleit solution at 37°C. The preparations were equilibrated for at least 1 h under an initial tension of 1 g with washing every 15 min with the Krebs-Henseleit solution. Responses were measured isometrically with a force-displacement transducer (Nihon Kohden TB-612T, Tokyo, Japan). After the equilibration period, each preparation was first stimulated with 60 mM KCl and the resultant contraction was used as a reference standard for the responses to ET-1, ET-3 and histamine. The tissues were washed 3 times every 15 min before the application of agonists. Thereafter, concentration-response curves for ET-1, ET-3 and histamine were made by their cumulative addition in logarithmic increments to the organ bath after reaching a plateau. BQ-123 (10 µM) was added 20 min prior to addition of ETs. At the end of the concentration-response measurements, 60 mM KCl was added again to check the contractile response of the tissues. Agonist-induced responses were expressed as percentages of the response to 60 mM KCl.

Statistical and Data Analyses. Independent data are expressed as mean ± s.e.m. and statistical significance was assessed by Student's *t* test. *P* < 0.05 was considered to be significant.

Comparison of cumulative concentration-dependent curves for contraction was performed by nonlinear regression analysis (21) based on a logistic equation (28),

$$T = T_{\max} C^{Hn} / (EC_{50}^{Hn} + C^{Hn}),$$

where *T* is the increased tension; *C*, the concentration of ET; *T*_{max}, the maximum tension achieved; and *Hn*, the slope factor or Hill coefficient. The fitted curves were compared using Dunnett's Multi-Range test. *P* < 0.05 was considered to be significant.

The concentration-inhibition curves and saturation-binding curves were analyzed by the least squares using the curve-fitting program, LIGAND (23).

Results

Binding Sites of ET_A and ET_B in Tracheal Smooth Muscle Membranes. Specific binding sites for ¹²⁵I-ET-1 and ¹²⁵I-ET-3 were detected in the membranes of tracheal smooth muscles from guinea pigs (Fig. 1-1). The apparent dissociation constant (K_d) and maximum binding capacities (B_{max}) estimated from the competitive binding studies are summarized in Table 1-1. The binding of 10 pM ¹²⁵I-ET-3 was inhibited by either unlabeled ET-1 or ET-3 with similar affinities, giving almost identical monophasic inhibition curves with K_d s for ET-1 and ET-3 of 6.2 pM and 8.3 pM, respectively (Fig. 1-1A). These results demonstrated the presence of ET_B in the tracheal smooth muscle. The ET_A antagonist, BQ-123, also showed a monophasic inhibition curve. However, the affinity of BQ-123 to ET_B was approximately 20,000-fold lower than that of either ET-1 or ET-3, as judged by its K_d (150 nM).

On the other hand, the binding of 10 pM ¹²⁵I-ET-1, a ligand common for both ET_A and ET_B, was inhibited in a biphasic manner by unlabeled ET-3 and BQ-123 (Fig. 1-1B). The binding of ¹²⁵I-ET-1 was displaced with the same affinity by either ET-1 or ET-3 in the range from 1 to 30 pM, indicating that ET_B was responsible for binding. One hundred- to one thousand-fold higher concentrations of ET-3 were necessary to obtain the same degree of inhibition of the remaining ¹²⁵I-ET-1 binding as that achieved by 30 pM to 1 μM ET-1, showing that ET_A was responsible for binding. The K_d of the high affinity site for ET-3 (ET_B) was 1.0 pM whereas the K_d for the low affinity site (ET_A) was 28 nM (Table 1-1B). The high affinity receptors (ET_B) represented 40% of the specific binding sites. The biphasic curve of inhibition by BQ-123 comprised a high affinity phase for ET_A from 1 to 100 nM and a low affinity phase for ET_B from 100 nM to 100 μM (Fig. 1-1B). The estimated K_d of the high affinity site for BQ-123 (ET_A) was 4.4 nM and the K_d for the low affinity site (ET_B) was 460 nM (Table 1-1B). The low affinity receptors (ET_B) represented 45% of the specific binding sites.

Since 1 nM ET-3 almost completely inhibited the binding of 10 pM ^{125}I -ET-3 to ET_B (Fig. 1-1A), I used 1 nM unlabeled ET-3 to mask the binding sites of ET_B for 10 pM ^{125}I -ET-1. In the presence of 1 nM ET-3, the binding of 10 pM ^{125}I -ET-1 was inhibited monophasically by unlabeled ETs and BQ-123 (Fig. 1-1C). The estimated K_d for unlabeled ET-1, ET-3 and BQ-123 to ET_A were 31 pM, 15 nM and 1.2 nM, respectively (Table 1-1C).

Analysis of the saturable binding of ^{125}I -ET-1 in the presence of 1 nM unlabeled ET-3 indicated a single class of binding sites for ET_A with a K_d of 38 pM and a B_max of 810 fmol/mg protein (Fig. 1-2A). The binding of ^{125}I -ET-3 to ET_B also showed a single class of binding sites, with a K_d of 5.1 pM and a B_max of 360 fmol/mg protein (Fig. 1-2B).

ET_A and ET_B in Primary Cultures of Tracheal Smooth Muscle Cells. ET_A and ET_B were also found on semi-confluent primary cultured tracheal smooth muscle cells. Analysis of the saturable binding of ^{125}I -ET-1 in the presence of 1 nM unlabeled ET-3 indicated a single class of binding sites for ET_A with a K_d of 51 pM and a B_max of 4.3 fmol/ 10^5 cells (Fig. 1-2C). The binding of ^{125}I -ET-3 to ET_B also showed a single class of binding sites, with a K_d of 18 pM and a B_max of 0.38 fmol/ 10^5 cells (Fig. 1-2D).

The ET_A and ET_B in low-densities of cultured cells were examined by autoradiography after incubation with 30 pM ^{125}I -ET-1 or ^{125}I -ET-3 in the presence or absence of various unlabeled ligands (Fig. 1-3). After incubation with 30 pM ^{125}I -ET-1, a ligand common for both ET_A and ET_B , almost all of the smooth muscle cells were intensely labeled (Fig. 1-3A). On the other hand, when 30 pM ^{125}I -ET-3 was used to label ET_B , the intensity decreased to approximately half of that observed with ^{125}I -ET-1 (Fig. 1-3B). When the ET_B binding sites were masked by the addition of 1 nM unlabeled ET-3 (Fig. 1-3C), the intensity of labeling with 30 pM ^{125}I -ET-1 decreased by approximately one half. Similarly, when the ET_A binding sites were masked by the addition of 10 μM BQ-123, the labeling intensity with 30 pM ^{125}I -ET-1 also decreased by one half (data not shown).

Labeling with both ^{125}I -ETs disappeared completely after incubation in the presence of an excess concentration (100 nM) of unlabeled ET-1 (Fig. 1-3D).

Increases in $[\text{Ca}^{2+}]_i$ Mediated by ET_A and ET_B in Fura-2-loaded Primary Cultured Cells. The increases in intracellular calcium level induced by ETs were investigated using low-densities of cultured cells. When the intracellular calcium level was monitored microscopically in a group of about 10 smooth muscle cells loaded with fura-2, ET-1 and ET-3 induced biphasic increases in the fluorescence ratio with transient and sustained phases, in a concentration-dependent manner. Typical time courses of the changes in the fluorescence ratio induced by 10 nM ET-1 and ET-3 are shown in Figure 1-4A. After addition of 10 nM ET-1 and ET-3, the estimated intracellular calcium concentration ($[\text{Ca}^{2+}]_i$) increased rapidly and transiently from the basal level of 130 ± 11 nM ($n = 20$) to a peak of 310 ± 15 nM for ET-1 ($n = 10$) and 230 ± 23 nM for ET-3 ($n = 10$) within 30 s. The $[\text{Ca}^{2+}]_i$ decreased gradually to 150 ± 14 nM ($n = 20$) within 3 min after stimulation by either ET-1 or ET-3, and maintained this level for more than 10 min. After chelation of extracellular Ca^{2+} by addition of 1.2 mM EGTA 30 s before the application of ETs, the transient increase in $[\text{Ca}^{2+}]_i$ remained unchanged but the sustained phase disappeared (data not shown), indicating that the transient increase in $[\text{Ca}^{2+}]_i$ was due to the release of Ca^{2+} from intracellular stores and the sustained phase to the influx of extracellular Ca^{2+} .

The concentration-dependencies of the peak $[\text{Ca}^{2+}]_i$ responses elicited by ET-1, ET-3 and histamine are shown in Figure 1-4B. Concentration-dependent increases in $[\text{Ca}^{2+}]_i$ were observed from 100 pM ET-1 and 300 pM ET-3 up to 300 nM of either peptide. Histamine (1 to 100 μM) also induced biphasic increases in $[\text{Ca}^{2+}]_i$. The ET-1-, ET-3- and histamine-induced increases in $[\text{Ca}^{2+}]_i$ were not maximal at the highest concentrations which were used.

When either 10 nM ET-1 or ET-3 was repeatedly applied to the smooth muscle cells at intervals of about 3 min, transient increases in $[\text{Ca}^{2+}]_i$ were observed only after the first stimulation, and not after subsequent applications (Fig. 1-5, A and B). The subsequent

addition of 10 nM ET-3 after the prior application of 10 nM ET-1 also did not elicit a second $[Ca^{2+}]_i$ transient increase (Fig. 1-5C). However, the application of 10 nM ET-1 after prior application of 10 nM ET-3 resulted in a second transient increase in $[Ca^{2+}]_i$ (Fig. 1-5D) with a peak of 180 ± 25 nM ($n = 8$), which was lower than the peaks obtained after prior stimulation with ET-1 (310 ± 15 nM; Fig. 1-5, A and C) or ET-3 (230 ± 23 nM; Fig. 1-5, B and D). These results indicated that ET-1 caused tachyphylaxis of both ET-1- and ET-3-induced $[Ca^{2+}]_i$ responses, while ET-3 caused tachyphylaxis of the ET-3-induced responses alone. When the ET_A -mediated response was blocked by incubation of the smooth muscle cells with 10 μ M BQ-123, the prior stimulation with 10 nM ET-3 induced a transient and a sustained increase in $[Ca^{2+}]_i$ but subsequent stimulation with 10 nM ET-1 had no effect on $[Ca^{2+}]_i$ (Fig. 1-5E). These results, taken together, indicated that the prior application of 10 nM ET-3 stimulated ET_B but not ET_A which was stimulated by the subsequent application of 10 nM ET-1, resulting in the second transient $[Ca^{2+}]_i$ increase. The data also suggested that prior stimulation of ET_B did not result in tachyphylaxis of the ET_A -mediated $[Ca^{2+}]_i$ increase. In all cases, stimulation with 100 μ M histamine at the end of the experiment resulted in a transient increase in $[Ca^{2+}]_i$ (Figs. 1-5 and -6), although the peak value (200 - 250 nM) was smaller than that induced by a single application of 100 μ M histamine (500 nM) (Fig. 1-4). Tachyphylaxis was, therefore, not considered to be due to exhaustion of intracellular Ca^{2+} stores.

Distribution of ET_A and ET_B in Single Tracheal Smooth Muscle Cells by Monitoring $[Ca^{2+}]_i$ Changes after Stimulation with ETs. As described above, prior stimulation of ET_B with 10 nM ET-3 resulted in tachyphylaxis of the ET_B -mediated transient $[Ca^{2+}]_i$ increase after further stimulation with ET-3 but not the response after stimulation of ET_A with 10 nM ET-1. Using this protocol, the cellular distribution of ET_A and ET_B was investigated by image analysis of the Ca^{2+} responses in a total of 100 individual single cells. For this purpose, video images of isolated cells were analyzed to avoid recording the changes in $[Ca^{2+}]_i$ caused by cell-to-cell communications. The Ca^{2+} responses were classified into

three distinct patterns, typical examples of which are shown in Figure 1-6, A-E. In 28 cells, which were considered to possess only ET_A, the prior application of ET-3 had no effect on [Ca²⁺]_i while the subsequent application of ET-1 evoked a transient increase in [Ca²⁺]_i (300 ± 35 nM at the peak) (Fig. 1-6A). By contrast, only the prior application of ET-3, but not the subsequent application of ET-1, evoked a Ca²⁺ response (290 ± 43 nM at a peak) in 17 cells (Fig. 1-6B). The cells showing this type of response were regarded as possessing ET_B alone. On the other hand, 50 cells showed transient Ca²⁺ increases after stimulation with both ET-3 and ET-1, with various ratios in the peak values evoked by the two isopeptides being observed (Fig. 1-6, C-E). These cells were considered to possess both ET_A and ET_B. Five of the 100 cells investigated showed no response to either peptide, indicating that a minor population of smooth muscle cells does not possess ET receptor. In all cases, stimulation with 100 μM histamine at the end of the experiment resulted in a transient increase in [Ca²⁺]_i.

Spatial Distribution of Ca²⁺ Levels of Single Smooth Muscle Cells after Stimulation with ETs. The spatial distribution of cytosolic Ca²⁺ levels was investigated by digital image analysis of the single cells. Figure 1-7 shows a typical series of pseudo-color images representing the spatial distribution of [Ca²⁺]_i in a single smooth muscle cell which possessed both ET_A and ET_B receptors, after consecutive stimulations with 10 nM ET-3 and ET-1. As observed in Fig. 1-7, B and D, which correspond to the images at the peaks of the increase in [Ca²⁺]_i (Fig. 1-6E), the [Ca²⁺]_i were heterogeneous within the cytoplasmic area of the single cell (from 100 nM to 500 nM). The regions of high [Ca²⁺]_i (400 to 500 nM) were seen to be clustered. Such spatial heterogeneity of the [Ca²⁺]_i signal was observed in all cells which I monitored at the peak of the transient [Ca²⁺]_i increase. These results are in good agreement with the fact that the transient [Ca²⁺]_i increases were due to the release of Ca²⁺ from the intracellular stores, probably the endoplasmic reticulum.

Tracheal Contraction Induced by ET-1 and ET-3. ET-1 and ET-3 caused long-lasting contraction of isolated guinea pig tracheal rings. Figure 1-8A shows typical time courses of the tracheal contraction induced by 100 nM ET-1 or ET-3. The contraction commenced immediately upon the addition of ETs and took 12 to 15 min to reach a plateau which for ET-1 and ET-3 respectively, corresponded to 80% and 66% of 60 mM KCl-induced contraction, and 88% and 73% of 100 μ M histamine-induced contraction. The responses to ETs were long-lasting (>20 min) and slow to washout, not reaching basal levels within 30 min. This can be compared with the rapid recovery from contraction induced by high K⁺ (60 mM) or histamine (100 μ M) with half times of 3.2 and 5.0 min, respectively.

Contractions were observed at 130 pM ET-1 and 430 pM ET-3, and muscle tension increased in a concentration-dependent manner (Fig. 1-8B). The contractile responses to 140 nM ET-1 or ET-3 were maximal. The data were fitted by a logistic equation and the parameters are compared in Table 1-2. The maximal contraction (T_{\max}) induced by ET-1 (79.6% of the KCl-induced contraction) was ~1.2 times stronger ($P < 0.025$) than that by ET-3 and ~90% of that induced by histamine. The estimated EC_{50} values were 1.94 ± 0.20 nM for ET-1 and 2.74 ± 0.33 nM for ET-3 (Table 1-2), being respectively 390- and 280-fold lower than that of histamine (760 ± 40 nM).

The ET_A antagonist, 10 μ M BQ-123, shifted the EC_{50} of the concentration-response curve for ET-1 to approximately 4-fold higher concentrations ($P < 0.025$) and reduced the T_{\max} to ~90% of the control value ($P < 0.05$). The T_{\max} for ET-3 both in the presence or absence of BQ-123 were also significantly different from the T_{\max} for ET-1 ($P < 0.025$). On the other hand, 10 μ M BQ-123 did not affect the contraction induced by 30 pM to 140 nM ET-3 but inhibited slightly the contraction by 440 nM ET-3 (Fig. 1-8B). These results indicated that the ET-3-induced contraction is mediated almost entirely by ET_B .

Hill plots were made of the concentration-dependency of the contractions. The Hill coefficients (H_n) estimated by non-linear least squares ($H_n \pm$ fitting error) were, $1.07 \pm$

0.06 for ET-1 in the presence of BQ-123, 1.09 ± 0.04 for ET-3 in the presence of BQ-123, and 1.01 ± 0.02 for ET-3 in the absence of BQ-123, indicating that there is no cooperativity in the ET_B-mediated contraction. On the other hand, the ET-1-induced contraction showed a biphasic relationship, with Hn of 1.66 ± 0.09 at low concentrations (30 pM-1.4 nM) and 0.60 ± 0.07 at high concentrations (1.4 nM-140 nM) (Fig. 1-8C). The value of 1 was not incorporated within the fitting error of the estimated Hn for ET-1 at the 95% confidence level. In the presence of BQ-123, Hn were 1.22 ± 0.10 at low concentrations and 0.96 ± 0.05 at high concentrations and could not be distinguished from 1 at the 95% confidence level. These results suggest that ET_A and ET_B cooperate positively in mediating the tracheal contraction induced by low concentrations of ET-1 and cooperate negatively at high concentrations of ET-1.

Discussion

In this chapter, I demonstrated by binding studies with ^{125}I -ET-1 and ^{125}I -ET-3 that guinea pig tracheal smooth muscle contains both ET_A and ET_B (Figs. 1-1 and -2). The receptors were visualized autoradiographically in primary cultured tracheal smooth muscle cells (Fig. 1-3). However, the distribution of these receptors at the level of single cells could not be identified by these methods. Therefore, the distribution of ET_A and ET_B in the cultured individual cells by monitoring of $[\text{Ca}^{2+}]_i$ after the stimulation with ETs (Figs. 1-4, -5, -6 and -7) was investigated. Based on the homologous desensitization of the transient increase in $[\text{Ca}^{2+}]_i$ after the stimulation of each subtype of receptor, it was found that both ET_A and ET_B coexist in a major population (~50%) of single tracheal smooth muscle cells. Furthermore, both ET_A and ET_B were shown to cooperate in mediating the potent and sustained contraction of tracheal rings induced by ET-1 (Fig. 1-8).

The coexistence of ET_A and ET_B at the tissue level has been demonstrated by binding assays with various radioligands, mRNA analyses and functional analyses in airways (12), lung (8) and various other organs (15, 22). No information has, however, been available about the cellular coexistence of ET_A and ET_B . Receptor subtypes for other classes of neurotransmitters and hormones are reportedly co-localized in several tissues and cell suspensions: β -1 and β -2 adrenergic receptors in human heart (13), A_1 - and A_2 -adenosine receptors in guinea pig ventricular cardiomyocytes (4), the inhibitory dopamine D-1 and excitatory D-2 receptors in cat caudate nucleus neurons (26), and histamine H_1 and H_2 receptors in rabbit papillary muscles (10). However, no report has referred to the coexistence of any receptor subtypes on single cells. To the best of my knowledge, this is the first report demonstrating the functional coexistence of receptor subtypes on single cells.

The proportion of ET_B decreases with increasing days in culture. The ratio of ET_B to ET_A was between 0.5 and 1 in the membrane preparations and ~1 in the cells after up to

6 days in culture, as judged by autoradiographic studies and Ca^{2+} -monitoring. However, the ratio was decreased in the semi-confluent cells after 7 to 8 days in culture ($B_{\text{max}}\text{ET}_B/B_{\text{max}}\text{ET}_A = 0.1$, Fig. 1-2), although the K_d values were not affected. Repetitive sub-culture of the cells resulted in the complete disappearance of ET_B binding sites and Ca^{2+} -responses to 10 nM ET-3 (data not shown).

ET_A and ET_B are known to couple to G-proteins and mediate increases in phosphatidylinositol hydrolysis and $[\text{Ca}^{2+}]_i$ in a wide variety of tissues and cells (3, 8). ET_A and ET_B in tracheal smooth muscle cells are also considered to activate the same signal transduction pathways as in other tissues and cells. The tracheal smooth muscle cells showed biphasic increases in $[\text{Ca}^{2+}]_i$ after stimulation with ETs (Fig. 1-4), i.e., transient peaks followed by sustained elevations above basal levels, similar to other types of ET-receptor-possessing cells. The transient increase of $[\text{Ca}^{2+}]_i$ is considered to be due to the release of Ca^{2+} from intracellular stores, and the sustained increase due to the influx of extracellular Ca^{2+} because although chelation of extracellular Ca^{2+} by the addition of EGTA did not affect the transient increase, the sustained increase was diminished.

The transient increase in $[\text{Ca}^{2+}]_i$ showed homologous desensitization after stimulation of ET_A and ET_B (Fig. 1-5). The tachyphylaxis is mainly due to the fact that the ET binding sites were occupied by the ligands, because ETs of a high concentration (10 nM) were used and were not washed out between applications. However, other factors such as rapid negative feedback via signal transduction pathways may, at least in part, be involved in the process of tachyphylaxis. For example, similar rapid desensitization to arginine vasopressin has been reported in vascular smooth muscle cells by measuring the $[\text{Ca}^{2+}]_i$ increase and intracellular pH changes (6). In this case, the activation of protein kinase C was demonstrated to be involved in the desensitization of those responses to arginine vasopressin.

Tachyphylaxis was not observed in the tracheal contraction assays with ETs. Sequential, twin additions of 10 nM ET-1 or ET-3 resulted in the same degree of

contraction as after a single addition of 20 nM ET-1 or ET-3 (data not shown). These results may suggest that the release of Ca^{2+} from the intracellular store sites contributes only weakly to the induction of contraction, although both the release from Ca^{2+} stores and the Ca^{2+} influx are believed to be involved in the ET-induced tracheal contraction (11, 24, 30).

As shown in Figs. 1-4B and 1-8B, when both ET_A and ET_B were simultaneously stimulated with ET-1, the EC_{50} s for the contraction (1.9 nM) was lower than the value for the stimulation of ET_B alone with ET-3 (2.7 nM). Furthermore, the threshold concentrations of ET-1 inducing contraction (~ 130 pM) and increases in $[\text{Ca}^{2+}]_i$ (~ 100 pM) were lower than those of ET-3 (~ 430 pM and 300 pM, respectively). However, ET-1 bound to ET_A with an affinity (K_d , 30-50 pM) lower than that with which ET-3 bound to ET_B (K_d , 1-20 pM). These results suggest that the responses mediated by ET_A and ET_B were enhanced in the case of the stimulation with ET-1 at low concentrations. On the other hand, the maximum contraction after the simultaneous stimulation of both ET_A and ET_B with ET-1 was only ~ 1.2 -fold higher than the maximum responses after the stimulation of ET_B alone with ET-3, although the B_{max} value of ET_A in the tracheal smooth muscle membranes (260-810 fmol/mg protein) was roughly equal to or 2-fold higher than the value of ET_B (250-440 fmol/mg protein). Thus, the responses mediated by both ET_A and ET_B stimulated by high concentrations of ET-1 can not be explained by a simple sum of the responses mediated independently by each of the receptors. The uppermost limits of these responses are not considered to be due to the limitation of capacities for the contraction, because the maximum contraction induced by ETs was obviously lower than that induced by histamine. ET_A and ET_B are thought to induce the $[\text{Ca}^{2+}]_i$ response with similar efficacy, because the peak values of transient $[\text{Ca}^{2+}]_i$ increase induced by the prior application of 10 nM ET-1 or ET-3 were almost identical in single smooth muscle cells containing ET_A alone, ET_B alone or both ET_A and ET_B (Fig. 1-6). Therefore, ET_A and ET_B are considered to cooperate in mediating the ET-1-induced contraction and $[\text{Ca}^{2+}]_i$

responses, positively after stimulation with low concentrations and negatively with high concentrations. The Hill coefficients given by the contraction data also support the possibility of such cooperativity (Fig. 1-8C).

Analysis of the specific saturable binding of ^{125}I -ET-1 to ET_A in the presence of 1 nM unlabeled ET-3 (Fig. 1-2A) indicated a single class of binding sites, and the Hill plot of the specific binding also showed a linear relationship with a slope of 1.1. Moreover, the pseudo-Hill plots of the displacement curve with ET-1, which is a receptor subtype non-selective agonist, on the binding of ^{125}I -ET-3 to ET_B in the tracheal membranes (Fig. 1-1A) showed a linear relationship with a slope of 0.98. These results suggest that there was no cooperativity between ET_A and ET_B in binding of ET-1. Therefore, the positive and negative cooperativities in the contraction and the $[\text{Ca}^{2+}]_i$ response induced by ET-1 are thought to occur at steps distal to receptor binding and prior to the increase in $[\text{Ca}^{2+}]_i$ in the smooth muscle cells. Although the precise mechanism remains to be elucidated, the cooperativity is predicted to be due to the fact that the two receptor subtypes coexist in a major population of the tracheal smooth muscle cells and stimulate common signal transduction pathways in the same cells. Similar cooperation may occur in other ET-1-induced actions mediated by both ET_A and ET_B in other tissues which contained both subtypes of the receptors.

Text Footnotes

*Part of this work was presented at the International Symposium "Smooth Muscle", Fukuoka, Japan, Jan. 29-Feb. 1, 1992.

References

1. **Advenier, C., B. Sarria, E. Naline, L. Puybasset, and V. Lagente.** Contractile activity of three endothelins (ET-1, ET-2 and ET-3) on the human isolated bronchus. *Br. J. Pharmacol.* 100: 168-172, 1990.
2. **Arai, H., S. Hori, I. Aramori, H. Ohkubo, and S. Nakanishi.** Cloning and expression of a cDNA encoding an endothelin receptor. *Nature.* 348: 730-732, 1990.
3. **Aramori, I., and S. Nakanishi.** Coupling of two endothelin receptor subtypes to differing signal transduction in transfected Chinese hamster ovary cells. *J. Biol. Chem.* 267: 12468-12474, 1992.
4. **Behnke, N., W. Müller, J. Neumann, W. Schmitz, H. Scholz, and B. Stein.** Differential antagonism by 1, 3-dipropylxanthine-8-cyclopentylxanthine and 9-chloro-2-(2-furanyl)-5, 6-dihydro-1, 2, 4-triazolo (1, 5-c) quinazolin-5-imine of the effects of adenosine derivatives in the presence of isoprenaline on contractile response and cyclic AMP content in cardiomyocytes. Evidence for the coexistence of A₁- and A₂-adenosine receptors on cardiomyocytes. *J. Pharmacol. Exp. Ther.* 254: 1017-1023, 1990.
5. **Black, P. N., M. A. Ghatei, K. Takahashi, D. Bretherton-Watt, T. Krausz, C. T. Dollery, and S. R. Bloom.** Formation of endothelin by cultured airway epithelial cells. *FEBS Lett.* 255: 129-132, 1989.
6. **Caramelo, C., P. Tsai, K. Okada, V. A. Briner, and R. W. Schrier.** Mechanisms of rapid desensitization to arginine vasopressin in vascular smooth muscle cells. *Am. J. Physiol.* 260: F46-F52, 1991.
7. **Cardell, L. O., R. Uddman, and L. Edvinsson.** A novel ET_A-receptor antagonist, FR139317, inhibits endothelin-induced contractions of guinea-pig pulmonary arteries, but not trachea. *Br. J. Pharmacol.* 108: 448-452, 1993.

8. **Cioffi, C. L., R. F. N. Jr, R. H. Jackson, and M. A. Sills.** Characterization of rat lung endothelin receptor subtypes which are coupled to phosphoinositide hydrolysis. *J. Pharmacol. Exp. Ther.* 262: 611-618, 1992.
9. **Gulati, A., and R. C. Strimal.** Endothelin mechanisms in the central nervous system: a target for drug development. *Drug Dev. Res.* 26: 361-387, 1992.
10. **Hattori, Y., H. Nakaya, M. Endou, and M. Kanno.** Inotropic, electrophysiological and biochemical responses to histamine in rabbit papillary muscles: evidence for coexistence of H₁- and H₂-receptors. *J. Pharmacol. Exp. Ther.* 253: 250-256, 1989.
11. **Hay, D. W. P.** Mechanism of endothelin-induced contraction in guinea-pig trachea: comparison with rat aorta. *Br. J. Pharmacol.* 100: 383-392, 1990.
12. **Hay, D. W. P., P. J. Henry, and R. G. Goldie.** Endothelin and the respiratory system. *Trends Pharmacol. Sci.* 14: 29-32, 1993.
13. **Hedberg, A., F. K. Jr, M. E. Josephson, and P. B. Molinoff.** Coexistence of beta-1 and beta-2 adrenergic receptors in the human heart: effects of treatment with receptor antagonists or calcium entry blockers. *J. Pharmacol. Exp. Ther.* 234: 561-568, 1985.
14. **Henry, P. J., P. J. Rigby, G. J. Self, J. M. Preuss, and R. G. Goldie.** Relationship between endothelin-1 binding site densities and constrictor activities in human and animal airway smooth muscle. *Br. J. Pharmacol.* 100: 786-792, 1990.
15. **Hori, S., Y. Komatsu, R. Shigemoto, N. Mizuno, and S. Nakanishi.** Distinct tissue distribution and cellular localization of two messenger ribonucleic acids encoding different subtypes of rat endothelin receptors. *Endocrinology.* 130: 1885-1895, 1992.
16. **Ihara, M., K. Noguchi, T. Saeki, T. Fukuroda, S. Tsuchida, S. Kimura, T. Fukami, K. Ishikawa, M. Nishikibe, and M. Yano.** Biological profiles of highly potent novel endothelin antagonists selective for the ET_A receptor. *Life Sci.* 50: 247-255, 1991.
17. **Inoue, A., M. Yanagisawa, S. Kimura, Y. Kasuya, T. Miyauchi, K. Goto, and T. Masaki.** The human endothelin family: three structurally and pharmacologically distinct

- isopeptides predicted by three separate genes. *Proc. Natl. Acad. Sci. USA.* 86: 2863-2867, 1989.
18. Martell, A. E., and R. M. Smith, *Amino Acids*. Vol. 1. 1974, New York: Plenum Press.
19. **Masaki, T., M. Yanagisawa, and K. Goto.** Physiology and pharmacology of endothelins. *Medical Research Reviews.* 12: 391-421, 1992.
20. **McKay, K. O., J. L. Black, and C. L. Armour.** Phosphoramidon potentiates the contractile response to endothelin-3, but not endothelin-1 in isolated airway tissue. *Br. J. Pharmacol.* 105: 929-932, 1992.
21. **Meddings, J. B., R. B. Scott, and G. H. Fick.** Analysis and comparison of sigmoidal curves: application to dose-response data. *Am. J. Physiol.* 257: G982-G989, 1989.
22. **Miller, R. C., J. T. Pelton, and J. P. Huggins.** Endothelins - from receptors to medicine. *Trends Pharmacol. Sci.* 14: 54-60, 1993.
23. **Munson, P. J., and D. Rodbard.** LIGAND: a versatile computerized approach for characterization of ligand-binding systems. *Anal. Biochem.* 107: 220-239, 1980.
24. **Ninomiya, H., Y. Uchida, M. Saotome, A. Nomura, H. Ohse, H. Matsumoto, F. Hirata, and S. Hasegawa.** Endothelins constrict guinea pig tracheas by multiple mechanisms. *J. Pharmacol. Exp. Ther.* 262: 570-576, 1992.
25. **Noguchi, K., Y. Noguchi, H. Hirose, M. Nishikibe, M. Ihara, K. Ishikawa, and M. Yano.** Role of endothelin ET_B receptors in bronchoconstrictor and vasoconstrictor responses in guinea-pig. *Eur. J. Pharmacol.* 233: 47-51, 1993.
26. **Ohno, Y., M. Sada, and S. Takaori.** Coexistence of inhibitory dopamine D-1 and excitatory D-2 receptors on the same caudate nucleus neurons. *Life Sci.* 40: 1937-1945, 1987.
27. Oiki, S., and Y. Okada, *Ca-EGTA buffers in physiological solutions*. *Seitai-no-kagaku*, Vol. 38. 1987, . 79-83.

28. **Randall, M. D., S. A. Douglas, and C. R. Hiley.** Vascular activities of endothelin-1 and some alanyl substituted analogues in resistance beds of the rat. *Br. J. Pharmacol.* 98: 685-699, 1989.
29. **Sakurai, T., M. Yanagisawa, Y. Takuwa, H. Miyazaki, S. Kimura, K. Goto, and T. Masaki.** Cloning of cDNA encoding a non-isopeptide-selective subtype of the endothelin receptor. *Nature.* 348: 732-735, 1990.
30. **Sarria, B., E. Naline, E. Morcillo, J. Cortijo, J. Esplugues, and C. Advenier.** Calcium dependence of the contraction produced by endothelin (ET-1) in isolated guinea-pig trachea. *Eur. J. Pharmacol.* 187: 445-453, 1990.
31. **Springall, D. R., P. H. Howarth, H. Counihan, R. Djukanovic, S. T. Holgate, and J. M. Polak.** Endothelin immunoreactivity of airway epithelium in asthmatic patients. *The Lancet.* 337: 697-701, 1991.
32. **Tschirhart, E. J., J. W. Drijfhout, J. T. Pelton, R. C. Miller, and C. R. Jones.** Endothelin: functional and autoradiographic studies in guinea pig trachea. *J. Pharmacol. Exp. Ther.* 258: , 1991.
33. **Yanagisawa, M., H. Kurihara, S. Kimura, Y. Tomobe, M. Kobayashi, Y. Mitsui, Y. Yazaki, K. Goto, and T. Masaki.** A novel potent vasoconstrictor peptide produced by vascular endothelial cells. *Nature.* 332: 411-415, 1988.

TABLE 1-1. Apparent dissociation constants and maximum binding capacities of ET_A and ET_B in tracheal smooth muscle membranes.

ligand	ET _A		ET _B	
	K _d	B _{max}	K _d	B _{max}
(A) ¹²⁵ I-ET-3	ET-1		8.3	260
	ET-3		6.2	250
	BQ-123		150 000	360
(B) ¹²⁵ I-ET-1	ET-1	N.D.*	N.D.*	N.D.*
	ET-3	28 000	670	1.0
	BQ-123	4 400	360	460 000
(C) ¹²⁵ I-ET-1 + 1 nM ET-3	ET-1	31	260	
	ET-3	15 000	300	
	BQ-123	1 200	260	

K_ds (pM) and B_{max}s (fmol/mg protein) were estimated from the corresponding data in Fig. 1-1 using the program, LIGAND (23).

(A) & (C) were fitted by a single-site model and (B) was fitted by a two-site model.

*N.D., not determined because the data could not be fitted by a two-site model.

TABLE 1-2. Statistical comparison of concentration-response curves of contraction

Data Set	T _{max} (% of 60 mM KCl)	EC ₅₀ (nM)
ET-1	79.6 ± 1.53	1.94 ± 0.20
ET-3	67.4 ± 1.58 †	2.74 ± 0.33 ‡
BQ-123 + ET-1	73.9 ± 1.94 *	7.32 ± 0.87 †
BQ-123 + ET-3	64.2 ± 1.65 † ‡	3.60 ± 0.46 † ‡

Values are the estimated parameters ± the fitting error.

* P < 0.05 compared with the data obtained with ET-1 alone

† P < 0.025 compared with the data obtained with ET-1 alone

‡ P < 0.025 compared with the data obtained with ET-1 in the presence of BQ-123

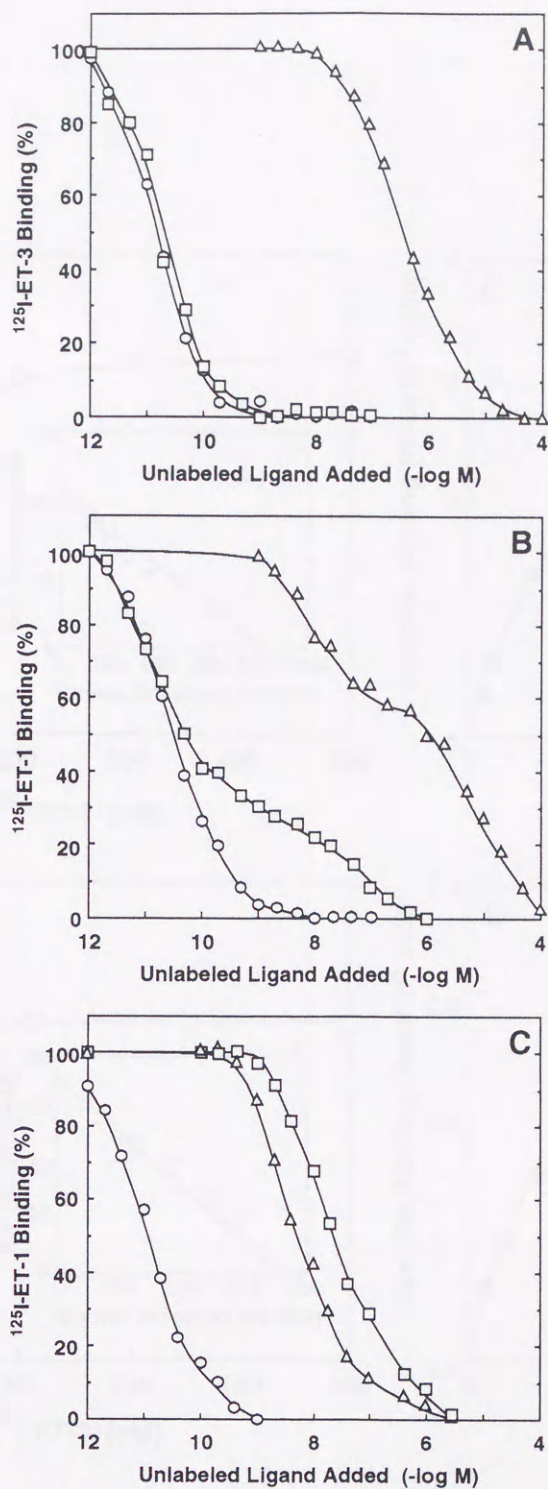


Fig. 1-1. Concentration-dependent inhibition of binding of 10 pM ^{125}I -ET-3 (A), 10 pM ^{125}I -ET-1 (B), 10 pM ^{125}I -ET-1 in the presence of unlabeled 1 nM ET-3 (C) to guinea pig tracheal smooth muscle membranes by unlabeled ET-1 (○), unlabeled ET-3 (□) and BQ-123 (△). The binding at each concentration of unlabeled peptide is expressed as a percentage of the specific binding with the radioligand alone (23 fmol/mg protein for A, 100 fmol/mg protein for B, and 50 fmol/mg protein for C). Values are the means of triplicate determinations.

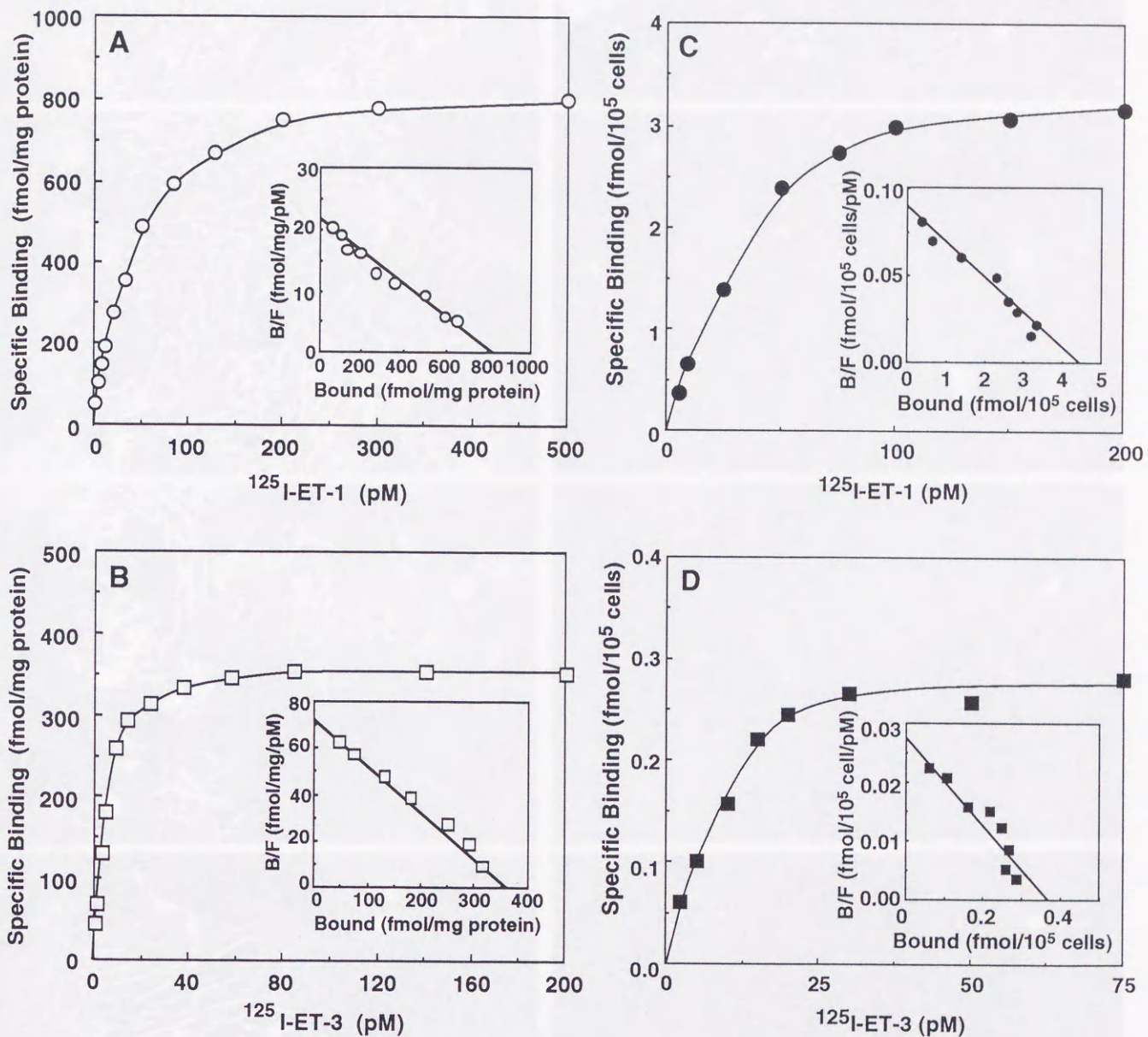


Fig. 1-2. The saturable binding of $^{125}\text{I-ET-1}$ in the presence of 1 nM unlabeled ET-3 (○, ●) and $^{125}\text{I-ET-3}$ (□, ■) to guinea pig tracheal smooth muscle (A, B) and primary cultured cells (C, D). Scatchard plots of the specific binding are shown in insets. Values are the means of triplicate determinations.

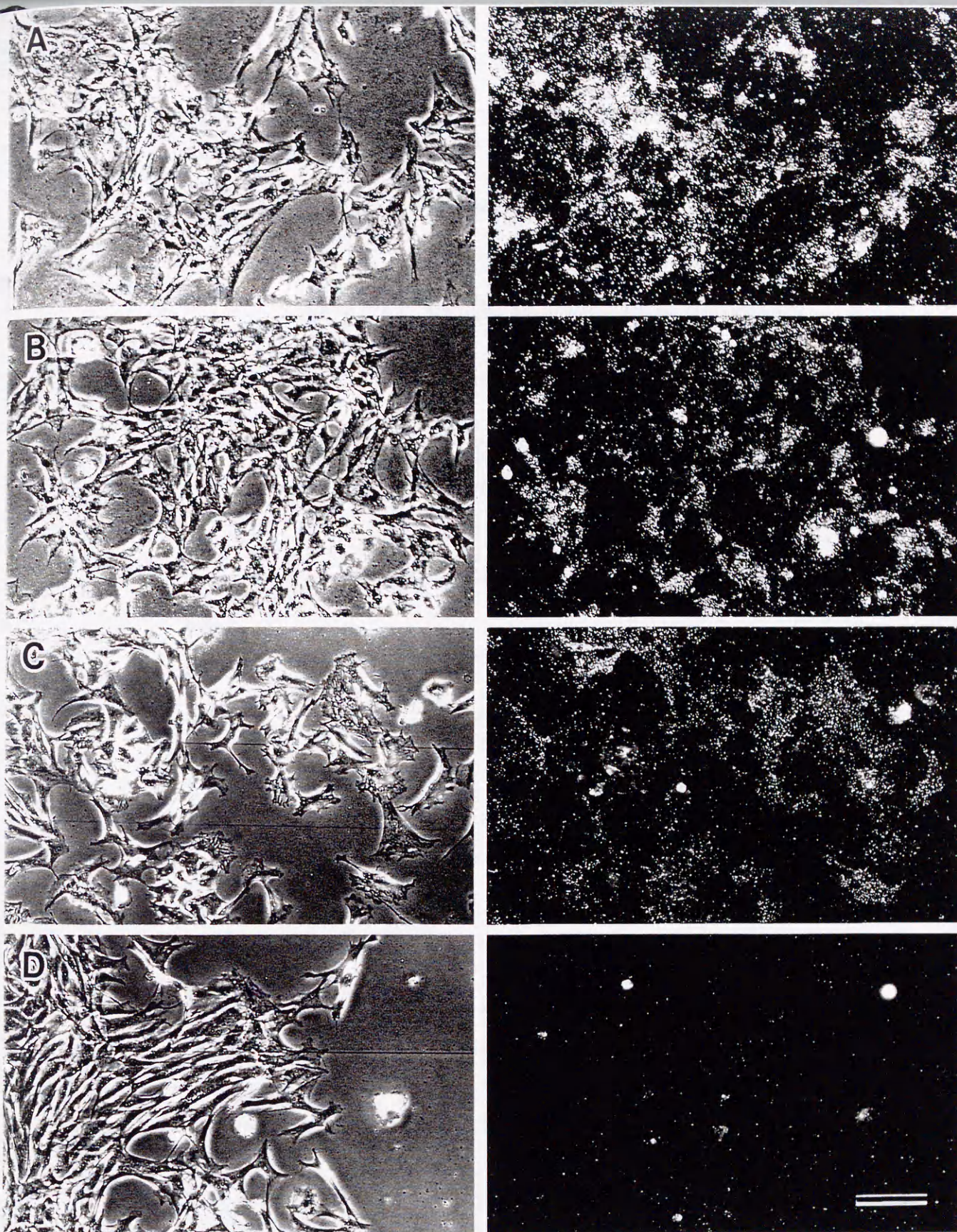


Fig. 1-3. Autoradiographic localization of binding sites for 30 pM ^{125}I -ET-1 (A), 30 pM ^{125}I -ET-3 (B), 30 pM ^{125}I -ET-1 in the presence of unlabeled 1 nM ET-3 (C), and 30 pM ^{125}I -ET-1 in the presence of unlabeled 100 nM ET-1 (as a nonspecific binding) (D) on the smooth muscle cells in primary culture. Photographs of the labeled cells under light (each left) and dark (each right) field illuminations are shown. Silver grains representing the binding sites were visualized as bright spots in a dark field. Bar, 100 μm .

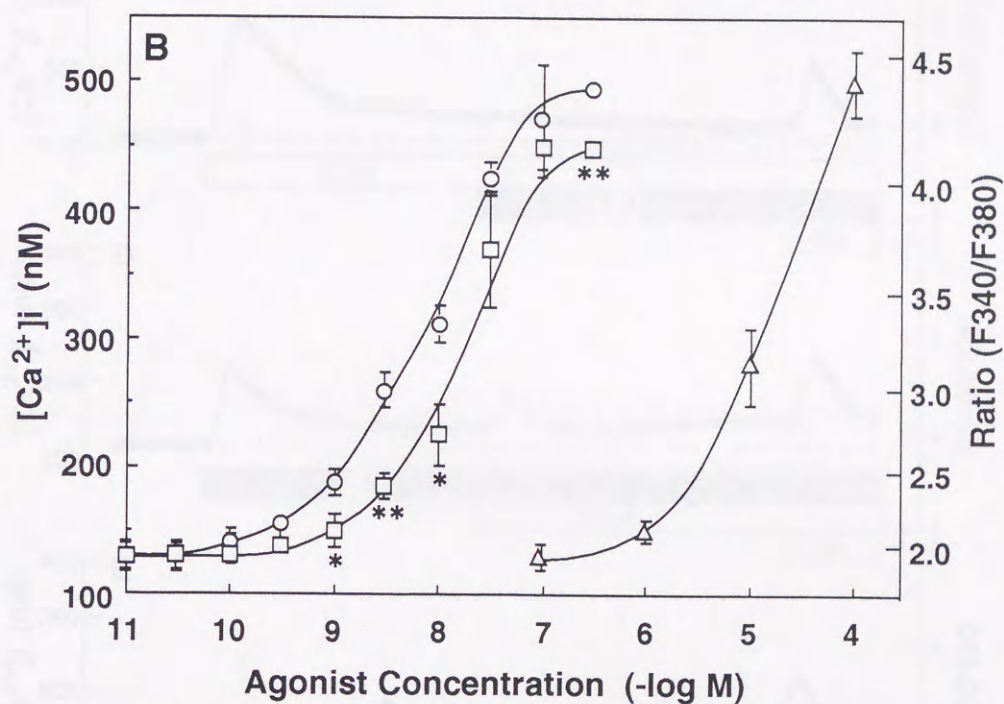
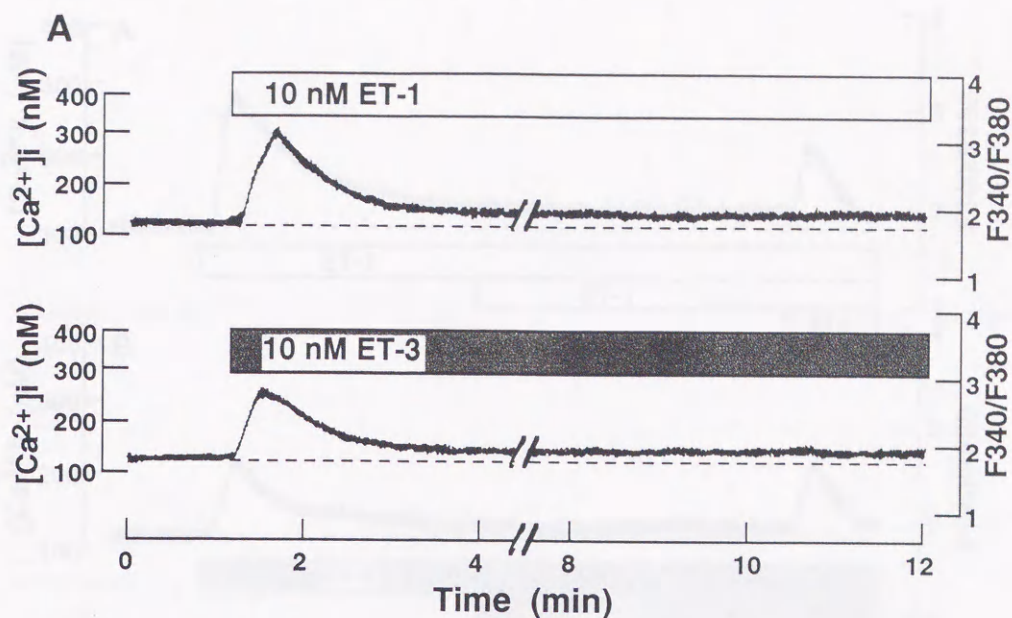


Fig. 1-4. A: Typical time courses of changes in $[Ca^{2+}]_i$ induced by 10 nM ET-1 and ET-3. B: The concentration dependencies of transient increases in $[Ca^{2+}]_i$ induced by ET-1 (\circ), ET-3 (\square) and histamine (\triangle). The average changes in the ratio of F340 to F380 were monitored using fura-2 in a group of about 10 tracheal smooth muscle cells using the photomultiplier tube. Data represent tentative estimates of $[Ca^{2+}]_i$ and are shown as the mean \pm s.e.m. of 3 to 10 experiments. * $P < 0.05$; ** $P < 0.01$ (comparison between the ET-1- and ET-3-induced $[Ca^{2+}]_i$ increases by unpaired Student's t-test). The data could not be fitted by a logistic equation.

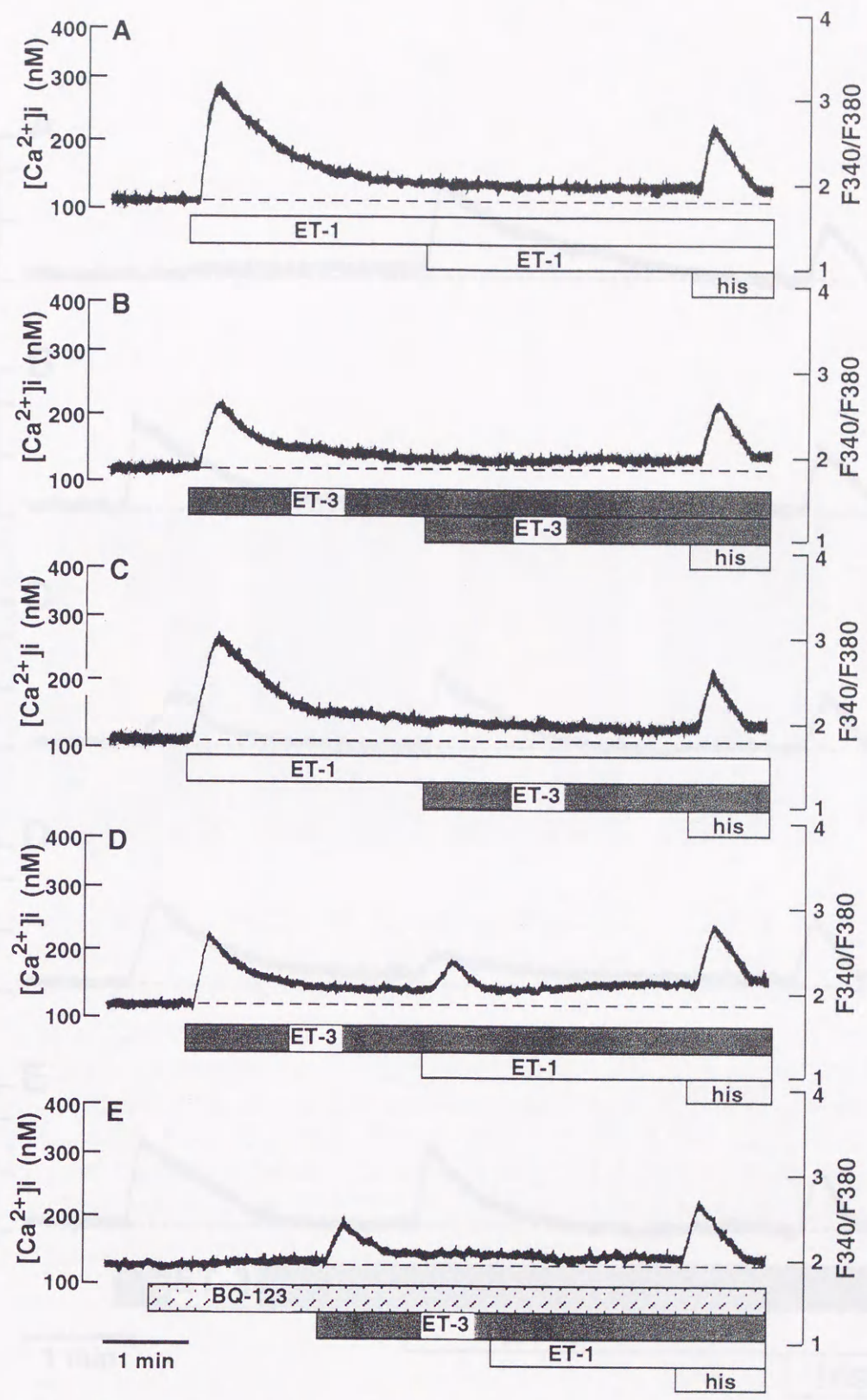


Fig. 1-5. Ca^{2+} responses in primary cultured cells induced by consecutive applications of 10 nM ET-1 followed by 10 nM ET-1 (A), 10 nM ET-3 followed by 10 nM ET-3 (B), 10 nM ET-1 followed by 10 nM ET-3 (C), 10 nM ET-3 followed by 10 nM ET-1 (D), and 10 μM BQ-123 followed by 10 nM ET-3 and 10 nM ET-1 (E). In all cases, 100 μM histamine (his) was added at the end of the experiment. Each signal represents the average signal from a group of about 10 cells monitored using the photomultiplier tube.

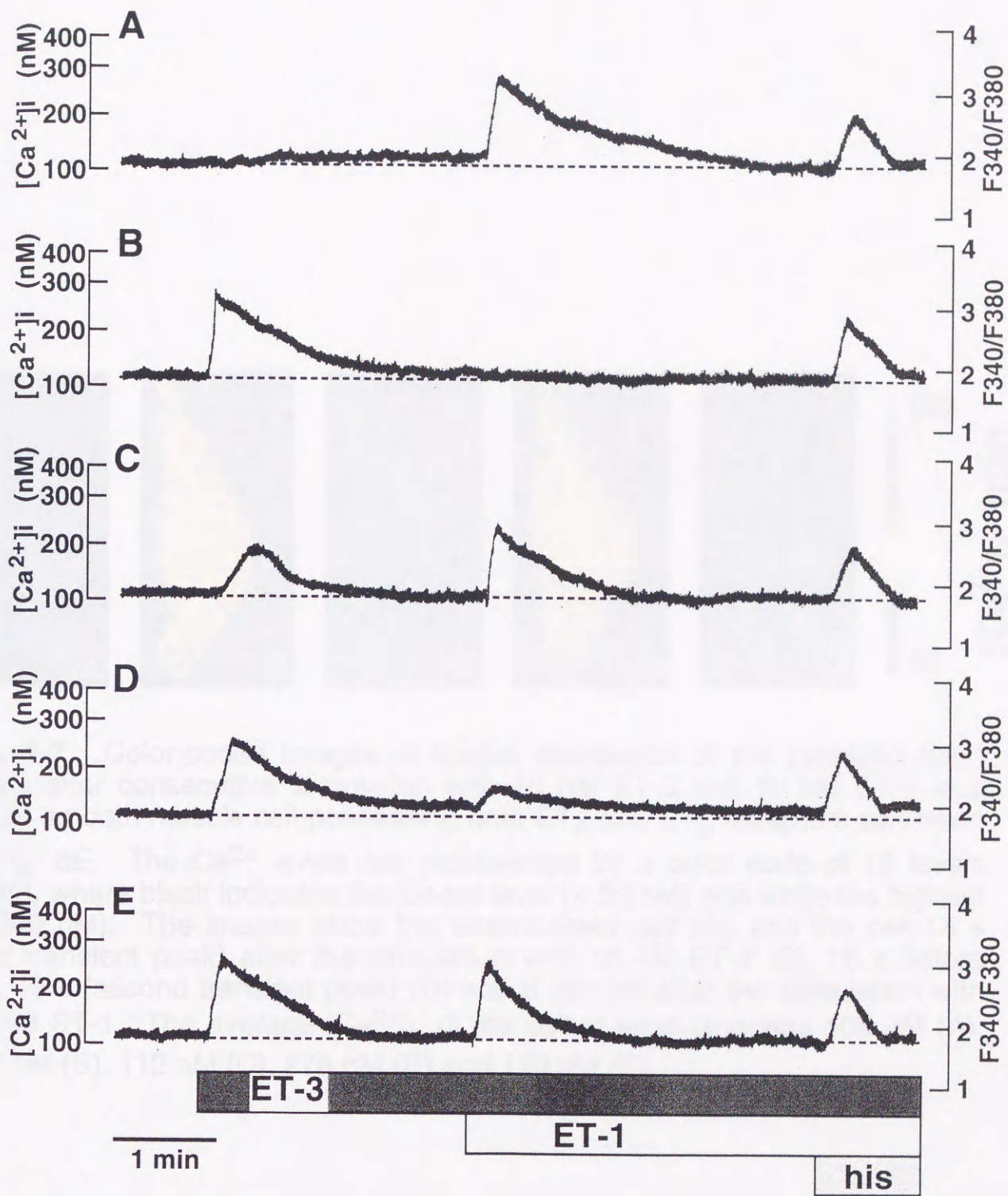


Fig. 1-6. Typical Ca^{2+} responses monitored using the CCD camera in single smooth muscle cells possessing ET_A (A), ET_B (B) and both receptors (C-E), after consecutive applications of 10 nM ET-3, 10 nM ET-1 and 100 μ M histamine (his).

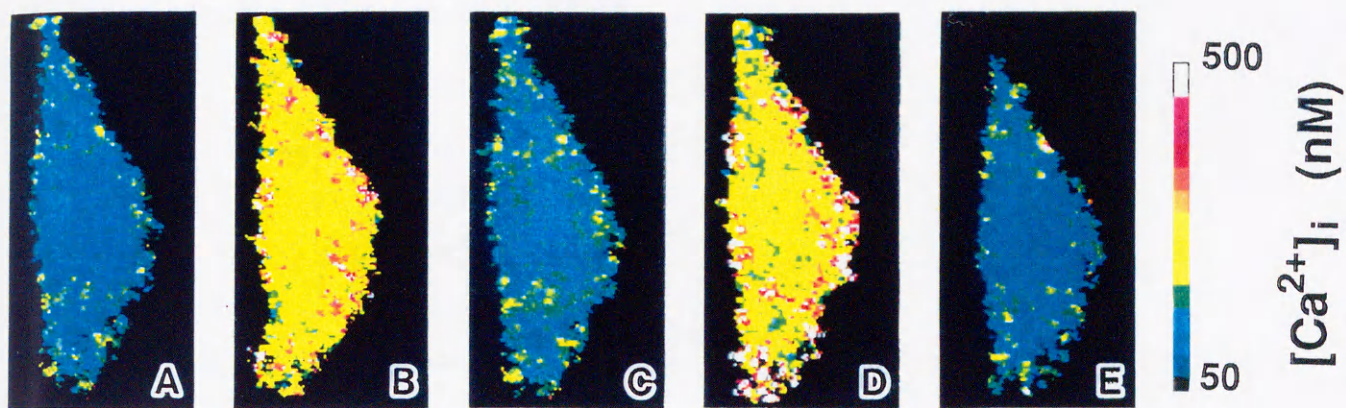


Fig. 1-7. Color-coded images of spatial distribution of the cytosolic Ca^{2+} levels after consecutive stimulation with 10 nM ET-3 and 10 nM ET-1 in a single smooth muscle cell possessing both ET_A and ET_B receptors as shown in Fig. 6E. The Ca^{2+} levels are represented by a color code of 16 levels (right), where black indicates the lowest level (< 50 nM) and white the highest (> 500 nM). The images show the unstimulated cell (A), and the cell 15 s (first transient peak) after the stimulation with 10 nM ET-3 (B), 10 s before (C), 15 s (second transient peak) (D) and 3 min (E) after the stimulation with 10 nM ET-1. The average $[\text{Ca}^{2+}]_i$ of the cell at each time was 108 nM (A), 284 nM (B), 112 nM (C), 278 nM (D) and 110 nM (E).

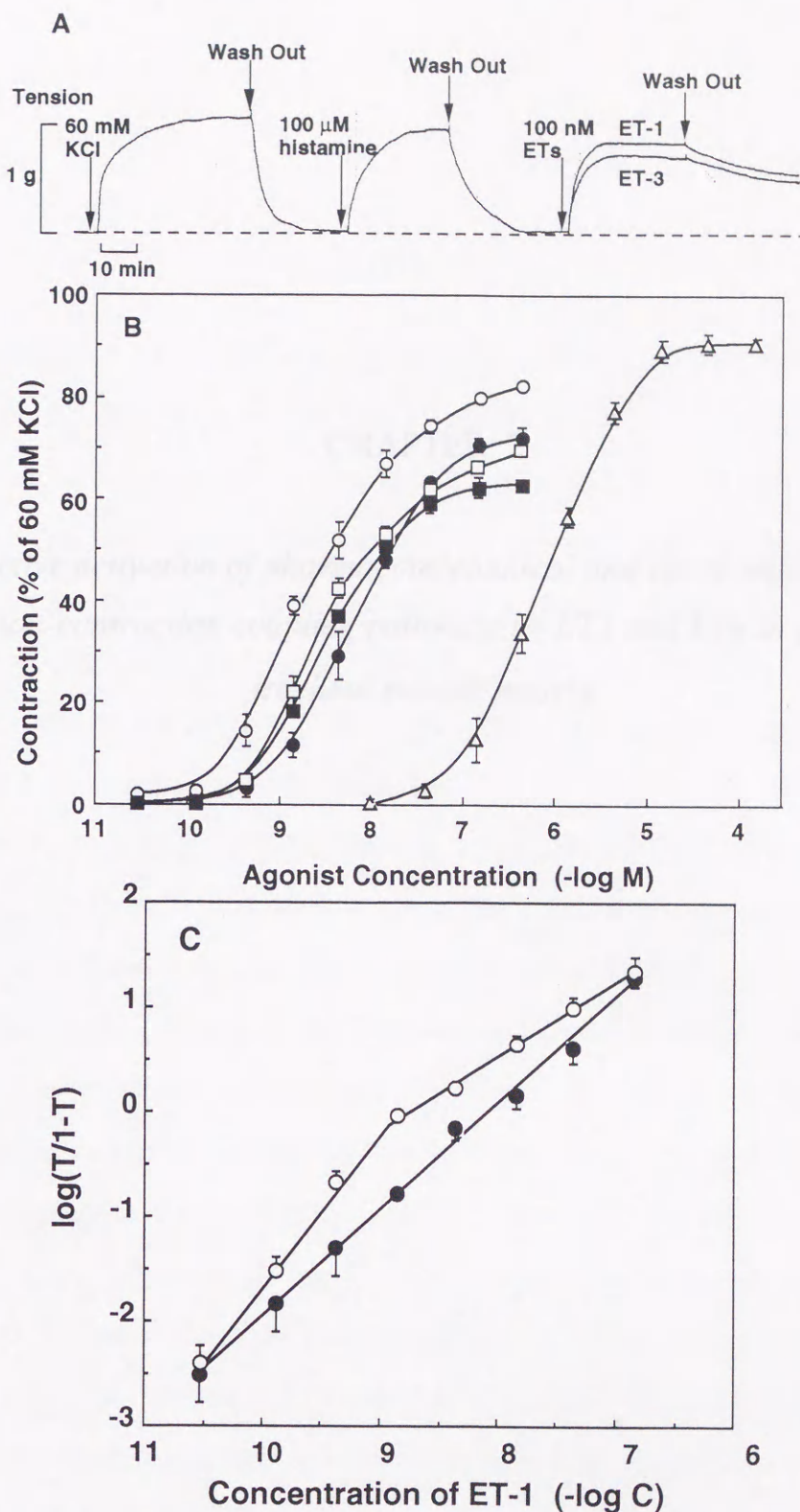


Fig. 1-8. A: Typical time course of tension development by the isolated, epithelium-denuded guinea pig tracheal rings in response to 60 mM KCl, 100 μ M histamine, 100 nM ET-1 and ET-3. B: Concentration-dependencies of the contraction of tracheal rings elicited by ETs and histamine. Symbols represent ET-1 (\circ), ET-3 (\square) and histamine (Δ), and ET-1 (\bullet) and ET-3 (\blacksquare) in the presence of 10 μ M BQ-123. BQ-123 itself showed no effect on the isolated trachea up to 10 μ M. C: Hill plots of the concentration-dependency of the contractions induced by ET-1 in the presence (\bullet) and absence (\circ) of 10 μ M BQ-123. Data are shown as mean \pm s.e.m. ($n = 5$).

CHAPTER 2

Selective activation of pharmacomechanical and electromechanical excitation-contraction coupling pathways by ET_A and ET_B in guinea pig tracheal smooth muscle

Abstract

Endothelin-1 (ET-1) induces contraction of airway smooth muscle of various species via activating ET_A and/or ET_B (3, 4, 11, 20, 26). In chapter 1, it was also demonstrated the cooperative contribution of ET_A and ET_B on guinea pig tracheal contraction. The physiological significance of the presence of the two receptor subtypes, however, remains unclear. I report in this chapter that, in guinea pig tracheal smooth muscle which expresses both ET_A and ET_B , the two receptor subtypes cooperate to fully mobilize the contractile apparatus by selectively activating pharmacomechanical and electromechanical excitation-contraction (E/C) coupling pathways. When stimulated independently, both ET_A and ET_B induced a long-lasting contraction of epithelium-denuded guinea pig trachea and in both cases, the contraction was totally dependent on Ca^{2+} influx from the extracellular space. The Ca^{2+} influx pathways activated by ET_A and ET_B were completely different; the ET_A -induced influx was due to the opening of voltage-independent Ca^{2+} channels whereas the ET_B -induced influx was due to the opening of L-type voltage-operated Ca^{2+} channels following membrane depolarization. ET_A , but not ET_B , induced phosphoinositide breakdown with resultant Ca^{2+} release and protein kinase C (PKC) activation. The released Ca^{2+} , however, did not induce contraction while the activated PKC indirectly contributed to contraction by increasing the Ca^{2+} -sensitivity of the contractile apparatus. These results revealed a unique mode of action of ET-1 among the smooth muscle constrictors which activate G protein-coupled receptors.

Introduction

Endothelins (ETs) are a family composed of three isopeptides, designated as ET-1, ET-2 and ET-3, each of which consists of 21 amino acid residues (8, 35). These three peptides have been increasingly revealed to have a variety of important effects in both

vascular and nonvascular systems (15). The functions of ETs are mediated by at least two distinct subtypes of receptors, namely ET_A receptors (ET_A) and ET_B receptors (ET_B). The ET_A has much greater selectivity for ET-1 and ET-2 than ET-3 (12), whereas the ET_B shows almost equal affinities for the three isopeptides (5). The activation of these receptors initiates several intracellular signal transduction events linked to a variety of biological actions, including an elevation of intracellular Ca^{2+} concentration ($[Ca^{2+}]_i$) and stimulation of phosphoinositide hydrolysis. In most preparations with cultured smooth muscle cells (2, 13, 18), ET-1-induced $[Ca^{2+}]_i$ increases occur in a biphasic manner: rapid initial transient and subsequent sustained phases which are caused by the release of intracellularly stored Ca^{2+} and transmembrane Ca^{2+} influx, respectively. Inositol 1,4,5-triphosphate (IP_3) and diacylglycerol (DG) produced by the phosphoinositide hydrolysis following G-protein-mediated activation of phospholipase C (PLC) serve as second messengers for the mobilization of intracellularly stored Ca^{2+} and the activation of protein kinase C (PKC), respectively (22, 32).

Recently both ET_A and ET_B receptors have been revealed to be involved in contractions induced by ET-1 in some vascular tissues and tracheal tissues (4, 28). In Chapter 1, I found out that ET_A and ET_B receptors coexist in major population of single smooth muscle cells of guinea pig trachea in primary culture and both receptors mediate long lasting contraction of its isolated trachea with their cooperation. These results show that the two receptor subtypes do not necessarily have clearly demarcated anatomic and functional territories. However, the signal transduction involved in these ET_A - and ET_B -mediated contraction is not completely understood, including its differences in their mediation. The ET-1-induced contraction of smooth muscle is slowly developing and long lasting, and depends greatly on extracellular Ca^{2+} existence, however it occurs even at low concentrations of ET-1 which do not induce the transient increase in $[Ca^{2+}]_i$. These evidences suggest that ET-1 may have unique properties for contractile mechanisms among

endogenous muscle constrictors, giving room for question whether the initial transient $[Ca^{2+}]_i$ increase induced by ET-1 contributes to the muscle contraction.

It is generally accepted that smooth muscle contraction is triggered by an increase in $[Ca^{2+}]_i$; the increased intracellular Ca^{2+} often forms a complex with calmodulin followed by the activation of enzymes such as myosin light chain kinase which results in the activation of cellular contractile mechanisms. Indeed, the contractile responses induced by ETs depend on the Ca^{2+} influx from extracellular space and the extracellular Ca^{2+} is indispensable to express the fully contractile responses to ETs. However, the relative contribution of these two sources of Ca^{2+} to muscle contraction remains unclear. In the case of ET receptors stimulation, the transient increase in $[Ca^{2+}]_i$ reaches the maximum level within 20 sec and declines to the lower sustained phase (lasting for at least 20 min.) within 5 min. On the other hand, the muscle contraction induced by ETs is generally slowly developing with time around 5 min to plateau and lasting for longer than 20 min. I have also reported in Chapter 1 that the transient increase in $[Ca^{2+}]_i$ induced by ETs was tachyphylactic in primary cultured smooth muscle cells of guinea pig trachea but in the tracheal contractile responses the tachyphylaxis was not observed, showing the poor correlation between the transient increase in $[Ca^{2+}]_i$ and the muscle contraction. From these facts, it is open to question whether the transient increase in $[Ca^{2+}]_i$ induced by ETs contributes to muscle contraction.

In Chapter 2, I elucidated that in the isolated guinea pig tracheal smooth muscle the contraction mediated by either ET_A or ET_B is basically initiated by the increase in $[Ca^{2+}]_i$ caused by extracellular Ca^{2+} influx and that the activation of ET_A stimulates the DG/PKC signaling pathway resulting in sensitization of contractile machinery to Ca^{2+} . It was also suggested that the IP_3 -induced transient increase in $[Ca^{2+}]_i$ never contributes to the contraction. Furthermore, the Ca^{2+} influx pathways activated by ET_A and ET_B were completely different; the ET_A -induced influx was due to the opening of voltage-independent Ca^{2+} channels whereas the ET_B -induced influx was due to the opening of L-

type voltage-dependent Ca^{2+} channels following membrane depolarization. These results revealed a unique mode of action of ET-1 among the smooth muscle constrictors which activate G protein-coupled receptors.

Materials: Nifedipine was from Dojin (Kure, Japan), nifedipine DL was from Kyokko Kagaku (Kyoto, Japan), BI-121 (7) was from Peninsula Laboratories, Inc. (Belmont, CA, U.S.A.), endothelin-1 and 17133 were from Funakoshi (Tokyo, Japan) and nifedipine and 17133 were from Sigma Chemical Company (St. Louis, MO, U.S.A.). NO-788 (9) was synthesized in my laboratory. All other chemicals were of analytical grade.

Animals: Male Hanley guinea pigs weighing 200-300 g were used in this study. The animals were housed in a temperature (22 ± 2°C) and humidity (70%) controlled room with a 12-hr light/dark cycle (lights on 5:00 A.M. and off at 7:00 P.M.). They were given standard guinea pig chow (TJCA Japan, Inc., Chofu, Japan) and tap water *ad libitum*.

Muscle Preparations and Contractile Assay. The guinea pig was sacrificed quickly and placed in oxygenated (95% O_2 -5% CO_2) Krebs-Henseleit solution of the following composition (mM): $NaCl$ 115.0, KCl 4.0, $CaCl_2$ 2.5, $MgSO_4$ 1.0, $NaHCO_3$ 25.0, NaH_2PO_4 0.5, $glucose$ 5.5, $HEPES$ 0.1, pH 7.4 at 37°C. After dissection, the muscle was quickly removed, the cruet was cut into rings of approximately 1 mm width. The epithelium was removed by gently using the rings in the jaws of a pair of Wescorner's forceps. The removal of the epithelium was confirmed histologically. The ring was placed into a 10 ml water-jacketed organ bath (Dwshiya UFR, Kyoto, Japan) containing the oxygenated Krebs-Henseleit solution at 37°C. The preparations were equilibrated for at least 1 hr under an initial tension of 1 g with washing every 15 min with the Krebs-Henseleit solution. Responses were measured isometrically with a micro-Joulemeter transducer (Nihon Kohden TB-6121, Tokyo, Japan). After 30 min of equilibration

Materials and Methods

Materials. ET-1, ET-3 and IRL 1620 (33) were purchased from the Peptide Institute Inc. (Osaka, Japan), fura-2-acetoxymethyl ester was from Dojin (Kumamoto, Japan), cremophor EL was from Nacalai Tesque (Kyoto, Japan), BQ-123 (7) was from Peninsula Laboratories Inc. (Belmont, CA, U.S.A.), calphostin C and 12-O-tetradecanoylphorbol-13-acetate (TPA) were from Funakoshi (Tokyo, Japan) and wortmannin and U73122 was from Sigma Chemical Company (St. Louis, MO, U.S.A.). BQ-788 (9) was synthesized in my laboratory. All other chemicals were of analytical grade.

Animals. Male Hartley guinea pigs weighing 350-500 g were used in this study. The animals were housed in a temperature- ($25 \pm 2^\circ\text{C}$) and moisture- (50%) controlled room with a 12-hr light/dark cycle (light on at 6:00 A.M. and off at 6:00 P.M.). They were given standard guinea pig chow (CLEA Japan, Inc., Osaka, Japan) and tap water *ad libitum*.

Muscle Preparations and Contraction Assay. The trachea was removed quickly and placed in oxygenated (95% O_2 -5% CO_2) Krebs-Henseleit solution of the following composition (mM): NaCl 113.0, KCl 4.8, CaCl_2 2.5, KH_2PO_4 1.2, MgSO_4 1.2, NaHCO_3 25.0 and glucose 5.5, EDTA 0.01, pH 7.4 at 37°C . After adherent fat and connective tissue had been carefully removed, the trachea was cut into rings of approximately 2 mm width. The epithelium was removed by gently turning the rings on the shaft of a pair of watchmaker's forceps. The removal of the epithelium was confirmed histologically. The ring was placed into a 4.0 ml water-jacketed organ bath (Iwashiyu UFER, Kyoto, Japan) containing the oxygenated Krebs-Henseleit solution at 37°C . The preparations were equilibrated for at least 1 h under an initial tension of 1 g with washing every 15 min with the Krebs-Henseleit solution. Responses were measured isometrically with a force-displacement transducer (Nihon Kohden TB-612T, Tokyo, Japan). After the equilibration

period, each preparation was first stimulated with 10 μ M carbachol (CCh) and the resultant contraction was used as a reference standard for the responses to ET-1, ET-3, IRL 1620 and histamine. The tissues were washed 3 times every 15 min before the application of agonists. Thereafter, concentration-response curves for ET-1, ET-3, IRL 1620 and histamine were made by their cumulative addition in logarithmic increments to the organ bath after reaching a plateau (Table I).

On the other hand, 100 nM ET-1 in the presence of 3 μ M BQ-788 or 10 μ M BQ-123 was applied for selective stimulation of ET_A and ET_B, respectively. The L-type voltage-dependent Ca²⁺ channel (L-VDCC) blockers, nifedipine and verapamil were applied 15 min after stimulation with ET-1 when the plateau tension level was achieved. The data shown are the relative forces of tension 20 min after application of the blockers. For low Na⁺ treatment, tissues were incubated at 37 °C for 30 min in a low Na⁺ Krebs solution (10 mM NaCl and 128 mM NMG-Cl) before stimulation. IAA-94, a Cl⁻ channel blocker, was applied 10 min before stimulation either in normal or low Na⁺ conditions. The data shown are the relative values of the plateau tension levels achieved (Table II).

Simultaneous Measurements between Intracellular Ca²⁺ Levels and Contraction.

Epithelium-denuded tracheal rings (~ 2 mm width) from guinea pig were opened into rectangle strips and treated with a lipophilic derivative of the Ca²⁺ fluorescent indicator fura-2-acetoxymethyl ester (fura-2/AM, 5 μ M) and a noncytotoxic detergent, cremophor EL (0.02%), which was added to increase solubility and cell-penetration of fura-2/AM, for 3 h at 30°C and then maintained for overnight at 4°C. After overnight-loading of fura-2/AM, the tracheal strip was rinsed with Krebs-Henseleit solution and held horizontally in a temperature-controlled (30°C), 5 ml organ bath which was attached to a fluorescence spectrometer. Changes in tension were monitored by a force-displacement isometric transducer. The central portion of strips was illuminated alternately at wavelengths of 340 and 380 nm, and the emitted fluorescence at 500 nm monitored. The contractile responses of fresh tissues and fura-2-loaded tissues induced by 10 μ M carbachol were

indistinguishable. The leakage of fura-2 from smooth muscle tissue was not seen at the experimental temperature of 30°C. $[Ca^{2+}]_i$ was estimated from the ratio of fluorescence intensities for excitation at 340 and 380 nm (F340/F380) according to the method described previously (27). BQ-788 or BQ-123 was added 20 min before ET-1 application. An inhibitor of PLC, U73122 (3 μ M), was added 30 min prior to addition of ET-1.

On the other hand, the extracellular Ca^{2+} -free condition was made by washing three times (over a 10 min period) with Ca^{2+} -free Krebs-Henseleit solution and adding 20 mM EGTA 20 sec before the application of ET-1, BQ-788 or BQ-123. In this condition, the basal level of $[Ca^{2+}]_i$ decreased to 58 ± 5 nM ($n = 8$).

Membrane Depolarization. Changes in membrane potential of the epithelium-denuded tracheal strips were monitored using the fluorescent dye bis-(1,3 dibutylbarbituric acid)-trimethine oxonol [DiBAC₄(3)] (excitation, 490 nm; emission, 518 nm) basically according to the technique similar to that used for cells by Takenaka et al. (34). In the present case, the tissue was bonded on quartz cover glass, and then transferred to a temperature-controlled (37°C) quartz cuvette in a fluorescence spectrometer. The tissue was incubated in Krebs-Henseleit solution containing 50 nM DiBAC₄(3) for 60 - 70 min. After the fluorescent trace reaching the plateau level, BQ-788, BQ-123 or BQ-123 and IAA-94 was/were added and then after 20 min incubation, ET-1 was applied. Traces presented are representative of three experiments.

Assay of [³H]-inositol Phosphate Turnover. The tracheal smooth muscle band, which lies between the cartilage horns along the posterior membrane of the trachea was dissected from the trachea and cut transversely into 5 pieces of equivalent size. Each tissue was preincubated for 45 min in 5 ml of Krebs-Henseleit solution at 37°C with washing every 15 min and then incubated with [³H]-*myo*-inositol (20 μ Ci) in 1 ml of oxygenated (95% O₂-5% CO₂) Krebs-Henseleit solution for 4 h at 37°C with gentle shaking. The tissues were washed three times with 1 ml of Krebs-Henseleit solution for 15 min to

remove excess [^3H]-*myo*-inositol. After washing, the tissues were incubated for a further 15 min in 1 ml Krebs-Henseleit solution containing 10 mM LiCl to inhibit the breakdown of inositol monophosphate to inositol and thus resulting in the accumulation of inositol phosphates. The tissues were stimulated for 20 min with 10 nM ET-1, 100 nM ET-3, 300 nM IRL 1620 and 10 μM histamine, and the tissues pretreated with 10 μM BQ-123 or 3 μM BQ-788 for 20 min were stimulated with 100 nM ET-1. The stimulation was terminated by freezing the tissues in liquid N_2 (-196°C). Each freezed tissue was exposed to 1 ml distilled water and 3 ml chloroform: methanol: hydrochloric acid (2: 1: 0.1, v/v) with vigorous shaking. The upper methanol/water phase was applied to an anion exchange chromatography column (0.6 ml of Dowex AG1-X8 in formate form). After washes with 10 ml of distilled water and 5 ml of a 5 mM sodium tetraborate and 60 mM sodium formate to remove [^3H]-inositol and [^3H]-glycerophosphoinositol respectively, [^3H]-inositol phosphates were eluted by two 2.5 ml additions of a buffer containing 0.1 mM formic acid and 0.75 M ammonium formate. The aliquots of the final fraction were mixed with 8 ml of Aquasol-2 liquid scintillation cocktail (Dupont, U.S.A.) and radioactivity counted in a liquid scintillation counter (Packard, Model 1900CA). Total [^3H]-inositol phosphates accumulation was expressed as d.p.m. mg^{-1} wet wt. tracheal smooth muscle.

Translocation of PKC α to Membrane. Tracheal strips were stimulated in Krebs-Henseleit solution for the time indicated with 100 nM ET-1 in the presence either BQ788 or BQ123. The reaction was halted by chilling in liquid nitrogen. Tissue was homogenized and centrifuged at 100,000 g for 30 min. PKC α in the membrane fraction was extracted from the pellet with 0.1 % Triton X-100. Samples (5 μg of protein) were subjected to SDS-PAGE (10 % acrylamide), Western transfer and immunoblotting with anti-PKC α antibody (GIBCO BRL). The blot was developed with ABC immunodetection kit (Vecstein) and Kodak HRP-1000.

Intracellular [Ca²⁺]-dependence on Contraction. The relative contribution of intra- and extra-cellular Ca²⁺ to the contractions induced by various concentrations of ET-1, and histamine were determined in the following manner. Extracellular Ca²⁺ was removed by washing three times every 10 min with Ca²⁺-free Krebs-Henseleit solution, and 20 μM EGTA was added to the organ bath before 20 sec until the tissues were exposed to the agonists. After stimulation with 100 nM ET-1 in the presence of BQ-123 or BQ-788, or 100 μM histamine in Ca²⁺-free Krebs-Henseleit solution containing 20 μM EGTA, consecutive cumulative concentration-response curves to CaCl₂ (0.01, 0.02, 0.03, 0.05, 0.1, 0.15, 0.2, 0.3, 0.4, 0.5, 0.6, 0.7, 0.8, 1.0, 1.2, 1.5, 2.0 and 2.5 mM final concentrations) were generated for each tissue. These concentrations of agonists (see above) were chosen as giving the maximum contraction. The free calcium concentrations at a each point of increasing CaCl₂ were calculated with a BASIC program using the stability constants of Ca²⁺, Mg²⁺ and H⁺ for EGTA (14), and taking into consideration the purity of EGTA and the activity of H⁺ (24).

Calphostin C (1 μM), a selective protein kinase C inhibitor, was added 30 min prior to addition of ET-1, histamine. In the preliminary study using guinea pig trachea, contractile responses to 1 μM TPA or KCl (66 mM) were obtained in the absence and presence of 1 μM calphostin C. Contractile responses induced by 1 μM TPA were completely inhibited by 1 μM calphostin C ($P < 0.01$), although 1 μM calphostin C slightly elicited the contraction ($35.5 \pm 4.6\%$ of the 10 μM CCh-induced contraction), whereas 1 μM calphostin C did not affect on 66 mM KCl-induced contraction. Therefore, in this study, I used 1 μM calphostin C as a selective protein kinase C inhibitor. Wortmannin (1 μM), a selective myosin light chain kinase (MLCK) inhibitor, was added 30 min prior to addition of histamine (19). Calphostin C (1 μM) and wortmannin (1 μM) did not change the fluorescence intensity at 500 nm excited at 340 nm and 380 nm.

Statistical and Data Analyses. All values are expressed as mean \pm s.e.m. and statistical significance was assessed by Student's *t* test. $P < 0.05$ was considered to be significant.

Comparison of cumulative concentration-dependent curves for contraction (Table I) was performed by nonlinear regression analysis (16) based on a logistic equation (25). The fitted curves were compared by the method of Dunnett's multiple comparison. $P < 0.05$ was considered to be significant.

Experimental protocol is summarized in Fig. 2-1.

Results

Tracheal Contraction Induced by ET-1, ET-3 and IRL 1620. ET-1, ET-3 and IRL 1620 (ET_B specific agonist) caused long-lasting and concentration-dependent contraction of isolated and epithelium-denuded guinea pig tracheal rings. The data were fitted by a logistic equation and parameters are compared in Table 2-1. The maximum contraction (T_{max}) induced by ET-1 ($87.3 \pm 2.03\%$ of the 10 μ M CCh-induced contraction) was ~ 1.3 times stronger ($P < 0.05$) than that by ET-3 and ~ 1.5 times stronger ($P < 0.01$) than that by IRL 1620, and the T_{max} value induced by IRL 1620 was not significantly different from that induced by ET-3. The half-maximally effective concentrations (EC₅₀) were 1.14 ± 0.12 nM for ET-1, 6.26 ± 0.37 nM for ET-3 and 8.72 ± 0.70 nM for IRL 1620 respectively, and the EC₅₀ value of IRL 1620 was not significantly different from that of ET-3. These results indicated that ET-1-induced contraction by which activated both ET_A and ET_B was more potent and efficient than ET-3- and IRL 1620-induced contraction by which activated only ET_B. These results also showed that IRL 1620 had almost same contractile activity to ET-3. The previous study of binding assays (33) have shown that IRL 1620 was more selective for ET_B than ET-3.

The ET_A antagonist, 10 μ M BQ-123, shifted the EC₅₀ value of the concentration-response curve for ET-1 to approximately 3-fold higher concentrations ($P < 0.05$) and reduced the T_{max} value to $\sim 64\%$ of the control value ($P < 0.05$, Table 2-1). On the other hand, the ET_B antagonist, 3 μ M BQ-788, entirely inhibited the contraction induced by 30 pM to 300 nM ET-3, however, did not significantly affect both EC₅₀ and T_{max} values of the concentration-response curve for ET-1.

Simultaneous Measurements of [Ca²⁺]_i and Muscle Tension. When stimulated in the presence of extracellular Ca²⁺ (2.5 mM), both ET_A and ET_B induced a sustained increase in the intracellular Ca²⁺ concentration ([Ca²⁺]_i) and contraction of epithelium-

denuded tracheal strips (Fig. 2-2). Figure 2-2A shows the representative time courses of $[Ca^{2+}]_i$ and force traces of a strip of trachea induced by ET-1. After stimulation of 100 nM ET-1 ($n = 4$), the $[Ca^{2+}]_i$ increased rapidly and transiently from the basal level (100 ± 18 nM) to a peak (350 ± 45 nM) within 30 sec, and contraction was initiated simultaneously. The $[Ca^{2+}]_i$ decreased gradually to 175 ± 20 nM within 5 min after stimulation by ET-1 and maintained this level for more than 20 min, and contraction was also long-lasting and maintained a plateau level for more than 20 min. In the presence of 3 μ M BQ-788, the ET_B antagonist, 100 nM ET-1 also induced both transient and sustained increases in $[Ca^{2+}]_i$ (364 ± 38 , 184 ± 26 nM, respectively, $n = 3$), but maximum contraction was slightly attenuated ($91 \pm 5\%$, Fig. 2-2B). However, IRL 1620 up to 300 nM ($n = 4$), induced the contraction and a sustained increase in $[Ca^{2+}]_i$ (190 ± 25 nM) without a transient increase in $[Ca^{2+}]_i$ (Fig. 2-2C). These contraction and sustained increase in $[Ca^{2+}]_i$ were also maintained a plateau level for more than 20 min. The ET_A antagonist, 10 μ M BQ-123, completely declined the transient increase in $[Ca^{2+}]_i$ elicited by 100 nM ET-1 (sustained increase in $[Ca^{2+}]_i$; 174 ± 19 nM, $n = 3$) and reduced the tension to almost equal level induced by 300 nM IRL 1620 (Fig. 2-2D). Moreover, 3 μ M BQ-788 completely inhibited both $[Ca^{2+}]_i$ and contraction elicited by 300 nM IRL 1620 ($n = 3$, Fig. 2-2E). As a reference, 100 μ M histamine ($n = 4$) induced a transient increase in $[Ca^{2+}]_i$ (380 ± 35 nM) followed by a sustained increase in $[Ca^{2+}]_i$ (174 ± 22 nM) and induced a contraction simultaneously (Fig. 2-2F). These results indicated that ET_A was apparently coupled to the mechanism of the Ca^{2+} release from intracellular stores, probably the sarcoplasmic reticulum, and linked to the influx of extracellular Ca^{2+} , whereas ET_B was linked to only the influx of extracellular Ca^{2+} .

After chelation of extracellular Ca^{2+} by addition of 5 mM EGTA at the end of the experiment in all cases, the sustained increases in $[Ca^{2+}]_i$ and the maintained contractile responses decreased promptly. These results, taken together, suggested that the influx of

Ca²⁺ from the extracellular space mainly contributes to the generation of contraction mediated by ET receptors.

Contribution of Transient and Sustained Increases in [Ca²⁺]_i to Contraction. The dependency on Ca²⁺ influx was more clearly demonstrated when extracellular Ca²⁺ was substituted after stimulation (Fig. 2-3). After removing extracellular Ca²⁺ by washing three times (over a 10 min period) with Ca²⁺-free Krebs-Henseleit solution, and adding 20 μM EGTA (the basal level of [Ca²⁺]_i decreased to 58 ± 5 nM, n = 8), 100 nM ET-1 induced only a transient increase in [Ca²⁺]_i (252 ± 23 nM, n = 3) without any sustained increase in [Ca²⁺]_i and also hardly induce contraction (Fig. 2-3A). Subsequently, the maximum contraction and sustained increase in [Ca²⁺]_i were obtained by increasing the extracellular Ca²⁺ concentration to 2.5 mM. These contraction and intracellular sustained Ca²⁺ level were almost equal to those obtained by the stimulation with 100 nM ET-1 in the presence of extracellular Ca²⁺ (see Fig. 2-2A). In the presence of 3 μM BQ-788, 100 nM ET-1 also induced a transient increase in [Ca²⁺]_i (198 ± 27 nM, n = 3) with no sustained increase in [Ca²⁺]_i and did not induce any contraction (Fig. 2-3B). Furthermore, 100 nM ET-1 in the presence of BQ-123 (Fig. 2-3C) or 300 nM IRL 1620 (data not shown) did not induce any contraction and [Ca²⁺]_i increase in the absence of extracellular Ca²⁺, however, the maximum contraction and sustained increase in [Ca²⁺]_i were also obtained by subsequent increasing of the extracellular Ca²⁺ to 2.5 mM, and they were almost equal to the results obtained in the presence of extracellular Ca²⁺.

On the other hand, 100 μM histamine induced not only a transient increase in [Ca²⁺]_i (271 ± 21 nM, n = 3) with no sustained increase in [Ca²⁺]_i but also a transient contraction simultaneously (Fig. 2-3D). And then the maximum contraction and sustained increase in [Ca²⁺]_i were obtained by subsequent increases of the extracellular Ca²⁺ to 2.5 mM after decreasing the transient contraction to the basal level. These results strongly indicated that the release of Ca²⁺ from intracellular store sites was not sufficient signal to

induce the tracheal contraction mediated by ET receptors, and ET-receptor-mediated contraction almost entirely depended on the influx of Ca^{2+} from extracellular space. However, the contractile profile was in marked contrast to histamine, which induced a transient contraction with a time course similar to the transient increase in $[\text{Ca}^{2+}]_i$ in the absence of extracellular Ca^{2+} .

Wortmannin (1 μM), a selective myosin light chain kinase inhibitor, was added 30 min prior to addition of histamine under the conditions of Ca^{2+} -free Krebs-Henseleit solution containing 20 μM EGTA. The level of a transient increase in $[\text{Ca}^{2+}]_i$ induced by 100 μM histamine (258 ± 34 nM, $n = 3$, Fig. 2-3E) was not different from that without the preceding addition of wortmannin, however, a transient contraction was abolished. The subsequent addition of 2.5 mM Ca^{2+} gave rise to the sustained increase in $[\text{Ca}^{2+}]_i$ whose level was almost same to that without the preceding addition of wortmannin, however, the contractile response was diminished (~20%). These results showed that histamine-induced transient contraction was caused by the activation of myosin light chain kinase (MLCK), and the sustained contraction was also caused by the activation of myosin light chain kinase.

ET_A-selective Activation of Phospholipase C and ET_B-mediated Ca²⁺ Influx via L-type Voltage-dependent Ca²⁺ Channel. As stimulation of ET_B did not cause the transient increase in $[\text{Ca}^{2+}]_i$, suggesting ET_A-selective activation of PLC. Further evidence for the independence from PLC of the ET_A-induced tension development was provided with the use of a PLC inhibitor U73122 (29). This drug abolished the initial transient increase in $[\text{Ca}^{2+}]_i$ without affecting the sustained increase in $[\text{Ca}^{2+}]_i$ and tension development (Fig. 2-4A). The dependence of the ET-1-induced contraction on Ca^{2+} influx prompted us to examine the differences in the Ca^{2+} influx pathways activated by ET_A and ET_B. I tested the effects of a series of Ca^{2+} channel blockers and found that L-VDCC blockers nifedipine and verapamil, abolished the influx and tension development mediated by ET_B while they barely affected those mediated by ET_A (Fig. 2-4B and Table II). A non-selective Ca^{2+}

channel blocker SK&F96365 (3 mM) (17) failed to inhibit either ET_A- or ET_B-induced Ca²⁺ influx (and tension development) although the divalent cation channel blocker Ni²⁺ (1 mM) (6) totally abolished both the ET_A- and ET_B-induced responses (data not shown).

Membrane Depolarization in ET_B-mediated Response. As the selective effects of L-VDCC blockers suggested the involvement of membrane depolarization in the ET_B-mediated response, I tested the effects of ET-1 on membrane potentials. Stimulation of ET_B, but not ET_A, caused depolarization of the membrane potentials which was comparable with that caused by 30 mM KCl (Fig. 2-5). The maximum shifts in membrane potential caused by ET_B-stimulation (> 20 mV) were large enough to induce Ca²⁺ influx through VDCC to elicit smooth muscle contraction (21). Both influx of Na⁺ and efflux of Cl⁻ were found to be responsible for the depolarization. A Cl⁻ channel blocker, indanyloxyacetic acid (IAA-94) (34) partially suppressed the ET_B-induced membrane depolarization and the inhibition was complete when extracellular Na⁺ was largely replaced with N-methylglucamine (NMG-Cl, Fig. 2-5). The same was the case for the ET_B-induced tension development. Either application of IAA-94 or depletion of extracellular Na⁺ partially suppressed the ET_B-induced tension development and the combination of these two procedures abolished it (Table II). Neither procedure affected the ET_A-induced tension development.

Phosphatidylinositol Turnover. To examine the physiological role of PI cascade in ET-1-induced contraction, I tested the possible modulation of Ca²⁺ sensitivity by ET-1. In the presence of extracellular Ca²⁺, the mean increase in [³H]-inositol phosphate accumulation in guinea pig trachea induced by 100 nM ET-1 was approximately 1.8-fold above basal level (407 ± 22 d.p.m./mg wet wt, P < 0.01, Fig. 2-6A). In comparison, 300 nM IRL 1620 did not induce significant accumulation of [³H]-inositol phosphates. On the other hand, ET-1-induced accumulation of [³H]-inositol phosphates was attenuated by 10 μM BQ-123, ET_A specific antagonist, to the basal level (P < 0.01), but was not significantly

attenuated by 3 μM BQ-788, ET_B specific antagonist. Histamine (100 μM), as a reference, induced [^3H]-inositol phosphate accumulation approximately 3.6-fold greater than basal level ($P < 0.01$).

In the absence of extracellular Ca^{2+} , a total [^3H]-inositol phosphate accumulation of basal level decreased to 76 ± 15 d.p.m./mg wet wt., however, the accumulations of [^3H]-inositol phosphates induced by 100 nM ET-1 in spite of the absence or the presence of 3 μM BQ-788 and 100 μM histamine were also significantly greater than basal level ($P < 0.01$, Fig. 2-6B). These results showed that inositol phosphates was specifically produced by ET_A , but not by ET_B .

Translocation of Protein Kinase C from Cytosol to Membrane Fractions. The Western blots showed the translocation of $\text{PKC}\alpha$ from cytosol to membrane fractions (Fig. 2-7). In case of ET_A stimulation (with 100 nM ET-1 in the presence of 3 μM BQ-788), the $\text{PKC}\alpha$ translocated to membrane fractions within 1 min after stimulation (Fig. 2-7A). The membrane association of $\text{PKC}\alpha$ sustained until 10 min, and then gradually decreased over 20 min. In contrast, in case of ET_B stimulation (with 100 nM ET-1 in the presence of 10 μM BQ-123), $\text{PKC}\alpha$ was not translocated to membrane fraction at any time (Fig. 2-7B). These data showed that the activation of PKC was specifically elicited by ET_A .

Cumulative Substitution of Extracellular Ca^{2+} . As the sustained increase in $[\text{Ca}^{2+}]_i$ was considered to have much contribution to ET-induced contraction than the transient increase in $[\text{Ca}^{2+}]_i$, the relationship between the extra- and intra-cellular Ca^{2+} and contraction to ET_A - or ET_B -stimulated strips of guinea pig trachea was investigated. Figure 2-8A shows a representative example of the effect of extra- and intra-cellular Ca^{2+} in the tracheal smooth muscle strip pre-stimulated with 100 nM ET-1 in Ca^{2+} -free Krebs-Henseleit solution containing 20 μM EGTA. The cumulative addition of CaCl_2 (0.01-2.5 mM) to the tracheal strip pre-stimulated with 100 nM ET-1 (both ET_A and ET_B activation) caused concentration-dependent increases in both $[\text{Ca}^{2+}]_i$ and tension. The threshold

concentration of CaCl_2 which increased $[\text{Ca}^{2+}]_i$ was $30 \mu\text{M}$ [the actual value of extracellular Ca^{2+} concentration ($[\text{Ca}^{2+}]_{\text{ex}}$) calculated with a BASIC program using the stability constants of Ca^{2+} , Mg^{2+} and H^+ for EGTA was $1.8 \mu\text{M}$] and the threshold concentration of $[\text{Ca}^{2+}]_{\text{ex}}$ which increased tension was $20.5 \mu\text{M}$. In case of pre-treatment with $3 \mu\text{M}$ BQ-788 and then stimulation with 100 nM ET-1 (ET_A activation), the threshold concentrations of $[\text{Ca}^{2+}]_{\text{ex}}$ which increased $[\text{Ca}^{2+}]_i$ and tension were also $1.8 \mu\text{M}$ and $20.5 \mu\text{M}$, respectively (Fig. 2-8B). In case of pre-treatment with $10 \mu\text{M}$ BQ-123 and then stimulation with 100 nM ET-1 (ET_B activation), the threshold concentrations of $[\text{Ca}^{2+}]_{\text{ex}}$ which increased $[\text{Ca}^{2+}]_i$ and tension were $1.8 \mu\text{M}$ and $120 \mu\text{M}$, respectively (Fig. 2-8C). These results indicated that extracellular Ca^{2+} sensitivity to ET_B -mediated contraction was lower than that of ET_A -mediated contraction. On the other hand, with the addition of $1 \mu\text{M}$ calphostin C (a selective PKC inhibitor) for 30 min before the stimulation with 100 nM ET-1, the cumulative addition of CaCl_2 resulted in a stepwise increase in both $[\text{Ca}^{2+}]_i$ and tension (Fig. 2-8D). A peak of transient increase in $[\text{Ca}^{2+}]_i$ induced by 100 nM ET-1 (both ET_A and ET_B activation) was slightly decreased ($80.0 \pm 10.0\%$, $n = 4$) as compared with control (see Fig. 2-8A). The Ca^{2+} -leakage from intracellular Ca^{2+} store sites might be caused by the removal of extracellular Ca^{2+} depending on the incubation time with Ca^{2+} -free Krebs-Henseleit solution. The threshold concentrations of $[\text{Ca}^{2+}]_{\text{ex}}$ which increased $[\text{Ca}^{2+}]_i$ and tension became $1.8 \mu\text{M}$ and $120 \mu\text{M}$, respectively. In case of ET_A activation in the presence of $1 \mu\text{M}$ calphostin C, the threshold concentrations of $[\text{Ca}^{2+}]_{\text{ex}}$ which increased $[\text{Ca}^{2+}]_i$ and tension became $1.8 \mu\text{M}$ and $120 \mu\text{M}$, respectively (Fig. 2-8E). However, in case of ET_B activation with the preceding addition of $1 \mu\text{M}$ calphostin C, the threshold concentrations of $[\text{Ca}^{2+}]_{\text{ex}}$ which increased $[\text{Ca}^{2+}]_i$ and tension were $1.8 \mu\text{M}$ and $120 \mu\text{M}$ respectively (Fig. 2-8F), and did not change to the values which were carried out without the preceding addition of $1 \mu\text{M}$ calphostin C (see Fig. 2-8C). These results showed that the inactivation of PKC caused by calphostin C decreased Ca^{2+} sensitivity to contractions mediated by ET_A .

In case of pre-stimulation with 100 μM histamine, both of the threshold concentrations of $[\text{Ca}^{2+}]_{\text{ex}}$ which increased $[\text{Ca}^{2+}]_{\text{i}}$ and tension were 0.16 μM (Fig. 2-8G). These results indicated that Ca^{2+} sensitivity to contraction induced by histamine was higher than that induced by ET-1. Furthermore, in case of pre-stimulation with 100 μM histamine with the preceding addition of 1 μM calphostin C (Fig. 2-8H), both peaks of transient increase in $[\text{Ca}^{2+}]_{\text{i}}$ and transient contraction were decreased ($72.0 \pm 11.5\%$ and $43.0 \pm 6.5\%$, respectively, $n = 4$) as compared with control (see Fig. 2-8G). It was considered that the transient contraction elicited by histamine undoubtedly depended on the transient increase in $[\text{Ca}^{2+}]_{\text{i}}$. The threshold concentrations of $[\text{Ca}^{2+}]_{\text{ex}}$ which increased $[\text{Ca}^{2+}]_{\text{i}}$ and tension became 0.16 μM and 71.0 μM .

For further elucidation of the relationship between $[\text{Ca}^{2+}]_{\text{i}}$ and tension development, $[\text{Ca}^{2+}]_{\text{i}}$ was plotted against the tension (Fig. 2-9). There are positive correlation between $[\text{Ca}^{2+}]_{\text{i}}$ increase and tension development produced by ET_A stimulation (Fig. 2-9A). However, the gradient of the $[\text{Ca}^{2+}]_{\text{i}}$ -tension relationship in ET_B -stimulated strips was lower than that obtained in ET_A -stimulated strips. Both a PLC inhibitor U73122 (3 μM) and a PKC inhibitor calphostin C (1 μM) caused rightward shifts of the $[\text{Ca}^{2+}]_{\text{i}}$ -tension relationship in ET_A -stimulated strips while neither of the drugs caused any change in the relationship in ET_B -stimulated strips (Fig. 2-9B). These results, taken together, clearly showed that ET_A -mediated contraction had much higher efficiency of intracellular Ca^{2+} to contraction than ET_B -mediated contraction, and the inactivation of PLC or PKC decreased Ca^{2+} sensitivity to contractions mediated by ET_A , but did not affect Ca^{2+} sensitivity to contractions mediated by ET_B .

Discussion

In Chapter 2, the different signal transduction systems mediated by ET_A and ET_B in guinea pig tracheal smooth muscle were reported. It was demonstrated by simultaneous measurements of $[Ca^{2+}]_i$ and muscle tension that ET_A was coupled to phosphoinositide turnover and the release of Ca^{2+} from intracellular store sites and also linked to the influx of extracellular Ca^{2+} , whereas ET_B was linked to only the influx of extracellular Ca^{2+} in guinea pig tracheal smooth muscles (Figs. 2-2, -3 and -6). The release of Ca^{2+} from intracellular store sites was not sufficient signal to induce the tracheal contraction mediated by ET_A , and the influx of Ca^{2+} from the extracellular space, mainly contributes to the generation of contraction mediated by ET_A or ET_B (Fig. 2-3). The contractile profile of ET-1 was found to be in marked contrast to histamine, which induced a transient contraction with a transient increase in $[Ca^{2+}]_i$ in the absence of extracellular Ca^{2+} (Fig. 2-3). Furthermore, it was shown that the ET_A -induced activation of PKC indirectly contributed to the contraction by increasing the Ca^{2+} -sensitivity of the contractile apparatus (Figs. 2-7, -8 and -9). This is the first report consolidating the multiple mechanism of tracheal smooth muscle contraction.

In this chapter, either ET_A - or ET_B -mediated contraction was shown to be caused by Ca^{2+} influx from extracellular space. Such situation promoted me to study which type of Ca^{2+} channel was involved in ET receptor-mediated contraction. According to the dependence on the activation of voltage-dependent Ca^{2+} channels (VDCCs) following membrane depolarization, the excitation-contraction (E/C) coupling pathways in smooth muscle cells can be divided into two categories; electromechanical and pharmacomechanical (31). The results clearly indicate the selective activation of pharmacomechanical and electromechanical E/C pathways by ET_A and ET_B , respectively. The mechanism of ET_B -activated electromechanical coupling was the opening of L-type voltage-dependent Ca^{2+} channels (L-VDCC) following membrane depolarization caused by

the opening of Na⁺ and Cl⁻-permeable channels (Figs. 2-4, -5 and Table 2-2). The mechanism of ET_A-activated pharmacomechanical coupling involved the opening of Ca²⁺ channels (non-selective cation channel) which did not require membrane depolarization. It is, however, generally accepted that the major mechanism of pharmacomechanical coupling is Ca²⁺ release by inositol 1,4,5-triphosphate generated by the phosphatidylinositol (PI) cascade and modulation of the sensitivity to Ca²⁺ (31).

The functional distinction between ET_A and ET_B has been reported by measuring the intracellular signal transduction in cells or tissues level. Nakanishi et al. (19) demonstrated that both ET_A- and ET_B-mediation showed PI hydrolysis and arachidonic acid release, however, ET_A-mediation showed the formation of cyclic AMP and ET_B-mediation showed an inhibitory action of cyclic AMP formation in receptor transfected cells. Henry et al. (4) reported that ET_A stimulation induces phosphoinositide turnover and subsequent release of intracellular Ca²⁺ whereas stimulation of ET_B facilitates the influx of extracellular Ca²⁺ in rat isolated tracheal tissues. In Chapter 1, I showed that both ET_A and ET_B mediated the [Ca²⁺]_i increases in primary culture of guinea pig tracheal smooth muscle cells, however, I could not show any differences of signal transduction mechanism between ET_A and ET_B. Then, in this chapter, I clearly indicate the selective activation of pharmacomechanical and electromechanical E/C pathways by ET_A and ET_B respectively in guinea pig trachea. These mechanisms might be generalized to the ET-mediated contraction of the other tissues.

In Chapter 1, it was shown that both ET-1 and ET-3 induced biphasic increases in [Ca²⁺]_i with a transient and a sustained phases in primary cultured cells derived from guinea pig tracheal smooth muscle, but ET-3-induced transient increases in [Ca²⁺]_i did not observe up to 100 nM in this study (data not shown). The transient increases in [Ca²⁺]_i induced by ET-1 was observed from the concentration of 1 nM in primary cultured cells, however, in tracheal tissues, the transient increases in [Ca²⁺]_i was observed from the stimulation of 10 nM ET-1. One of the reasons for this discrepancy is considered to be the

differences of ligand permeability between tissues and cells. The experiments in which extracellular Ca^{2+} was removed suggest that the main source of mobilized Ca^{2+} for the initial transient increase in $[\text{Ca}^{2+}]_i$ is an intracellular pool (presumably the sarcoplasmic reticulum) and that the main source of mobilized Ca^{2+} during the sustained phase is an extracellular space. However, the relative contribution of mobilized Ca^{2+} from these two sources to contractile responses in airway smooth muscle, especially the contribution of transient increase in $[\text{Ca}^{2+}]_i$, is not clear. I have already described in Chapter 1 that tachyphylaxis was not observed in the tracheal contraction assays with ETs, although the transient increase in $[\text{Ca}^{2+}]_i$ showed homologous desensitization after stimulation of ET receptors in primary cells, therefore, the ET-induced Ca^{2+} release from the intracellular store sites only weakly contributed to the induction of contraction. The present data clearly proved by the method of simultaneous measurements of $[\text{Ca}^{2+}]_i$ and muscle tension that a transient increase in $[\text{Ca}^{2+}]_i$ induced by ET-1 in the absence or presence of BQ-788, ET_B specific antagonist, did not accompany with any contraction in Ca^{2+} -free Krebs-Henseleit solution by comparing with the contractile response of histamine. In the case of histamine, a transient increase in $[\text{Ca}^{2+}]_i$ accompanied with a transient contraction. With regard to the peak values of transient increases in $[\text{Ca}^{2+}]_i$, there were not significant differences between ET-1- and histamine-induced $[\text{Ca}^{2+}]_i$ increases. Therefore, the quantity of transient increases in $[\text{Ca}^{2+}]_i$ is not considered to be essential for transient contraction, although it is well known that contraction of airway smooth muscle is dependent upon the concentration of intracellular free Ca^{2+} (1, 30). The Ca^{2+} localization by stimulation of the different Ca^{2+} store sites with ETs and histamine might be one of the cause of this difference, however, it remains to be elucidated.

Recently a number of hormones and neurotransmitters have been shown to cause polyphosphoinositide breakdown in several tissues. The resulting products, inositol 1,4,5-triphosphate (IP_3) and diacylglycerol (DG), have been shown to function as intracellular messengers in the action of the particular agonist (4, 22). DG in the plasma membrane is

believed to be a physiological factor which activates the PKC *in situ* (10, 23). The present data showed that phosphoinositide (PI) turnover and transient increase in $[Ca^{2+}]_i$ occurred by the ET_A mediation, and that the PKC-inhibitor, calphostin C, suppressed Ca^{2+} -sensitivity to ET_A -stimulated contraction. Therefore, it is considered that the stimulation of ET_A activates PKC, and elevates intracellular Ca^{2+} -sensitivity to muscle contraction, while the activation of ET_B does not activate PKC, because PI turnover did not occur.

In conclusion, the absolute requirement of Ca^{2+} influx for ET-1 to induce tracheal smooth muscle contraction was clearly distinct from the mode of action of other constrictors that bind to G protein-coupled receptors such as histamine, which could induce a transient increase in tension corresponding to the transient increase in $[Ca^{2+}]_i$ (not shown). The lack of contribution by the transient increase in $[Ca^{2+}]_i$ indicated that the high potency of ET-1 resides in other intracellular signaling events unique to this ligand. I suggest that the ability of ET-1 to activate diverse sets of Ca^{2+} channels, by activating both ET_A and ET_B , may underlay the high potency of the peptide as a smooth muscle constrictor. The ET_A -selective activation of PI cascade, which in turn leads to the activation of PKC, potentiates the effect of ET-1. The combination of the non-selective ligand ET-1 and the two receptor subtypes coupled with distinct signaling pathways enables the full mobilization of the contractile apparatus. Thus, ET-1 is the first example of a single ligand which activates both pharmacomechanical and electromechanical pathways, via two receptor subtypes specialized to each E/C coupling pathway.

References
Text Footnotes

1. Ellis, R. S., D. F. Bohr, and J. C. Kling. Endothelin-induced calcium responses in human vascular smooth muscle cells. *Am. J. Physiol.* 263: C144-C147, 1992.

2. Hay, D. W. P., P. J. Henry, and R. G. Gentle. Endothelin and the nervous system. *Trends Pharmacol. Sci.* 14, 29-32, 1993.

3. Henry, P. J. Endothelin-1 (ET-1) activates expression of an unusual form of Ca^{2+} and Cl^{-} channels and calcium-activated potassium currents. *Br. J. Pharmacol.* 110: 443-451, 1992.

4. Honda, K., K. Nakata, H. Araki, S. Suga, Y. Ozawa, M. Kobayashi, Y. Shirakami, Y. Saito, S. Nakamura, and H. Inoue. Cloning and expression of human endothelin-1 receptor cDNA. *FEBS Lett.* 257: 23-26, 1991.

5. Hurrell, L. Pharmacology of calcium channels and smooth muscle. *Ann. Rev. Pharmacol. Toxicol.* 36: 225-258, 1996.

6. Ibari, H., K. Nagata, T. Sasaki, S. Takarada, A. Tawarida, S. Hirose, Y. Fukami, K. Ishikawa, M. Nishikino, and M. Yanai. Biological profile of highly potent novel vasopressin analogs selective for the V_{1a} receptor. *Life Sci.* 50: 267-285, 1991.

7. Inoue, A., M. Yanai, S. Kikuchi, Y. Nambu, T. Miyazaki, K. Goto, and T. Masaki. The human endothelin family: three structurally and pharmacologically distinct peptides produced by three separate genes. *Proc. Natl. Acad. Sci. USA* 86: 2863-2867, 1989.

8. Ishikawa, K., M. Ibari, K. Nagata, T. Masu, N. Miya, T. Sasaki, T. Takarada, T. Fukami, S. Ozaki, T. Nagata, M. Nishikino, and M. Yanai. Biochemical and pharmacological profile of a potent and selective endothelin B receptor antagonist, DQ-702. *Proc. Natl. Acad. Sci. USA* 91: 4892-4895, 1994.

References

1. **Filo, R. S., D. F. Bohr, and J. C. Ruegg.** Glycerinated skeletal and smooth muscle: calcium and magnesium dependence. *Science*. 147: 1581-1583, 1965.
2. **Gardner, J. P., G. Tokudome, H. Tomonari, E. Maher, D. Hollander, and A. Aviv.** Endothelin induced calcium responses in human vascular smooth muscle cells. *Am. J. Physiol.* 262: C148-C155, 1992.
3. **Hay, D. W. P., P. J. Henry, and R. G. Goldie.** Endothelin and the respiratory system. *Trends Pharmacol. Sci.* 14: 29-32, 1993.
4. **Henry, P. J.** Endothelin-1 (ET-1)-induced contraction in rat isolated trachea: involvement of ET_A and ET_B receptors and multiple signal transduction systems. *Br. J. Pharmacol.* 110: 435-441, 1993.
5. **Hosoda, K., K. Nakao, H. Arai, S. Suga, Y. Ogawa, M. Mukoyama, G. Shirakami, Y. Saito, S. Nakanishi, and H. Imura.** Cloning and expression of human endothelin-1 receptor cDNA. *FEBS Lett.* 287: 23-26, 1991.
6. **Hurwitz, L.** Pharmacology of calcium channels and smooth muscle. *Annu. Rev. Pharmacol. Toxicol.* 26: 225-258, 1986.
7. **Ihara, M., K. Noguchi, T. Saeki, T. Fukuroda, S. Tsuchida, S. Kimura, T. Fukami, K. Ishikawa, M. Nishikibe, and M. Yano.** Biological profiles of highly potent novel endothelin antagonists selective for the ET_A receptor. *Life Sci.* 50: 247-255, 1991.
8. **Inoue, A., M. Yanagisawa, S. Kimura, Y. Kasuya, T. Miyauchi, K. Goto, and T. Masaki.** The human endothelin family: three structurally and pharmacologically distinct isopeptides predicted by three separate genes. *Proc. Natl. Acad. Sci. USA.* 86: 2863-2867, 1989.
9. **Ishikawa, K., M. Ihara, K. Noguchi, T. Mase, N. Mino, T. Saeki, T. Fukuroda, T. Fukami, S. Ozaki, T. Nagase, M. Nishikibe, and M. Yano.** Biochemical and pharmacological profile of a potent and selective endothelin B-receptor antagonist, BQ-788. *Proc. Natl. Acad. Sci. USA.* 91: 4892-4896, 1994.

10. **K-S. Ha, a. J. H. E.** Differential translocation of protein kinase C isozymes by thrombin and platelet-derived growth factor. *J. Biol. Chem.* 268: 10534-10539, 1993.
11. **Knott, P. G., A. C. D'Aprile, P. J. Henry, D. W. P. Hay, and R. G. Goldie.** Receptors for endothelin-1 in asthmatic human peripheral lung. *Br. J. Pharmacol.* 114: 1-3, 1995.
12. **Lin, H. Y., E. H. Kaji, G. K. Winkel, H. E. Ives, and H. F. Lodish.** Cloning and functional expression of a vascular smooth muscle endothelin-1 receptor. *Proc. Natl. Acad. Sci. USA.* 88: 3185-3189, 1991.
13. **Little, P. J., C. B. Neylon, V. A. Tkachuk, and A. Bobik.** Endothelin 1 and endothelin 3 stimulate calcium mobilization by different mechanisms in vascular smooth muscle. *Biochem. Biophys. Res. Commun.* 183: 694-700, 1992.
14. Martell, A. E., and R. M. Smith, *Amino Acids.* Vol. 1. 1974, New York: Plenum Press.
15. **Masaki, T., M. Yanagisawa, and K. Goto.** Physiology and pharmacology of endothelins. *Medical Research Reviews.* 12: 391-421, 1992.
16. **Meddings, J. B., R. B. Scott, and G. H. Fick.** Analysis and comparison of sigmoidal curves: application to dose-response data. *Am. J. Physiol.* 257: G982-G989, 1989.
17. **Merritt, J. E., W. P. Armstrong, C. D. Benham, T. J. Hallam, R. Jacob, A. Jaxa-Chamiec, B. K. Leigh, S. A. McCarthy, K. E. Moores, and T. J. Rink.** SK&F 96365, a novel inhibitor of receptor-mediated calcium entry. *Biochem. J.* 271: 515-522, 1990.
18. **Nakamura, M., T. J. Abell, A. M. Richards, H. Ikram, E. A. Espiner, and T. G. Yandle.** Endothelin induced changes in intracellular calcium concentration in rat vascular smooth muscle cells. *Heart Vessels.* 7: 37-41, 1992.
19. **Nakanishi, S., S. Kakita, I. Takahashi, K. Kawahara, E. Tsukuda, T. Sano, K. Yamada, M. Yoshida, H. Kase, Y. Matsuda, Y. Hashimoto, and Y. Nonomura.**

- Wortmannin, a microbial product inhibitor of myosin light chain kinase. *J. Biol. Chem.* 267: 2157-2163, 1992.
20. **Nally, J. E., R. McCall, L. C. Young, M. J. O. Wakelam, N. C. Thomson, and J. C. McGrath.** Mechanical and biochemical responses to endothelin-1 and endothelin-3 in human bronchi. *Eur. J. Pharmacol.* 288: 53-60, 1994.
21. **Nelson, M. T., J. B. Patlak, J. F. Worley, and N. B. Standen.** Calcium channels, potassium channels, and voltage dependence of arterial smooth muscle tone. *Am. J. Physiol.* 259: C3-C18, 1990.
22. **Nishimura, J., S. Moreland, H. Y. Ahn, T. Kawase, R. S. Moreland, and C. v. Breemen.** Endothelin increases myofilament Ca^{2+} sensitivity in alpha toxin permeabilized rabbit mesenteric artery. *Circ. Res.* 71: 951-959, 1992.
23. **Nishizuka, Y.** Intracellular signaling by hydrolysis of phospholipids and activation of protein kinase C. *Science.* 258: 607-613, 1992.
24. Oiki, S., and Y. Okada, *Ca-EGTA buffers in physiological solutions.* *Seitai-no-kagaku*, Vol. 38. 1987, . 79-83.
25. **Randall, M. D., S. A. Douglas, and C. R. Hiley.** Vascular activities of endothelin-1 and some alanyl substituted analogues in resistance beds of the rat. *Br. J. Pharmacol.* 98: 685-699, 1989.
26. **Rubanyi, G. M., and M. A. Polokoff.** Endothelins: Molecular Biology, Biochemistry, Pharmacology, Physiology, and Pathophysiology. *Pharmacol. Rev.* 46: 325-415, 1994.
27. **Sato, K., H. Ozaki, and H. Karaki.** Changes in cytosolic calcium level in vascular smooth muscle strip measured simultaneously with contraction using fluorescent calcium indicator Fura 2. *J. Pharmacol. Exp. Ther.* 246: 294-300, 1988.
28. **Seo, B., B. S. Oemar, R. Siebenmann, L. v. Segesser, and T. F. Lüscher.** Both ET_A and ET_B receptors mediate contraction to endothelin-1 in human blood vessels. *Circulation.* 89: 1203-1208, 1994.

29. **Smith, R. J., L. M. Sam, J. M. Justen, G. L. Bundy, G. A. Bala, and J. E. Bleasdale.** Receptor-coupled signal transduction in human polymorphonuclear neutrophils: effects of a novel inhibitor of phospholipase C-dependent processes on cell responsiveness. *J. Pharmacol. Exp. Ther.* 253: 688-697, 1990.
30. **Somlyo, A. P., and B. Himpens.** Cell calcium and its regulation in smooth muscle. *FASEB J.* 3: 2266-2276, 1989.
31. **Somlyo, A. P., and A. V. Somlyo.** Signal transduction and regulation in smooth muscle. *Nature.* 372: 231-236, 1994.
32. **Sunako, M., Y. Kawahara, K. Kariya, S. Araki, H. Fukuzaki, and Y. Takai.** Endothelin induced biphasic formation of 1,2 diacylglycerol in cultured rabbit vascular smooth muscle cells mass analysis with a radioenzymatic assay. *Biochem. Biophys. Res. Commun.* 160: 744-750, 1989.
33. **Takai, M., I. Umemura, K. Yamasaki, T. Watakabe, Y. Fujitani, K. Oda, Y. Urade, T. Inui, T. Yamamura, and T. Okada.** A potent and specific agonist, Suc-[Glu⁹, Ala^{11,15}]-endothelin-1(8-21), IRL 1620, for the ET_B receptor. *Biochem. Biophys. Res. Commun.* 184: 953-959, 1992.
34. **Takenaka, T., M. Epstein, H. Forster, D. W. Landry, K. Iijima, and M. S. Goligorsky.** Attenuation of endothelin effects by a chloride channel inhibitor, indanyloxyacetic acid. *Am. J. Physiol.* 262: F799-F806, 1992.
35. **Yanagisawa, M., H. Kurihara, S. Kimura, Y. Tomobe, M. Kobayashi, Y. Mitsui, Y. Yazaki, K. Goto, and T. Masaki.** A novel potent vasoconstrictor peptide produced by vascular endothelial cells. *Nature.* 332: 411-415, 1988.

TABLE 2-1. *Statistical comparison of the concentration-contractile response curves*

Data Set	T _{max} (% of 10 μM carbachol)	EC ₅₀ (nM)
ET-1	87.3 ± 2.03	1.14 ± 0.12
ET-3	68.2 ± 0.98 ^b	6.26 ± 0.37 ^a
IRL 1620	58.1 ± 1.29 ^a	8.72 ± 0.70 ^a
ET-1 + 10 μM BQ-123	55.8 ± 1.69 ^{a d}	3.55 ± 0.43 ^{b d}
ET-1 + 3 μM BQ-788	77.1 ± 1.48	2.23 ± 0.18 ^c
ET-3 + 3 μM BQ-788	1.90 ± 1.04 ^{a c}	N. D.

Values are the estimates of parameters ± SE based on nonlinear regression analysis using a logistic equation. T_{max}, maximum contraction, EC₅₀, half-maximally effective concentration. ^a P < 0.01; ^b P < 0.05 compared with the data obtained with ET-1; ^c P < 0.01; ^d P < 0.05 compared with the data obtained with ET-3 (Dunnett's multiple comparison).

TABLE 2-2. *Effects of L-VDCC blockers, IAA-94 and low Na⁺ condition on ET-1-induced contraction of epithelium-denuded guinea pig trachea.*

Treatment	Contraction (% of that induced by 66 mM KCl)	
	ET _A	ET _B
None	113 ± 7	89 ± 3
Nifedipine (1 μM)	100 ± 3	0*
Verapamil (10 μM)	87 ± 7	0*
IAA-94 (30 μM)	101 ± 2	44 ± 2*
Low Na ⁺ (10 mM)	106 ± 10	66 ± 2*
Low Na ⁺ (10 mM) plus IAA-94 (30 μM)	117 ± 13	2 ± 0*

Values are means ± s.e. of more than 4 independent determinations. * p < 0.01 compared with the control contraction mediated by ET_B.

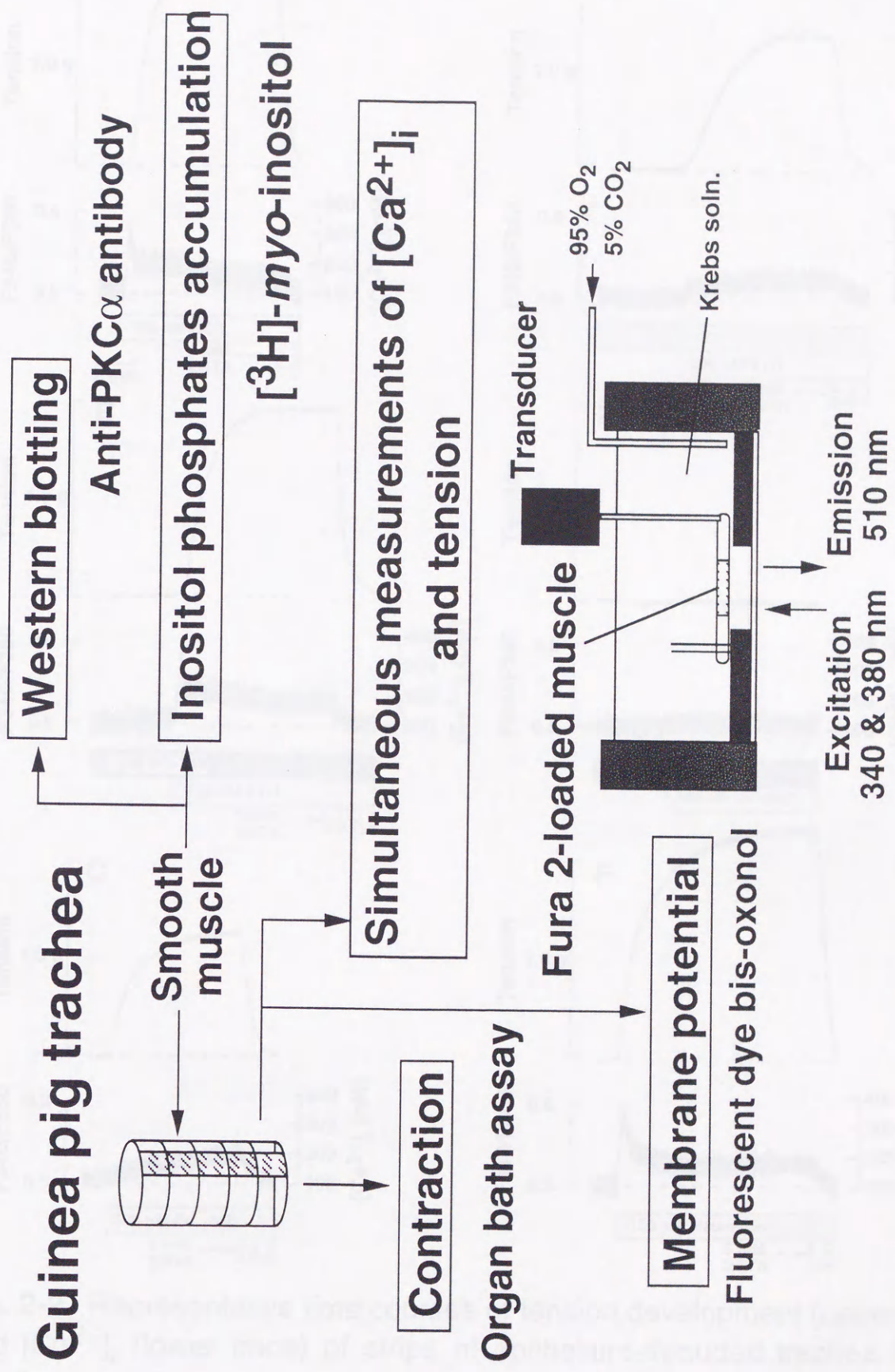


Fig. 2-1. Experimental protocol.

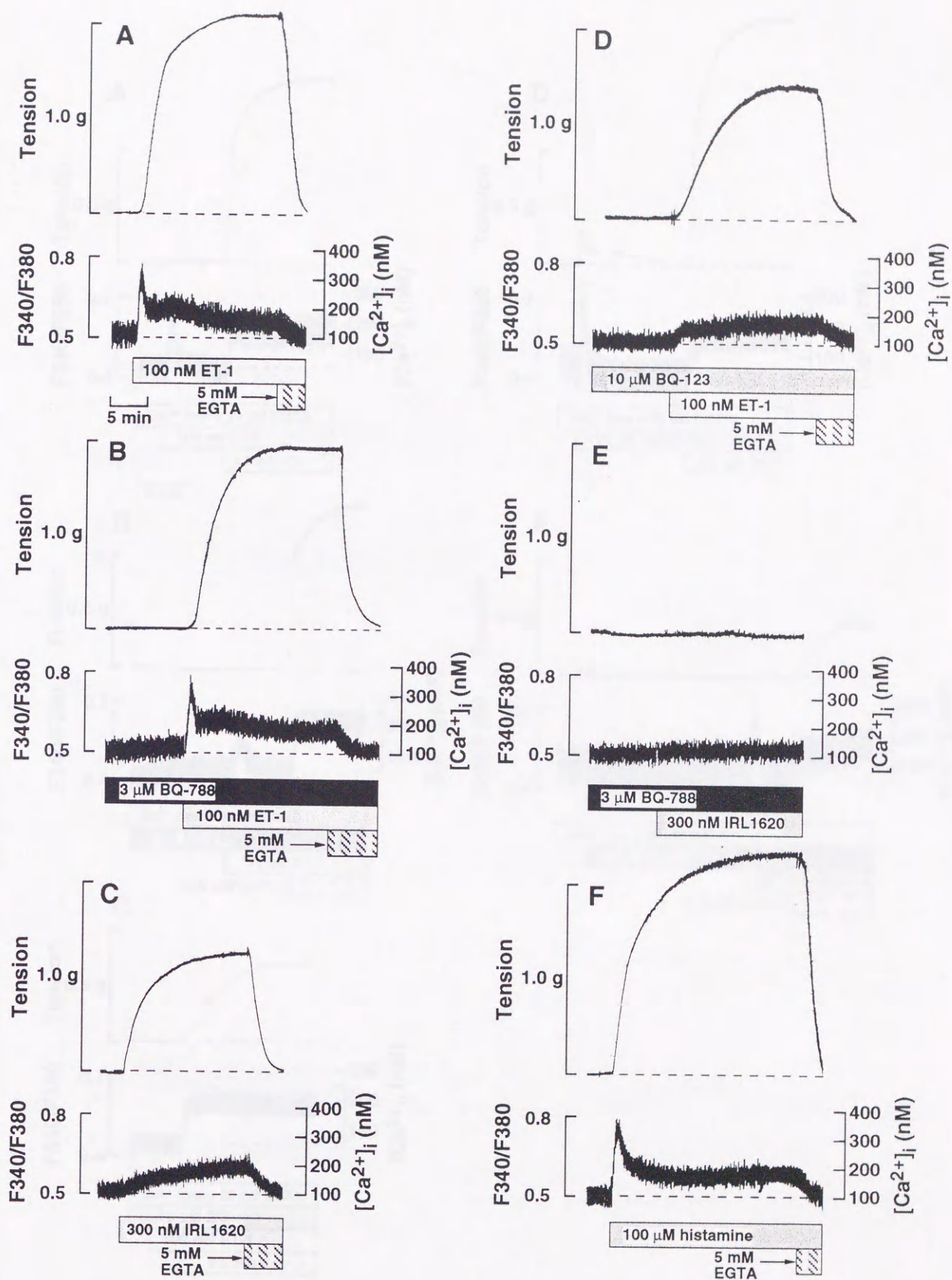


Fig. 2-2. Representative time courses of tension development (upper trace) and $[Ca^{2+}]_i$ (lower trace) of strips of epithelium-denuded trachea loaded with fura-2. Stimulation of both ET_A and ET_B (A), ET_A (B), ET_B (C, D), ET_B in the presence of $3 \mu M$ BQ-788 (E), and stimulation with $100 \mu M$ histamine (F). Dotted lines show basal levels of tension and $[Ca^{2+}]_i$.

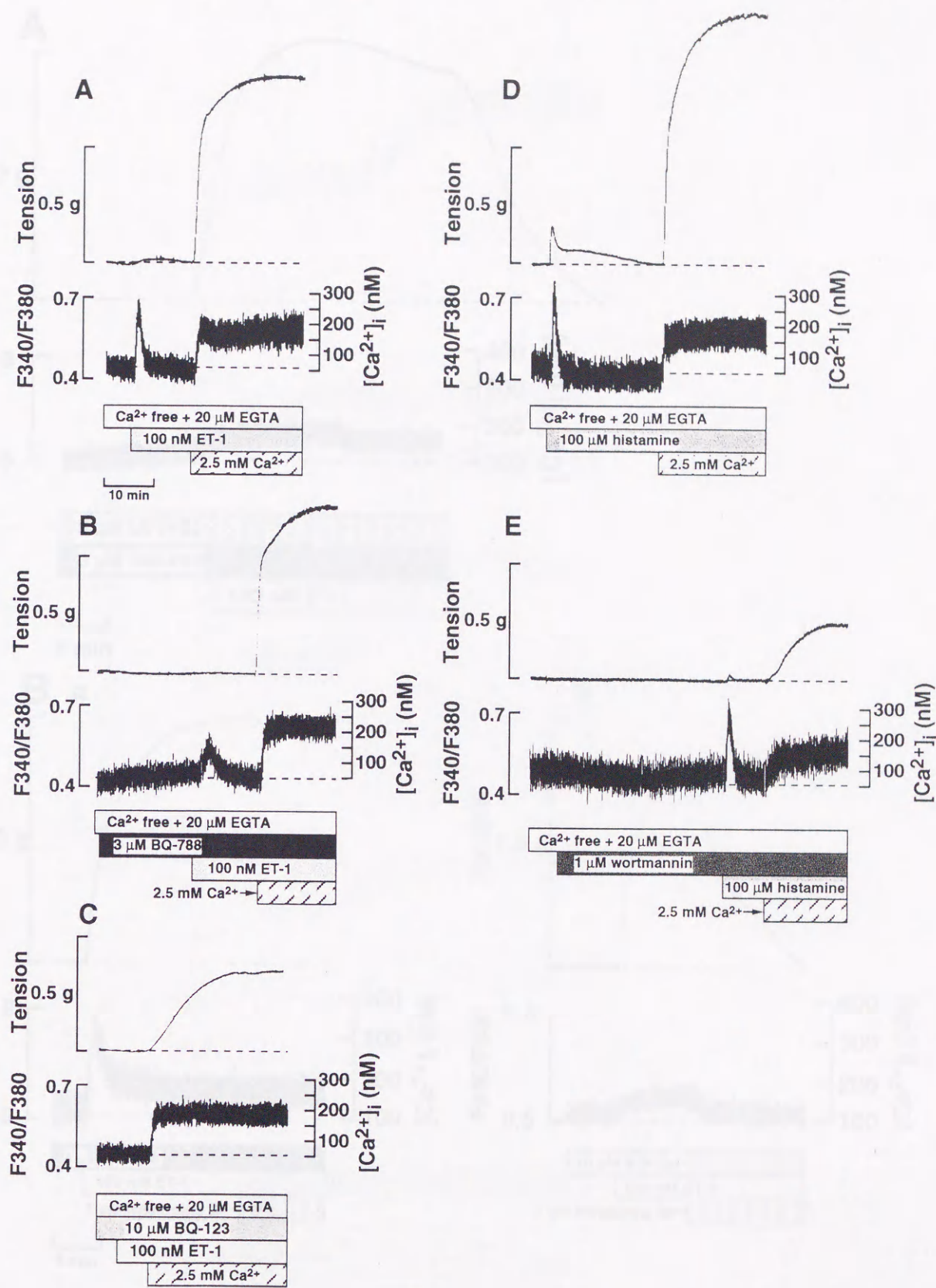


Fig. 2-3. Effects of ET-1 in the absence or presence of BQ-788, BQ-123 and histamine on tension development (upper trace) and $[Ca^{2+}]_i$ (lower trace) in the absence of external Ca^{2+} . Stimulation of both ET_A and ET_B (A), ET_A (B), ET_B (C) and 100 μ M histamine (D) were carried out. Effects of pre-treatment with 1 μ M wortmannin induced by 100 μ M histamine (E) in the absence of external Ca^{2+} .

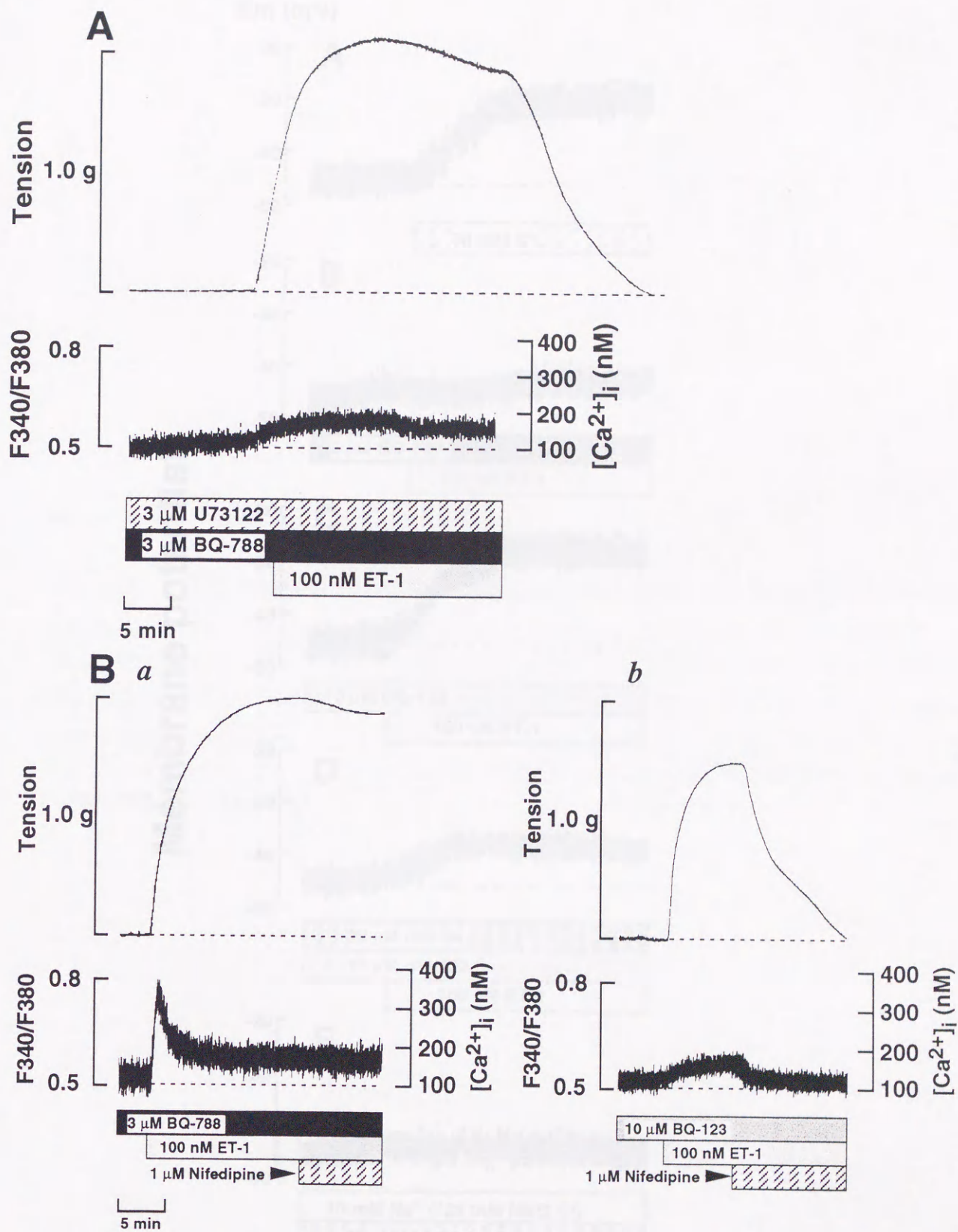
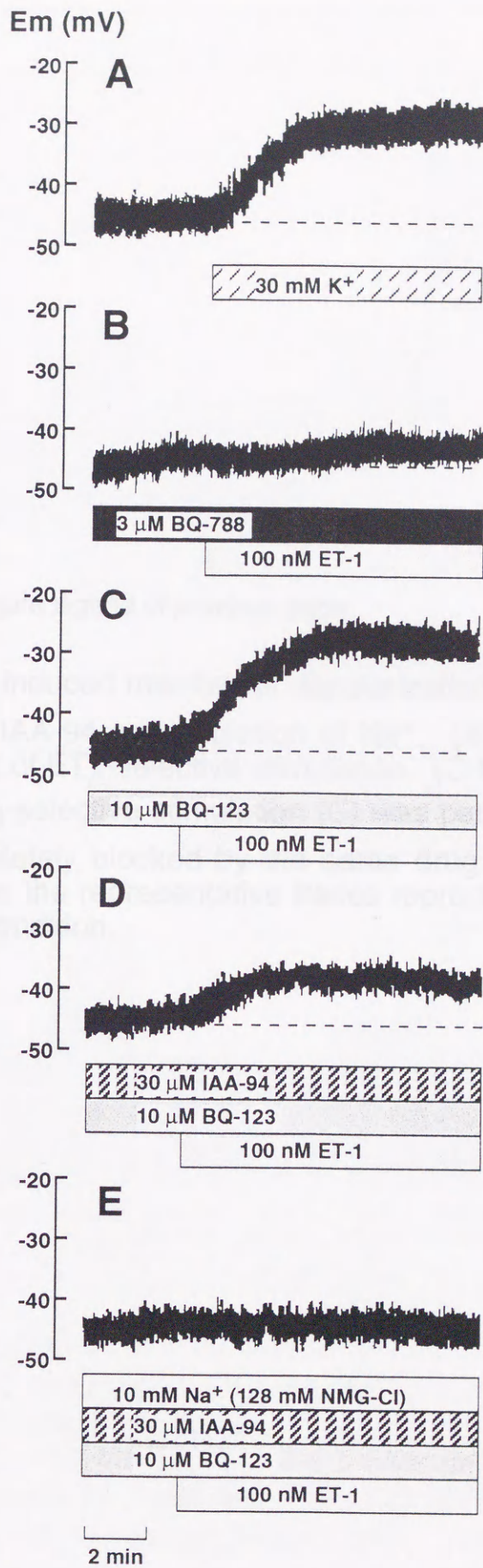


Fig. 2-4. (A) Effects of U73122 on ET_A -induced increases in $[Ca^{2+}]_i$ and tension in the presence of extracellular Ca^{2+} . (B) Effects of nifedipine on either ET_A - (a) or ET_B - (b) induced increases in $[Ca^{2+}]_i$ and tension. Another L-VDCC blocker verapamil (10 μ M) gave essentially the same results (not shown). Shown are the representative traces obtained in more than three independent experiments.

Membrane potential





← Figure legend of previous page

Fig. 2-5. ET_B-induced membrane depolarization of tracheal smooth muscle and effects of IAA-94 and depletion of Na⁺. (A) Effect of 30 mM KCl. (B) Negative effect of ET_A-selective stimulation. (C-E) Membrane depolarization caused by ET_B-selective stimulation (C) was partially blocked by IAA-94 (D) and was completely blocked by the same drug under a low Na⁺ condition (E). Shown are the representative traces reproduced at least twice for each experimental condition.



Fig. 2-5. Accumulation of [³H]-inositol phosphates in epithelium-denuded tracheal smooth muscles. [³H]-inositol phosphate accumulation were measured under basal conditions or following stimulation with 100 nM ET-1, 300 nM IRL 1620, 100 nM ET-1 in the presence of 10 μM BQ-123, 100 nM ET-1 in the presence of 3 μM BQ-788, 100 μM histamine in the presence (A) and absence (B) of extracellular Ca²⁺. Accumulation of [³H]-inositol phosphates are expressed as d.p.m. mg⁻¹ wet wt. tracheal smooth muscle. Data are shown as the mean ± S.E. of 3-5 independent experiments. Significant difference based on Student's t test, a P < 0.01.

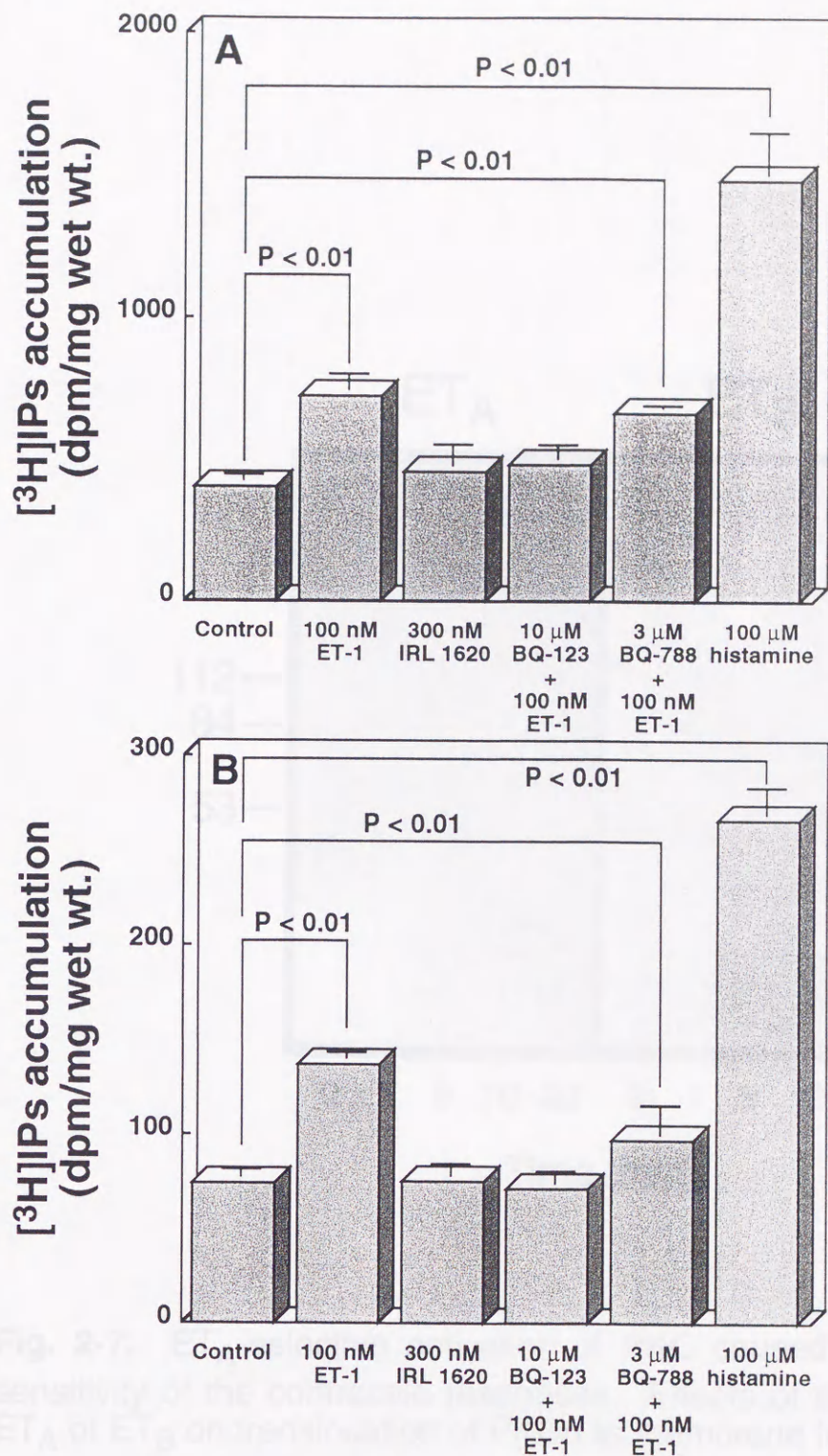


Fig. 2-6. Accumulation of [³H]-inositol phosphates in epithelium-denuded tracheal smooth muscles. [³H]-inositol phosphate accumulation were measured under basal conditions or following stimulation with 100 nM ET-1, 300 nM IRL 1620, 100 nM ET-1 in the presence of 10 μM BQ-123, 100 nM ET-1 in the presence of 3 μM BQ-788, 100 μM histamine in the presence (A) and absence (B) of extracellular Ca²⁺. Accumulation of [³H]-inositol phosphates are expressed as d.p.m. mg⁻¹ wet wt. tracheal smooth muscle. Data are shown as the mean ± S.E. of 3-5 independent experiments. Significant difference based on Student's t test, a P < 0.01.

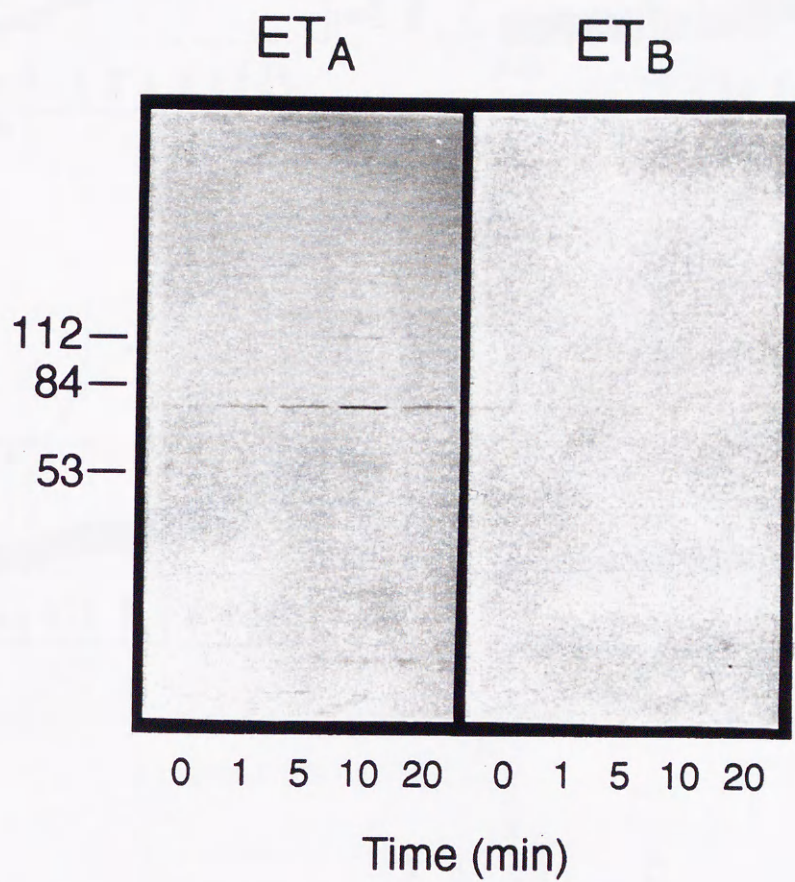


Fig. 2-7. ET_A-selective activation of PKC caused an increase in Ca²⁺ sensitivity of the contractile responses. Effects of selective stimulation of ET_A or ET_B on translocation of PKC α to membrane fractions.

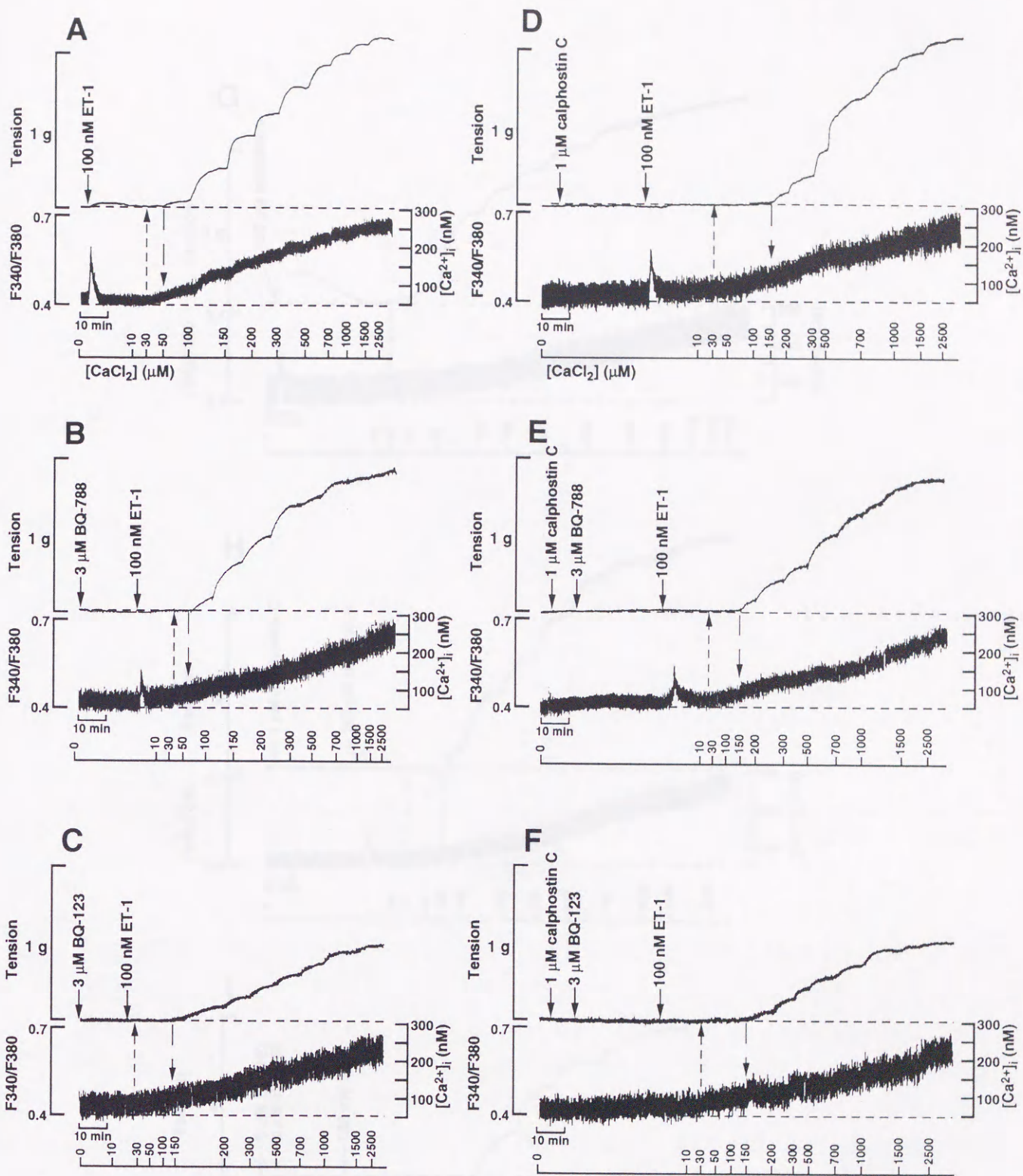


Fig. 2-8. Representative concentration-dependent increases in tension (upper trace) and $[Ca^{2+}]_i$ (lower trace) in tracheal strips induced by cumulative addition of $CaCl_2$ in Ca^{2+} -free Krebs-Henseleit solution containing $20 \mu M$ EGTA pre-stimulated with $100 nM$ ET-1 (A), in the presence of $3 \mu M$ BQ-788 (B), or $10 \mu M$ BQ-123 (C) and $100 \mu M$ histamine (G), and with $100 nM$ ET-1 (D), in the presence of BQ-788 (E), or $10 \mu M$ BQ-123 (F) and $100 \mu M$ histamine (H) in the presence of $1 \mu M$ calphostin C. Dotted lines show basal levels of tension and $[Ca^{2+}]_i$.

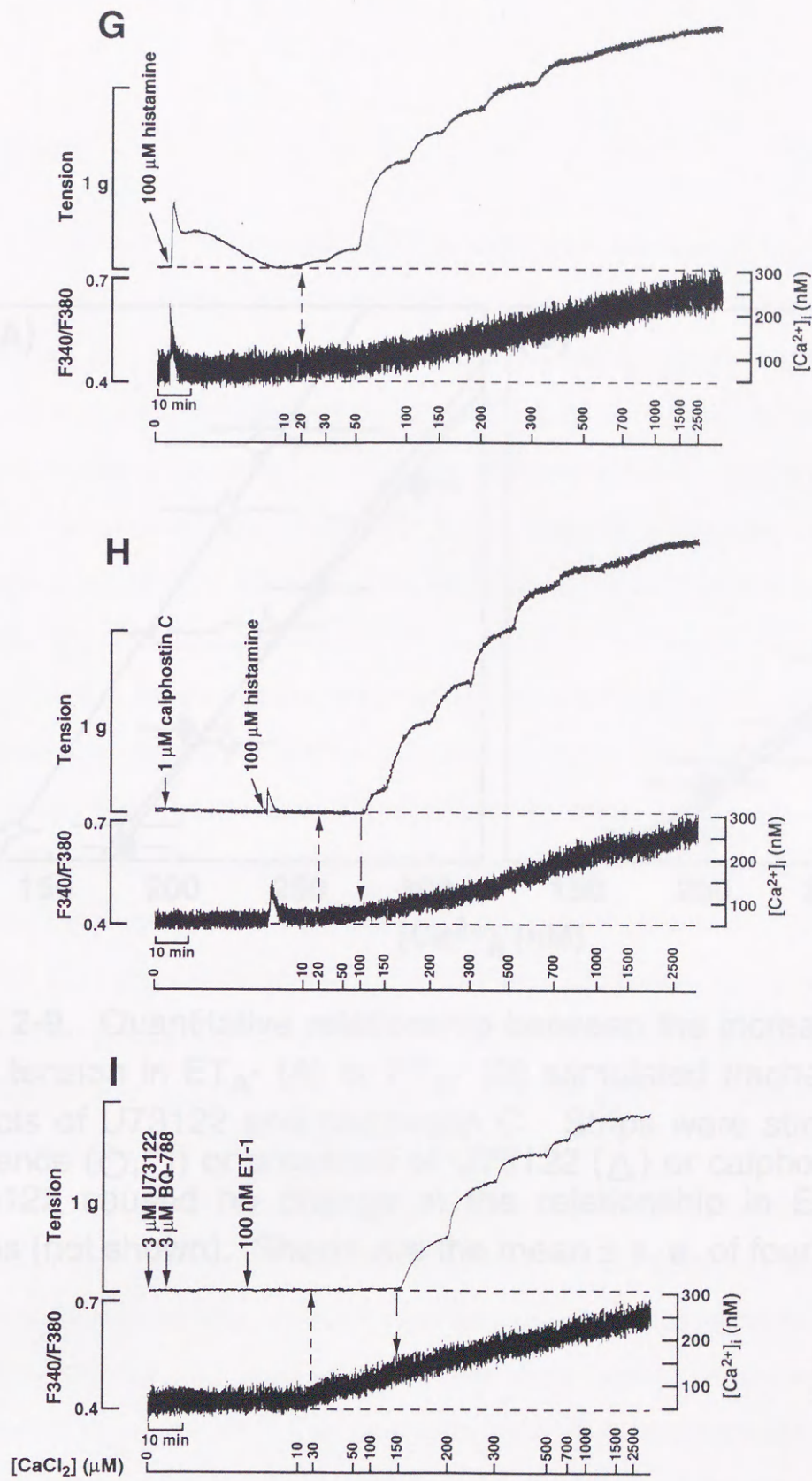


Fig. 2-8-I. Effect of U73122 on ET_A-stimulated strips.

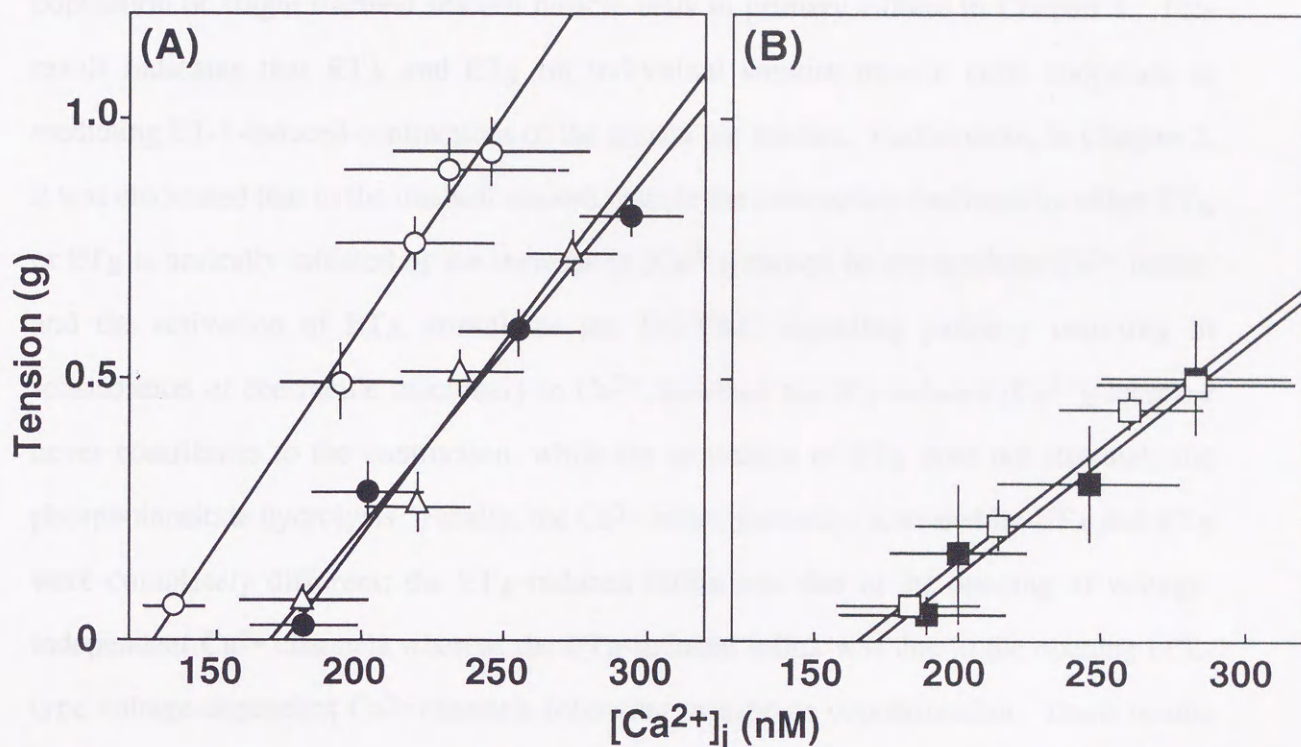


Fig. 2-9. Quantitative relationship between the increases in $[Ca^{2+}]_i$ and tension in ET_A - (A) or ET_B - (B) stimulated tracheal strips, and effects of U73122 and calphostin C. Strips were stimulated in the absence (○, □) or presence of U73122 (△) or calphostin C (●, ■). U73122 caused no change in the relationship in ET_B -stimulated strips (not shown). Shown are the mean \pm s. e. of four experiments.

Conclusion

In this thesis, the two subtypes of ET receptor were found to coexist in a major population of single tracheal smooth muscle cells in primary culture in Chapter 1. This result indicates that ET_A and ET_B on individual smooth muscle cells cooperate in mediating ET-1-induced contractions of the guinea pig trachea. Furthermore, in Chapter 2, it was elucidated that in the tracheal smooth muscle the contraction mediated by either ET_A or ET_B is basically initiated by the increase in $[Ca^{2+}]_i$ caused by extracellular Ca^{2+} influx, and the activation of ET_A stimulates the DG/PKC signaling pathway resulting in sensitization of contractile machinery to Ca^{2+} , however the IP₃-induced $[Ca^{2+}]_i$ increase never contributes to the contraction, while the activation of ET_B does not stimulate the phosphoinositide hydrolysis. Finally, the Ca^{2+} influx pathways activated by ET_A and ET_B were completely different; the ET_A-induced influx was due to the opening of voltage-independent Ca^{2+} channels whereas the ET_B-induced influx was due to the opening of L-type voltage-dependent Ca^{2+} channels following membrane depolarization. These results revealed that ET-1 plays a unique mode of action among the smooth muscle constrictors which activate G protein-coupled receptors, and that ET-1 is the first example of a single ligand which activates both pharmacomechanical and electromechanical pathways, via two receptor subtypes specialized to each E/C coupling pathway (Fig. 3).

To date, research has focused, to a large extent, on the contractile effects of the ETs. This activity of the ETs is the most facile to study, but for several pulmonary disorders it is unlikely to be the most relevant. Thus, for many lung diseases, including asthma, a chronic inflammatory disorder, it is important that future studies should be directed towards examination of the effects of ET on parameters other than bronchoconstriction *e.g.*, influence on nerves, inflammatory cell function, also the effects of chronic exposure on smooth muscle and fibroblast proliferation and other structural components of the lung. Another critical area of research will be the elucidation and classification of the ET receptor

subtypes mediating these effects; the availability of potent and selective receptor antagonists for the ET receptors will assist greatly in this endeavor. For the purpose of these requirements, in this study, I suggest that the development of specific bifunctional antagonist against both ET_A and ET_B receptors could be therapeutically expected to counteract pathological states such as asthma.

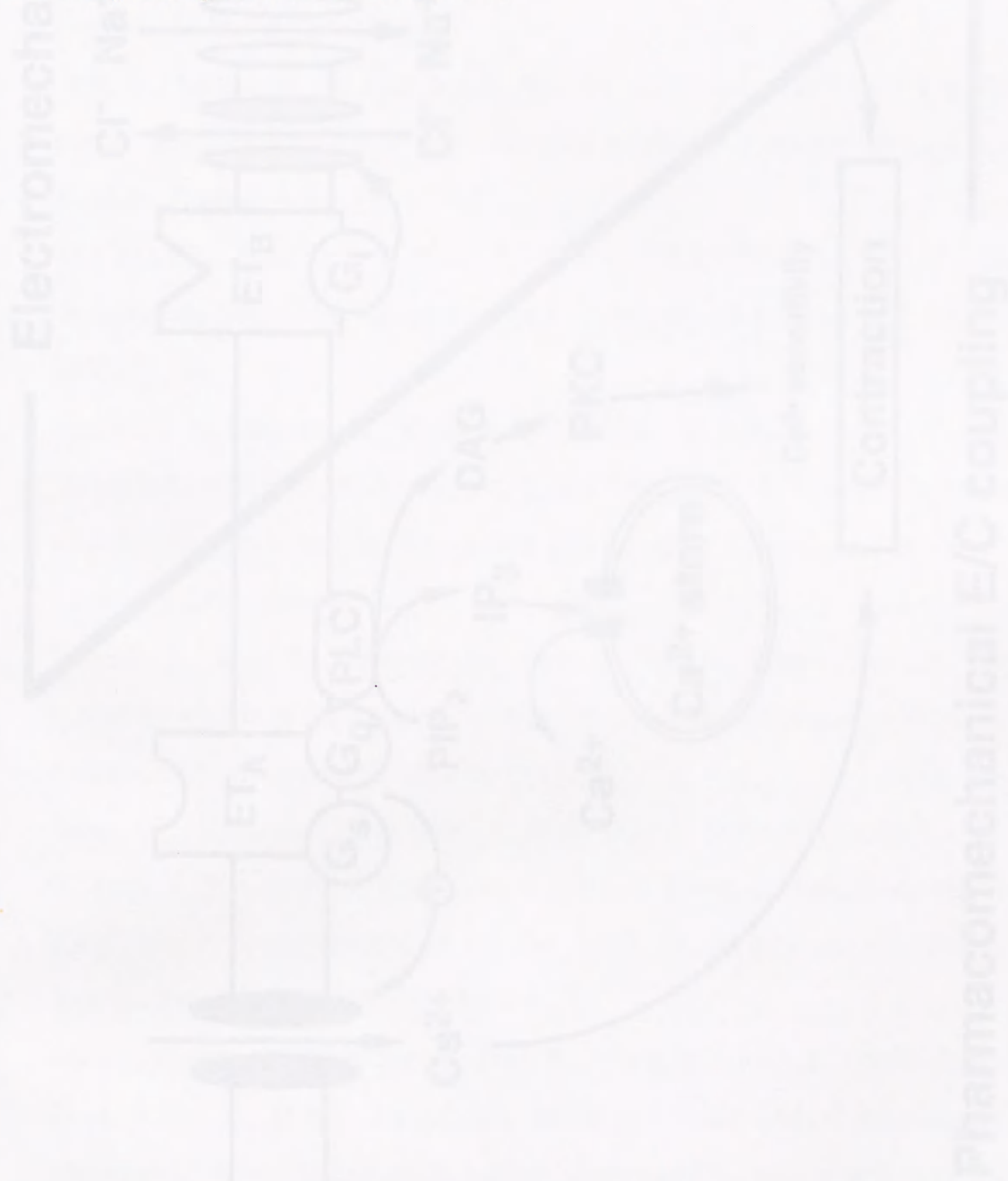


Fig. 3. Scheme of ET_A or ET_B -mediated signal transduction mechanism on tracheal smooth muscle cells.

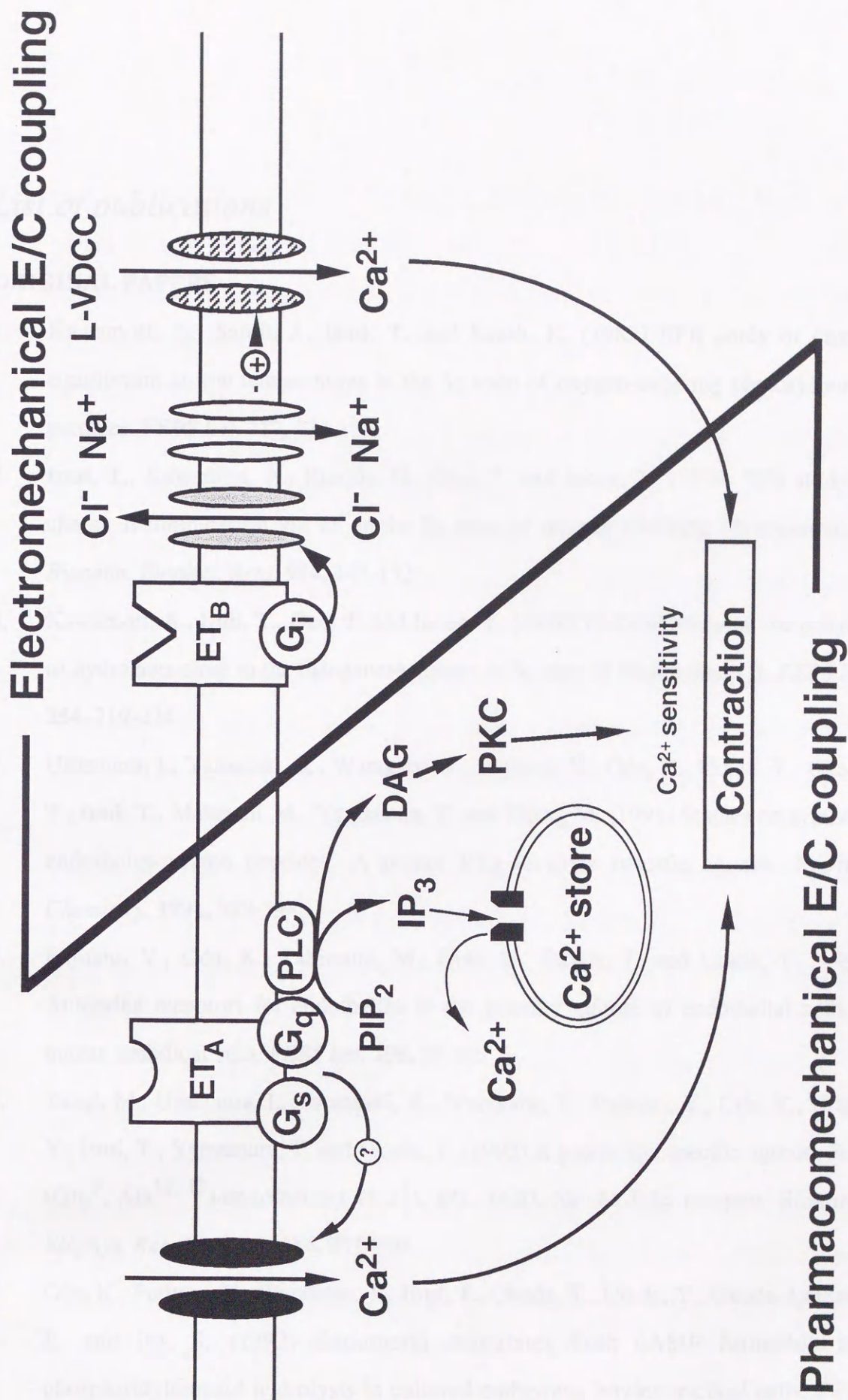


Fig. 3. Scheme of ET_A - or ET_B -mediated signal transduction mechanisms on tracheal smooth muscle cells.

List of publications

ORIGINAL PAPERS

1. Kawamori, A., Satoh, J., **Inui, T.** and Satoh, K. (1987) EPR study of charge equilibrium at low temperatures in the S₂ state of oxygen-evolving photosystem II particles. *FEBS lett.* **217**, 134-138.
2. **Inui, T.**, Kawamori, A., Kuroda, G., Ono, T. and Inoue, Y. (1989) EPR study of charge recombination via D⁺ in the S₂ state of oxygen evolving Photosystem II. *Biochim. Biophys. Acta.* **974**, 147-152.
3. Kawamori, A., **Inui, T.**, Ono, T. and Inoue, Y. (1989) ENDOR study on the position of hydrogens close to the manganese cluster in S₂ state of Photosystem II. *FEBS lett.* **254**, 219-224.
4. Umemura, I., Yamasaki, K., Watakabe, T., Fujitani, Y., Oda, K., Urade, Y., Okada, T., **Inui, T.**, Makatani, M., Yamamura, T. and Takai, M. (1991) Studies on synthetic endothelin-related peptides -A potent ET_B-receptor specific agonist. *Peptide Chemistry.* **1991**, 389-394.
5. Fujitani, Y., Oda, K., Takimoto, M., **Inui, T.**, Okada, T. and Urade, Y. (1992) Autocrine receptors for endothelins in the primary culture of endothelial cells of human umbilical vein. *FEBS lett.* **298**, 79-83.
6. Takai, M., Umemura, I., Yamasaki, K., Watakabe, T., Fujitani, Y., Oda, K., Urade, Y., **Inui, T.**, Yamamura, T. and Okada, T. (1992) A potent and specific agonist, Suc-[Glu⁹, Ala^{11, 15}]-endothelin-1 (8-21), IRL 1620, for the ET_B receptor. *Biochem. Biophys. Res. Commun.* **184**, 953-959.
7. Oda, K., Fujitani, Y., Watakabe, T., **Inui, T.**, Okada, T., Urade, Y., Okuda-Ashitaka, E. and Ito, S. (1992) Endothelin stimulates both cAMP formation and phosphatidylinositol hydrolysis in cultured embryonic bovine tracheal cells. *FEBS lett.* **299**, 187-191.

8. **Inui, T.**, Urade, Y., Fujitani, Y., Oda, K., Takimoto, M., Watakabe, T., Ochi, A., Okada, T. and Yamamura, T. (1992) Distribution of two subtypes of receptors for endothelins in single smooth muscle cells isolated from guinea pig trachea. *Jpn. J. Pharmacol.* **58**, suppl. 2, 280P.
9. James, A., Fujitani, Y., **Inui, T.**, Katsume, Y., Oda, K., Urade, Y. and Okada, T. (1992) Responses of A10 cells to Arg⁸-vasopressin and endothelin-1: The role of divalent cations. *Jpn. J. Pharmacol.* **58**, suppl. 2, 354P.
10. Takimoto, M., **Inui, T.**, Okada, T. and Urade, Y. (1993) Contraction of smooth muscle by activation of endothelin receptors on autonomic neurons. *FEBS lett.* **324**, 277-282.
11. **Inui, T.**, James, A., Fujitani, Y., Takimoto, M., Okada, T., Yamamura, T. and Urade, Y. (1994) ET_A and ET_B receptors on single smooth muscle cells cooperate in mediating guinea pig tracheal contraction. *Am. J. Physiol.* **266**, L113-L124.
12. Früh, Th., Saika, H., Svensson, L., Pitterna, Th., Sakaki, J., Okada, T., Urade, Y., Oda, K., Fujitani, Y., Takimoto, M., Yamamura, T., **Inui, T.**, Makatani, M., Takai, M., Umemura, I., Teno, N., Toh, H., Hayakawa, K. and Murata, T. (1996) IRL 2500: a potent and ET_B selective endothelin antagonist. *Bioorganic & Medicinal Chemistry letters*. in press.
13. Higashi, T., Ishizaki, T., Shigemori, K., Nakai T., Miyabo S., **Inui, T.** and Yamamura, T. (1997) Pharmacological heterogeneity of constrictions mediated by endothelin receptors in rat pulmonary arteries. *Am. J. Physiol.* in press.
14. **Inui, T.**, Ninomiya, H., Sasaki, Y., Makatani, M., Urade, Y., Masaki, T. and Yamamura, T. Selective activation of pharmacomechanical and electromechanical excitation-contraction coupling pathways by endothelin_A and endothelin_B in guinea pig tracheal smooth muscle. (submitted)

15. **Inui, T.**, Ishibashi, O., Inaoka, T., Origane, Y., Kumegawa, M., Kokubo, T. and Yamamura, T. (1997) Cathepsin K antisense oligodeoxynucleotide inhibits osteoclastic bone resorption. *J. Biol. Chem.* in press.
16. **Inui, T.**, Origane, Y., Ishibashi, O., Kokubo, T., Kumegawa, M. and Yamamura, T. Pit assay for osteoclastic bone resorption. (in preparation).

INTERNATIONAL MEETINGS/ABSTRACTS

1. Kawamori, A., **Inui, T.**, Kuroda, G. and Kobayashi, Y. (1988) Local ENDOR of photosystem II particles. The XIIIth International Conference on Magnetic Resonance in Biological Systems, Wisconsin, USA.
2. **Inui, T.**, Makatani, M., Sasaki, Y., Oda, K., Urade, Y. and Yamamura, T. (1994) Transient calcium increases mediated by the ET_A receptor do not induce muscle contraction in guinea pig trachea. The XIIth International Congress of Pharmacology, Montréal, Canada.
3. Yamamura, T., Makatani, M., **Inui, T.**, Fujitani, Y., Oda, K., Takimoto, M., Urade, Y., Okada, T., Sakaki, J. and Früh, T. (1995) Pharmacological profiles of a potent ET_B receptor selective antagonist, IRL 2500. The ICth International Conference on Endothelin, London, U.K.
4. Higashi, T., **Inui, T.**, Makatani, M., Ishizaki, T. and Yamamura, T. (1995) Mediation by ET_A and ET_B for vaso-action of endothelins in rat pulmonary artery. The ICth International Conference on Endothelin, London, U.K.

Acknowledgments

I wish to express my sincere gratitude to Professor Susumu Takayama, Biological Laboratory, School of Science, Kwansei Gakuin University for his invaluable advice, discussion, and intimate encouragement.

The present investigation was carried out under the guidance of Dr. Takaki Yamamura at the Analytics & Informatics (A&I) Department, International Research Laboratories, Ciba-Geigy Japan Ltd. from 1989-1996. I am deeply grateful to Dr. Takaki Yamamura and Dr. Yoshihiro Urade of Osaka Bioscience Institute for their constant guidance, valuable discussions, and encouragement. I also wish to express my hearty thanks to Professor Asako Kawamori of Kwansei Gakuin University, Professor Tatsuo Yagura of Kwansei Gakuin University, Professor Tomoh Masaki of Kyoto University, the late Emeritus Professor Ryo Sato of Osaka University and Professor Hideaki Karaki of the University of Tokyo for their helpful advice and discussions. Thanks are also due to Dr. Haruaki Ninomiya of Kyoto University and Dr. Andrew F. James of King's College London for their helpful advice, invaluable discussion and technical assistance. I give my gratitude to Dr. Christian d'Hondt of the A&I department head for his great support and encouragement in the early stage of this study. I also deeply thank to Dr. Toshikazu Okada, Dr. Michihiro Takai, Dr. Yukio Sasaki, Dr. Misato Takimoto, Dr. Yasushi Fujitani and Ms. Maki Makatani for their helpful advice and fruitful discussions, and technical assistance. I am greatly indebted to Mr. H. Saiki, Mr. T. Watakabe, Mr. T. Nishi, Ms. A. Ochi and Ms. Y. Katsume-Sugimoto for their excellent technical assistance. Finally, I greatly appreciate to my parents, Kiyoshi and Kazuko, and my wife, Hisami, for their unfailing understanding and affectionate encouragement.

Spring, 1997

Takashi Inui

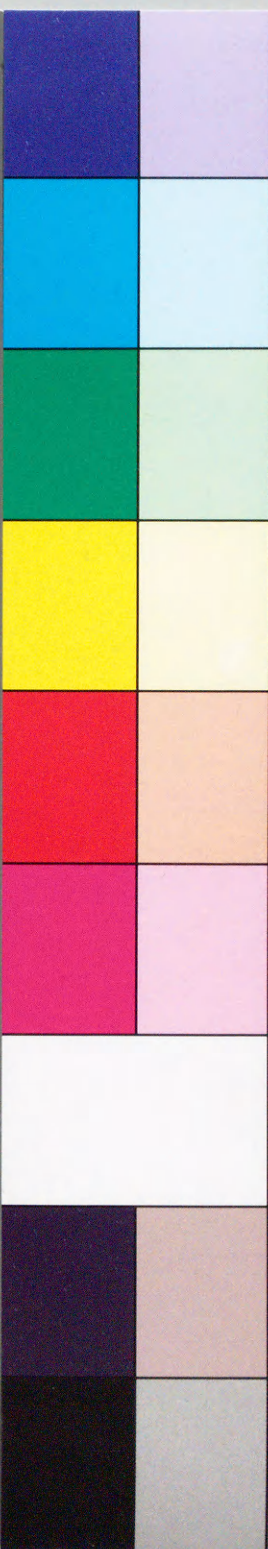


Inches 1 2 3 4 5 6 7 8
cm 1 2 3 4 5 6 7 8 9 10 11 12 13 14 15 16 17 18 19

Kodak Color Control Patches

© Kodak, 2007 TM: Kodak

Blue Cyan Green Yellow Red Magenta White 3/Color Black



Kodak Gray Scale



© Kodak, 2007 TM: Kodak

A 1 2 3 4 5 6 M 8 9 10 11 12 13 14 15 B 17 18 19

